INVERSION OF SUCROSE SOLUTION

BY

ION EXCHANGE

A Thesis

Submitted to the Department of Chemical Engineering

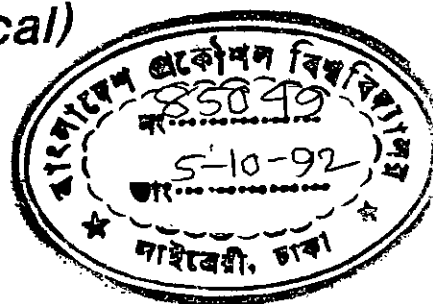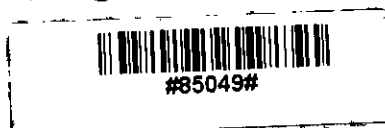*in partial fulfilment of the requirements for the degree of*

Master of Science

in

Engineering (Chemical)

by

SIRAJUL HAQUE KHAN

Chemical Engineering Department

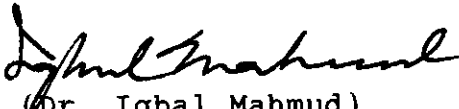*Bangladesh University of Engineering and Technology, Dhaka.*

August, 1992.

BANGLADESH UNIVERSITY OF ENGINEERING AND TECHNOLOGY
DEPARTMENT OF CHEMICAL ENGINEERING
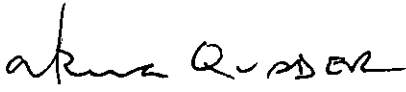
CERTIFICATION OF THESIS WORK

We, the undersigned, certify that **SIRAJUL HAQUE KHAN**, candidate for the degree of **Master of Science in Engineering (Chemical)** has presented his thesis on the subject **INVERSION OF SUCROSE SOLUTION BY ION EXCHANGE**, that the thesis is acceptable in form and content, and that the student demonstrated a satisfactory knowledge of the field covered by this thesis in an oral examination held on August 24, 1992.

(Dr. Khaliqur Rahman)
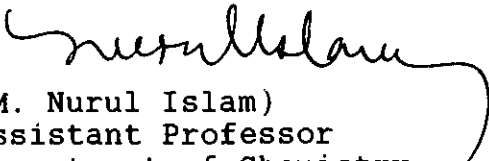Professor
Chemical Engineering Department

Chairman
Examination Committee

(Dr. Iqbal Mahmud)
Professor and Head
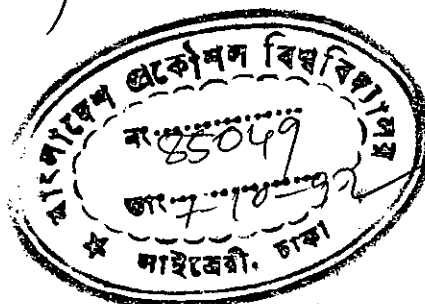Chemical Engineering Department

Member

(Dr. A.K.M.A. Quader)
Professor
Chemical Engineering Department

Member

(M. Nurul Islam)
Assistant Professor
Department of Chemistry

External Member

ABSTRACT

Inversion of sucrose solution was studied in a packed column with a strongly acidic cation exchange resin as catalyst. The variables studied were: reaction temperature, feed flow rate, feed concentration, and resin particle size. The inversion reaction can be described as a first order irreversible reaction and experimental results showed that the over-all rate decreases with increasing particle size of resin and increases with temperature. Experiment was performed with 20, 30, and 40% sucrose solutions and it was found that the specific rate constant increases with concentration of the feed solution.

From the experimental data the values of specific rate constant, distribution co-efficient and effective diffusivity were estimated by non-linear regression analysis. Distribution co-efficient for the system was found to be around 1. For 30% sucrose solution the specific rate constant varied from 0.01148 to 0.73909 min^{-1} in the temperature range of 30 to 70^0C. Effective diffusivity varied from 3.826 x 10^{-8} to 18.951 x 10^{-8} cm^2/sec for the above concentration and range of temperature.

Activation energy and Arrhenius constant for over-all rate and intrinsic rate were obtained. For intrinsic rate they were 24.93 Kcal/mol and 7.657 x 10^{15} min^{-1} respectively. For 30% sucrose solution the limiting value of over-all activation energy varied from 16.765 to 14.628 Kcal/mol for resin diameter 0.326 to 1.09 mm.

It was found that at high space-time mass transfer rate in the liquid film was important. This was of the order of 10^{-5} cm/sec.

ACKNOWLEDGEMENT

CONTENTS

CONTENTS - continued

LIST OF TABLES

LIST OF GRAPHS

LIST OF GRAPHS - CONTINUED

NOMENCLATURE

A   –   Arrhenius constant

c   –   Concentration of a component

c_0 –   Concentration of a component on resin surface

C_A –   Concentration of sucrose in solution

$\overline{C_A}$ –   Concentration of sucrose in resin phase

C_{Ai} –   Concentration of sucrose at interface

D_{eff} –   Effective diffusivity, cm^2/sec

E   –   Activation energy of chemical reaction

E_{app} –   Apparent activation energy

E_{diff} –   Activation energy of diffusion

k   –   Rate constant, min^{-1} (for first-order reaction)

$\overline{k}$ –   Rate constant in the resin phase, min^{-1}

K_L –   Mass transfer co-efficient, cm/sec

q   –   Column cross-section

Q_A –   Amount of sucrose in solution

$\overline{Q_A}$ –   Amount of sucrose in resin phase

$\widehat{Q}$ – $= (Q_A + \overline{Q_A})$ = Total amount of sucrose

r   –   Radial distance

r_i –   Intrinsic rate

r_0 –   Radius of resin particle

r_{obs} –   Observed rate

R   –   Gas constant, 1.987 $cal/{}^0C$-mol

t   –   time or space time

T   –   Temperature, absolute

v — Flow rate (solution volume per unit time and unit bed cross-section)

V — Total volume of resin

W — Thiele modulus

z — Downstream distance along the resin bed

Z — Total length of resin bed.

GREEK LETTERS:

β — Void fraction of the resin bed

λ — Distribution co-efficient

π — 3.1416

η — Effectiveness factor

CHAPTER-1

INTRODUCTION

CHAPTER-1

INTRODUCTION
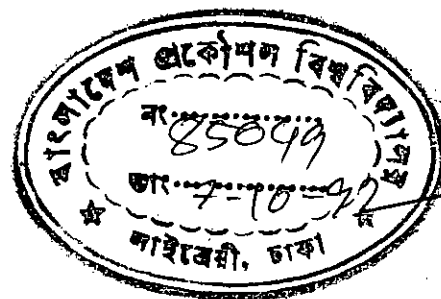
Hydrolysis of sucrose leads to a mixture of glucose and fructose.

Sucrose + H_2O -----> Glucose + Fructose
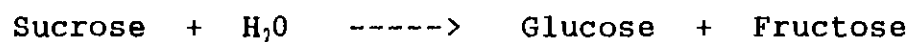
Technically this process is known as inversion of sugar and is utilized to produce artificial honey and liquid sugar. Liquid sugar has a significant market in the food industry and is used in phermaceuticals, confectioneries, bakeries and for sweetening soft drinks.

The above reaction is catalyzed by H^+ ions (e.g. hydrochloric acid). It is well known that strong cation exchange resins in hydrogen form are just as capable as hydrochloric acid for this purpose. Hydrolysis by free acid may be described as a homogeneous catalysis, and it may thought that ion exchange resins act as heterogeneous catalysts. However, the H^+ ions in the resin phase are mobile and solvated and thus in a condition which is not different from that in a corresponding homogeneous solution and catalysis of liquid phase reactions by ion exchange resin thus is not a true case of heterogeneous catalysis, but may be described more adequately as homogeneous catalysis in the resin phase. The main difference with the hydrolysis in free acid system and the ion exchange system is that in the former case homogeneous reaction occurs throughout the entire volume whereas in the latter case homogeneous reaction occurs throughout the dispersed solid phase.

In the inversion process, sucrose solution is heated to about 50-70^{0}C in an acid medium, either a strong mineral acid or a strong cation exchange resin of specific porosity and particle size. In both the cases, the reaction may be described as a first order reaction.

The use of solid ion exchanger has the major disadvantage that it has low reaction rate, since the actual reaction is accompanied by the necessary diffusion of the reactants to the catalytic centers. However, this limitation is more than compensated for by the following advantages:

1.   By simple filtration step, catalyst free products can be obtained.

2.   The catalyst can be recovered frequently by means of a simple filtration step.

3.   Continuous reaction can be obtained by passage of the reactants through beds of ion exchange resin catalysts.

4.   Unusual selectivity effects are possible.

5.   Side reactions can be kept at a minimum.

6.   Special corrosion-resistant equipment is not necessary as with soluble catalysts.

The catalyst can be used for a long period without further regeneration if not contaminated with any other cations. Increased stability and specified control of structure have led to the increased use of cation exchange resins as catalysts for inversion process.

The first experimental work (1,2) on inversion of sucrose by ion exchange resins was done quite early and several other studies (3,4,5) are available in the literature. However, none of these studies report fundamental kinetic and mass transfer data on the system. In the literature only over-all rate data are available. The main objective of the present study was to obtain (a) basic kinetic data and (b) basic data on mass transfer rate during hydrolysis of sucrose solution by ion exchange (of) resins.

Experimental work for the present study was performed with Duolite C-20, which is one of the widely used commercial resins. Duolite C-20 is a strongly acidic gel type cationic exchange resin with 8% divinyl benzene crosslinking.

The experiment was performed to study the effect of following operating variables:

(i)   Concentration of sucrose solution

(ii)   System temperature

(iii)   Solution flow rate

(iv)   Particle size of the resin.

CHAPTER-2

LITERATURE REVIEW

CHAPTER-2

LITERATURE REVIEW

2.1 CATALYSIS BY ION EXCHANGER

Many chemical reactions, both inorganic and organic, can be catalyzed by ion exchange materials and many processes have been employed commercially. This is true for reactions of gases and of liquids and solutes. Typical catalyzed gas reactions are the synthesis of ammonia, cracking of olefins, hydrogenations, reductions such as preparation of aniline from nitrobenzene, oxidations such as preparation of sulfur trioxide from sulfur dioxide, and other technically important processes. Reactions of liquids and solutes include esterification, ester hydrolysis, sucrose inversion, dehydration of alcohols, hydration of acetylene derivatives, and aldol, acyloin, and Knoevenagel condensations (6).

Early workers found that various naturally occurring zeolites were effective as catalysts for certain oxidative reactions. Jaeger (7) prepared a zeolite catalyst containing vanadium which was effective for the oxidation of sulfur dioxide to sulfur trioxide.

The catalytic properties of soils and clays were studied intensively by Rice (8) and Puri (9,10), who found that acid or hydrogen forms to possess the ability to catalyze the inversion of sucrose and hydrolysis of ethyl acetate. Rice and Puri also found that they were able to correlate the catalytic activity with the amount of exchangeable hydrogen ions in the exchange complex.

Probably the largest consumer of ion exchange materials as catalysts is the petroleum-refining industry in its cracking and refining processes. In this application, natural clays and synthetic aluminosilicates are employed in the hydrogen form. Thomas (11) studied the structural relationships of alumina – silica zeolites and suggested that the active site is located in the acidic hydrogen of the gel ($HAlSiO_4$).

2.2.1   INVERSION OF SUCROSE BY ION EXCHANGE

The catalysis of sucrose inversion by ion exchange is by no means a new field of study. The inversion of sucrose by soils was described in 1911 by Tacke and Suchting (12) and in 1914 by Hanley (13). These workers believed the inversion to be catalyzed by the humic acids present in the soils, and this view persisted until 1918. In the latter year Rice and Osugi (8) showed convincingly that the inversion must be attributed in a large measure to the mineral portion of soils as well. Rice and Osugi extended their work to various siliceous minerals and to colloidal silicic acid. Further work on the measurement of soil acidity and sucrose inversion was reported by Parker and Bryan (14) in 1923 and by Puri and Dua (10) in 1938. In 1946, Sussman (15) reported the inversion of sucrose by Zeo-karb H, a sulfonated coal, but gave no quantitative data.

Mariani (1,2) reported studies of the inversion of sucrose catalyzed by the hydrogen form of the cation exchange resin Amberlite IR-100, a sulfonic resin of the phenolic type. Mariani found that resin particle size influenced the rate of inversion

markedly-- finer mesh resin giving a more rapid reaction-- and concluded that the rate of diffusion of sucrose into the resin particle was an important factor in controlling the rate of inversion.

Bodamer and Kunin (3) studied the effectiveness of various cation exchange resins for the inversion of sucrose. They studied the variables of resin particle size, cross-linka e of the resin copolymer, and temperature. They found marked effects of particle size on the reaction rate constant. The sulfonic exchanger used in the study were commercially available sulfonated styrene type ion exchange resin Amberlite IR-120 as well as several modifications differing in porosity. The carboxylic resins were commercially available Amberlite IRC-50 and a more porous analog.

Table 2.1

Effect of Porosity on Reactivity of Resin Catalyst (3)

Temperature	$K \times 10^4$			Activation Energy cal/mol
	25^0C	50^0C	75^0C	
Resin porosity, % Cross-linkage				
1 - Sulfonic Type	7.6	199.2	-	25,800
4 - Sulfonic Type	5.2	110.3	-	24,200
10- Sulfonic Type	0.7	26.3	117.0	27,600
15- Sulfonic Type	-	3.0	48.6	25,100
20- Sulfonic Type	-	0.7	23.2	31,600
1 - Carboxylic	-	-	50.0[a]	-
2 - Carboxylic	-	-	9.0	25,900

[a]at 100^0C.

Table 2.1 summarizes their findings on the effect of porosity and temperature on reaction constant and energy of activation. While these results show definite trends in activity as a function of porosity, the accuracy of the measurements was such that no consistent correlation exists between resin porosity and activation energy. The values obtained are somewhat lower than those reported for homogeneous catalysis and this may indicate that diffusional resistances are controlling to such a degree that the energies cannot be compared directly. Since the inversion is only pseudo-first order, the methods of interpretation are open to some question.

Most of the published works on sucrose inversion by ion exchange were performed using the stirring test and involving quite highly dilute solutions. Siegers and Martinola (5) studied inversion of sucrose solutions with strongly acidic cation exchange resins. The conditions selected were similar to the practical conditions encountered in sugar refineries. They studied the variables of resin particle size, temperature and sucrose concentration and also compared gel type resins with varying degrees of cross-linking with macroporous exchange resins. They found that rate constant decreases from 0.054 min^{-1} to 0.036 min^{-1} with increasing bead diameter from 0.4 mm to 0.85 mm at 40^0C for 60^0 Brix, which is a result expected for a resin. The rate constant also tripled between 40^0C and 70^0C from 0.039 min^{-1} to 0.125 min^{-1} for 0.76 mm bead size for 60^0 Brix. They also found an increase in the rate constant between 30^0 and 50^0 Brix from 0.034 to 0.045 min^{-1} although it ceased to rise for 60^0 Brix where rate constant was 0.44 min^{-1}.

Recently Ananda and Rauha (16) studied inversion of 40% sucrose solution with a strongly acidic cation exchange resin in a packed column. The resin used was styrene type with 8% divinyl benzene cross-linking, however, the brand name has not been mentioned. They found that the rate of inversion decreased with increasing particle size and feed flow rate. The over-all rate constant decreased from 0.042 to 0.023 min^{-1} for resin size 0.46 mm to 0.80 mm at 45^0C. Apparent activation energy varied from 20.6 to 17.3 Kcal/mol for the same particle range. The true rate constant varied from 0.023 to 0.35 min^{-1} in the temperature range 35 to 65^0C, and the true activation energy was 24.97 Kcal/mol. Distribution co-efficient was around 1.5 and diffusivity varied from $7x10^{-9}$ to $50x10^{-9}$ cm^2/sec in the temperature range of 35 to 65^0C.

2.2.2 Behaviour of different ion exchanger

Most works on sucrose inversion by ion exchange were done on gel-type resins with a cross-linking of about 8% divinyl benzene. Gilliand and others (4) mentioned the use of a macroporous cation exchange resin with a high degree of cross-linking, but without specifying precise details. This resin proved inferior to the gel-type resins cross-linked with 8% DVB. Sieger and Martinola (5) compared gel-type resins with varying degrees of cross-linking with macroporous exchange resins. From the plot of rate constant as a function of the degree of cross linking, they found that a higher level of cross linking considerably impedes the inversion reaction. Between the gel type and macroporous resin, the latter one is slightly superior, especially at elevated degree of crosslinking.

Inner surface or pore diameter, determined according to BET, have only a minor effect compared to the influence of cross-linkage. They also concluded from the results of Gilliand and others(4) that the macroporous resin used there consisted of highly crosslinked beads regarding the faster reaction of the gel type resins.

2.2.3   SECONDARY REACTIONS DURING INVERSION

One undesirable phenomenon accompanying acid hydrolysis of sucrose is the formation of hydroxymethylfurfural (HMF). This slightly yellowish compound with an extinction maximum at 283 nm is difficult to remove and gives the evaporated liquid sugar an unpleasant colour. Siegers and Martinola (5) found that at 40^0C HMF formation was nearly zero but at 70^0C it was 3.5 g/lit solution. Consequently, the inversion rate cannot be increased at will be raising the temperature.

CHAPTER-3

THEORETICAL BACKGROUND

CHAPTER-3

THEORETICAL BACKGROUND

Inversion of sucrose is a pseudo-first order irreversible reaction.

$$C_{12}H_{22}O_{11} \quad + \quad H_2O \quad \xrightarrow{\quad H^+ \quad} \quad C_6H_{12}O_6 \quad + \quad C_6H_{12}O_6$$

Sucrose $\hspace{6cm}$ Glucose $\hspace{1cm}$ Fructose
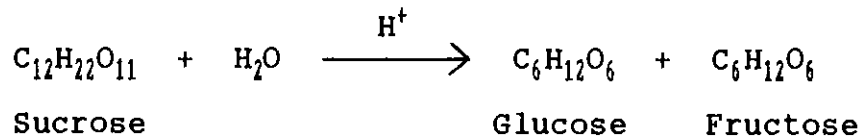
rate,

$$- \frac{dQ_A}{dt} = kQ_A \qquad \ldots \qquad \ldots \qquad (3.1)$$

where,

$\quad Q_A$ = amount of sucrose in moles

$\quad t$ = time

$\quad k$ = rate constant

In concentration term the above equation becomes:

$$- \frac{dC_A}{dt} = kC_A \qquad \ldots \qquad \ldots \qquad (3.2)$$

In a solid phase, there is a difference between the kinetics of the actual chemical reaction at the catalytically active site and the kinetics of the over-all process which includes diffusion of the reactants and products to and from the active site. The rate of the over-all process can be computed when the rate of actual chemical reaction and other data such as diffusion co-efficients of the reactants and products, etc. are known.

3.1 REACTION MECHANISM IN ION EXCHANGE RESIN

The pores of an ion exchange resin which is in contact with a solution contain solvent, solutes, and counter ions. The counter ions are mobile and solvated and thus in a condition which is, in principle, not different from that in a corresponding homogeneous solution. It can therefore be expected that counter ions which display catalytic activity in homogeneous solutions are equally active in the pores of a resin, and that the reaction mechanism in homogeneous catalysis by a dissolved electrolyte and heterogeneous catalysis by a resin is essentially the same. These conclusions are reasonably well confirmed by experimental observations which show that the order of the actual chemical reaction is the same in both cases and that the activation energy is similar (17).

3.2 THE RATE-DETERMINING STEP

In order for the reaction to occur, reactant molecules must migrate from the solution into the ion exchanger and must react; the reaction products must then migrate back into the solution. The mass transfer in the bulk solution is effected by agitation or solution flow and is fast as compared with any other step, so that concentration differences in the bulk solution

Figure 3.1: Resin-catalyzed reaction A --> B + C

are instantaneously leveled out. However, the catalyst particles are surrounded by an adherent liquid layer, called film, across

which mass transfer can occur by diffusion only. Thus three phenomena can affect the rate of the over-all process:

Diffusion of reactants and products across the film

Diffusion of reactants and products in the interior of the catalyst particle

The actual chemical reaction at the active sites.

If film diffusion is much slower than the chemical reaction, it must obviously be rate controlling since, in this limiting case, all reactant molecules react as soon as they reach the surface of the catalyst particle (Fig. 3.2, bottom). If the chemical reaction
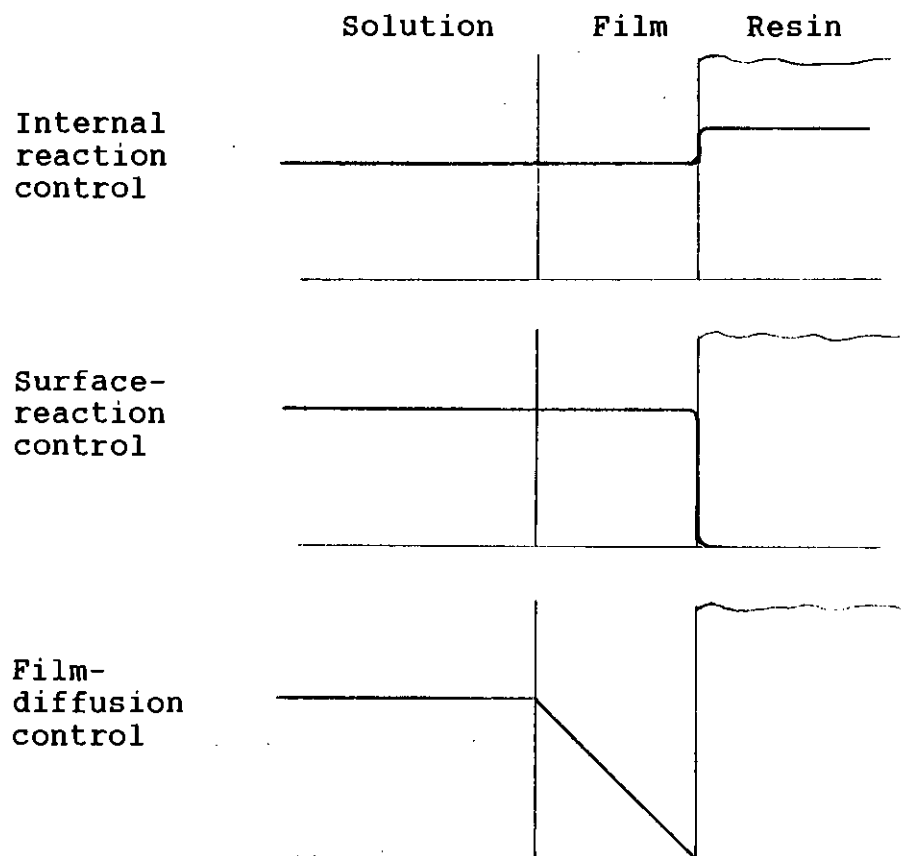
Figure 3.2: Concentration profiles of the reactant in a first-order, irreversible reaction with rate control by internal reaction (top), surface reaction (middle), and film diffusion (bottom).

is much slower than the diffusion processes, sorption equilibrium of the reactants is established and upheld throughout the catalyst particle since diffusion is fast enough to make up for the disappearance of reactants by chemical reaction (Fig. 3.2, top). The overall rate thus is controlled by the rate of the chemical reaction throughout the particle. If intraparticle diffusion is much slower than the chemical reaction, the reactant molecules will react before they have time to penetrate into the interior of the catalyst particle. In this latter limiting case, the reaction occurs only in a thin layer at the particle surface, and its rate is controlled by either film diffusion or chemical reaction at the surface (Fig. 3.2, middle), whichever of these two processes is the slower one. These considerations show that, in the three limiting cases, the overall rate is controlled by:

Film diffusion

Chemical reaction throughout the particles

Chemical reaction at the particle surfaces.

Intermediate cases arise if the rates of the individual steps are comparable.

The rate of the internal chemical reaction (with a given amount of catalyst) is independent of the resin particle size, whereas the rates of both film diffusion and surface reaction are proportional to the resin surface area. Smaller particle size thus favors internal reaction control. Film diffusion obviously is rate controlling if it is slower than the surface reaction. This situation is exceptional and can only arise if the chemical reaction is very fast.

In publication of experimental results it has often been stated that the over-all rate depends on the particle size of the catalyst (3,15,18,19). However, the detailed investigations by Hammett and Collaborators (18,20), who also carried out comparative measurements with superficially sulfonated resin particles, show strong evidence that the overall rate is controlled by a combination of intraparticle reaction and intraparticle diffusion. Unambiguous evidence for exclusive rate control by film diffusion or surface reaction has so far not been reported (17).

3.3 DIFFUSION IN A SINGLE PARTICLE

Consider a first-order reaction occurring on the spherical catalyst particle of radius r_0.
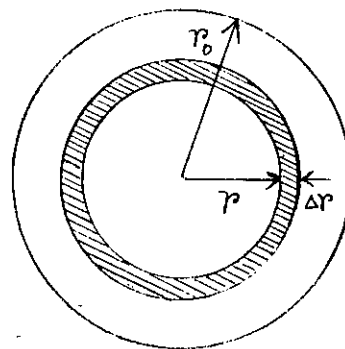
Figure 3.3: Mass balance on a spherical particle.

The mass balance equation is

$$\frac{d}{dr} \left(r^2 D_{eff} \frac{dc}{dr} \right) - \bar{k} c r^2 = 0 \qquad \cdots \qquad (3.3)$$

B.C.s are:

1. at $r = r_0$, $c = c_0$

2. at $r = 0$, $\frac{dc}{dr} = 0$

Define a Thiele type modulus W as

$$W = r_o (\frac{\bar{k}}{D_{eff}})^{\frac{1}{2}} \qquad (3.4)$$

Equation (3.3) becomes

$$\frac{d^2c}{dr^2} + \frac{2}{r} \frac{dc}{dr} - (\frac{W}{r_o})^2 c = 0 \qquad (3.5)$$

The solution of this equation is well known (21) and is given by

$$\frac{c}{c_o} = \frac{r_o}{r} \frac{\sinh (Wr/r_o)}{\sinh W} \qquad (3.6)$$

At steady-state,

Observed rate = Diffusion rate

$$r_{obs} = 4\pi r_0^2 D_{eff} (\frac{dc}{dr})_{r=r_0}$$

$$r_{obs} = 4\pi r_0 D_{eff} c_0 W (\frac{1}{\tanh W} - \frac{1}{W})$$

If the entire active volume of the spherical particle were exposed to reactant at a concentration c_0, then the intrinsic rate

$$r_i = (\frac{4}{3} \pi r_o^3) \bar{k} c_o$$

So effectiveness factor

$$\eta = \frac{r_{obs}}{r_i}$$

$$\eta = \frac{3}{W}\left(\frac{1}{\tanh W} - \frac{1}{W}\right) \qquad (3.7)$$

Effectiveness factor (η) is a function of the Thiele modulus

(W) only. Effectiveness factor indicates the degree of catalyst utilization. Figure 3.4 shows the relation between effectiveness factor and Thiele modulus.

For W >15 equation (3.7) reduces to

$$(\eta) \quad = 3/W \qquad\qquad (3.8)$$
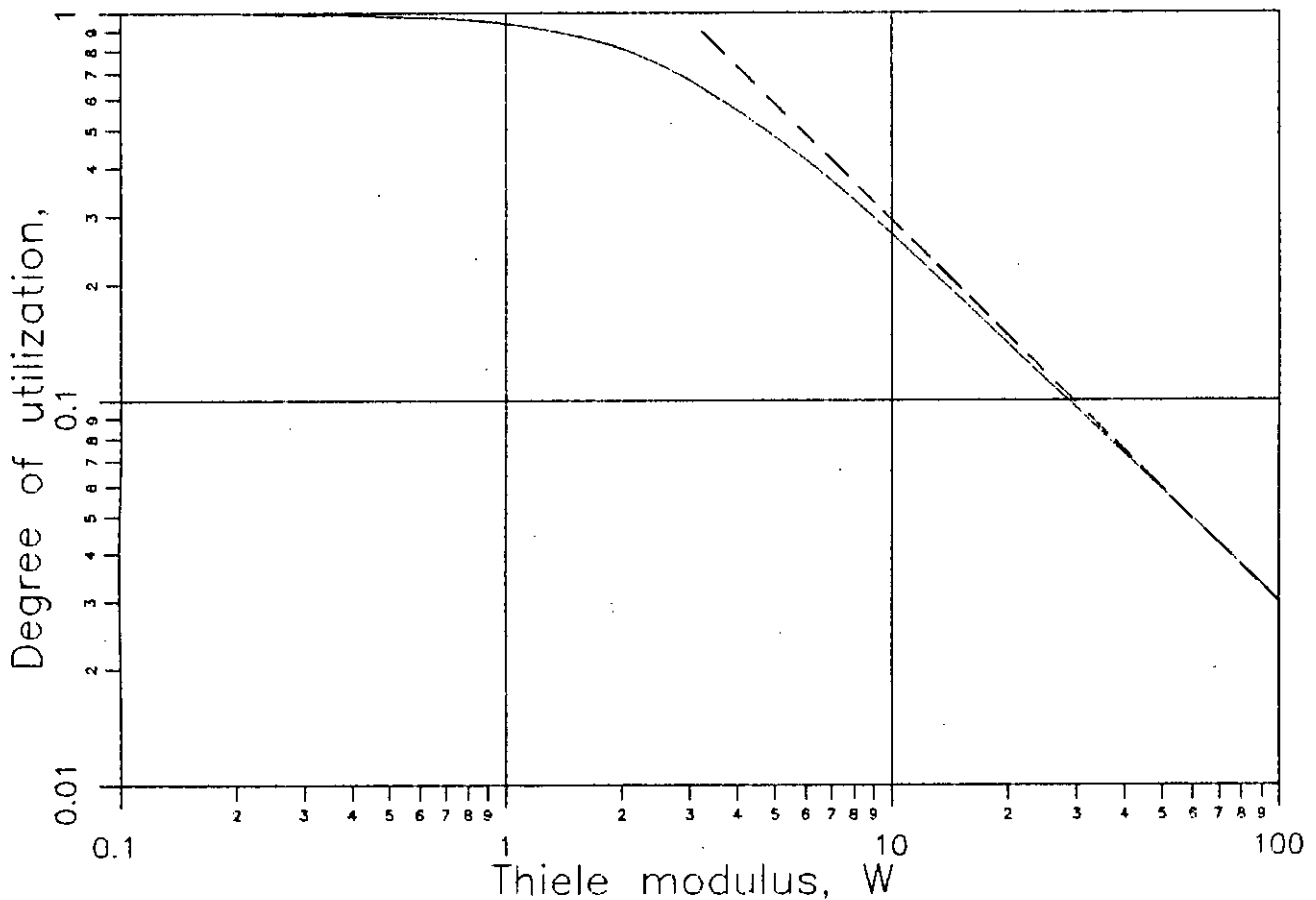
Figure 3.4: Degree of catalyst utilization as a function of the Thiele modulus, for a first—order irreversible reaction. The broken line is for the relation $\eta = 3/W$, which is approached at high values of the Thiele modulus.

Combining equation (3.4) and (3.8)

$$\eta = \frac{3}{r_o(\overline{k}/D_{eff})^{\frac{1}{2}}}$$

Multiplying both sides with kλ

$$\overline{k}\lambda\eta = \frac{3\overline{k}\lambda}{r_o(\frac{\overline{k}}{D_{eff}})^{\frac{1}{2}}} = \frac{3(\overline{k}\,D_{eff})^{\frac{1}{2}}\lambda}{r_o}$$

$$\log\,(\overline{k}\lambda\eta) = \log\,(3(\overline{k}\,D_{eff})^{\frac{1}{2}}\,\lambda\,) - \log\,r_o \qquad (3.9)$$

Equation (3.9) shows that a log-log plot of $\overline{k}\lambda\eta$ vs. r_0 will give a straight line of slope -1 and intercept $3(\overline{k}D_{eff})^{1/2}\lambda$.

3.4 INTERNAL REACTION CONTROL

With internal reaction control, sorption equilibrium of the reactant A between the resin and the solution is rapidly established and is maintained throughout the process.

Thus

$$\overline{C}_A = \lambda_A C_A \qquad (3.10)$$

The molar distribution coefficient λ_A of the reactant is assumed to be constant. The chemical reaction occurs only within the resin, and the concentration of the reactant in the resin is uniform. The rate law equation 3.1 can then be written as

$$- d\widetilde{Q}_A = \overline{k}\overline{Q}_A = \overline{k}\,\lambda_A C_A V \qquad (3.11)$$

where,

V = total volume of the catalyst

$\overline{k}$ = rate constant of the reaction in the catalyst

$\widetilde{Q}_A = (\overline{Q}_A + Q_A)$ = total amount of reactant

$\overline{Q}_A$ = amount of reactant in catalyst

Q_A = amount of reactant in solution.

3.5 COLUMN OPERATION

The reaction can be carried out in a continuous operation in which the solution is passed through a fixed-bed of catalyst in a column. A steady state in the bed is attained, provided that the feed composition and the flow rate are kept constant. In the steady state, the solution concentration in any layer normal to the column axis remains constant, and so does the reaction rate in the layer.
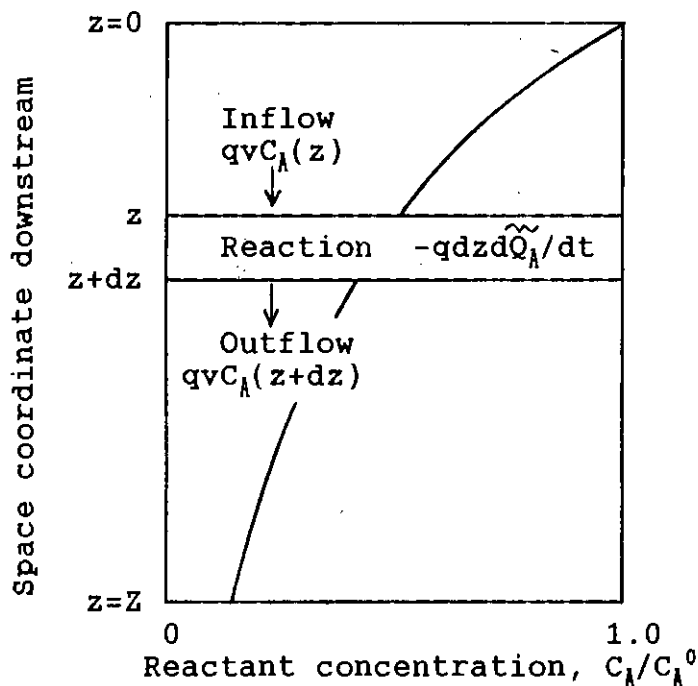
Figure 3.5: Steady-state axial concentration profile of the reactant in continuous operation with a fixed catalyst bed, and material balance in a layer of the bed.

A material balance in an arbitrary layer between z and z+dz (z = space co-ordinate in direction of column axis) can be set up by equating inflow minus outflow of the reactant to the amount which reacts in the layer. Neglecting longitudinal diffusion and temperature effects one can write

$$qvC_A(z) - qvC_A(z+dz) = qdz(1-\beta)\overline{k} \lambda_A C_A \qquad (3.12)$$

inflow   outflow   amount reacting

where,

q = column cross-section

v = Linear flow rate (solution volume per unit time and unit bed cross-section)

β = fractional void volume of the bed.

This gives

$$\frac{dC_A}{dz} = - \overline{k} \lambda_A C_A \frac{1 - \beta}{v} \qquad (3.13)$$

Integration of this equation with the initial condition

$$z = 0 , \quad C_A(0) = C_A^0$$

gives the axial concentration profile of the reactant in the column

$$C_A(z) = C_A^0 \exp(-\overline{k} \lambda_A \frac{1 - \beta}{v} z) \qquad (3.14)$$

The concentrations in the effluent of a column are obtained from equation (3.14) by replacing z by the bed length Z.

Then

$$\frac{Z}{v} = t = \text{space time}$$

and equation (3.14) becomes

$$C_A(z) = C_A^0 \exp(-\overline{k} \lambda_A (1 - \beta)t) \qquad (3.15)$$

3.6 EFFECT OF INTRAPARTICLE DIFFUSION

Slow intraparticle diffusion may reduce the overall rate, especially if the reactant molecules are large and thus have a low mobility in the resin catalyst. In such cases, sorption equilibrium of the reactant is not attained since a substantial fraction of the molecules react before they can reach the center of the particle. The catalyst is not fully utilized since the catalytically active ions in the particle centers rarely see a reactant molecule and thus remain essentially useless. In the limiting case of extremely slow particle diffusion, the reaction occurs only in a thin layer at the particle surface.

In a continuously operated column, a steady-state is attained. Accordingly, the intraparticle concentration profiles in any layer of the column become time-independent and can be expressed as a function of the solution concentration, $C_A(z)$, in the layer. The axial concentration profiles and the effluent concentration can be derived in exactly the same way as in the case of internal reaction control. The only difference in the calculations and results is that the product $\eta.z$ appears instead of z :

$$C_A(z) = C_A^{0}\exp(-\overline{k}\lambda_A \frac{(1 - \beta)}{v}\eta z) \qquad (3.16)$$

For effluent concentration, z becomes Z (column length) then,

$$\frac{Z}{v} = t = \text{space time}$$

and equation (3.16) becomes

$$\frac{C_A(Z)}{C_A^{0}} = \exp(-\overline{k}\lambda_A(1 - \beta)\eta t) \qquad (3.17)$$

3.7 EFFECT OF FILM DIFFUSION RESISTANCE

When film diffusion resistance becomes important, the gradient of concentration in the film is to be taken into account. In this case, the right hand side in Eq. (3.12) must be expressed in terms of interfacial concentration C_{Ai} instead of bulk concentration, C_A. Eq. (3.13) will be then modified as follows:

$$\frac{dC_A}{dz} = -\bar{k}\,\lambda_A C_{Ai}\,\frac{(1-\beta)}{v} = \frac{-3k_L(1-\beta)}{vr_0}\,(C_A - C_{Ai}) \qquad (3.18)$$

Equating the middle and right hand terms in Eq. (3.18), the interfacial concentration can be expressed as

$$C_{Ai} = \frac{C_A}{1 + \dfrac{\bar{k}\,\lambda_A r_0}{3\,k_L}} \qquad (3.19)$$

Replacing C_{Ai} from the middle term in Eq. (3.18) by Eq. (3.19), the mass balance equation may be readily integrated to yield

$$\frac{C_A(z)}{C_A^0} = \exp\frac{-(\bar{k}\,\lambda_A(1-\beta)t)}{1 + \dfrac{\bar{k}\,\lambda_A r_0}{3\,K_L}} \qquad (3.20)$$

It may be seen that when film diffusion control is not important i.e. when the value of mass transfer co-efficient, k_L is high $\bar{k}\,\lambda_A r_0/3k_L \ll 1$ and Eq. (3.20) reduces to Eq. (3.17).

CHAPTER-4

EXPERIMENTAL SET-UP
AND
METHOD OF EXPERIMENT

CHAPTER-4

EXPERIMENTAL SET-UP AND METHOD OF EXPERIMENT

4.1 GENERAL ARRANGEMENT OF THE EXPERIMENTAL SET-UP

A flow diagram of the experimental set-up is shown in figure 4.1. The cation exchange resin was placed in a 1/2 inch borosilicate glass column fitted with sintered glass bottom and a bottom valve with PTFE stem. A scale was glued to the outside of this column to measure the bed height which varied slightly with solution concentration.

The column was jacketed with a 3 inch glass tube and water from a thermostatic bath was circulated through the jacket. A thermometer was placed in the jacket to measure the temperature.

A rectangular tank made of polymethylmethacrylate was used as feed tank in this experiment. The feed tank was placed at a height from the resin bed such that gravity head was sufficient for required solution flow through the resin bed.

Two rotameters, one for measuring low flow rates and the other for higher flow rates, connected in series, were used to control and to monitor steadiness of solution flow.

Different units of the experimental set-up were interconnected with PVC tubings.

Optical rotation of the samples taken from the column outlet was measured by a polarimeter. Each sample was cooled to 30^0C and the rotation readings was taken at that temperature. A separate thermostatic bath was used for this purpose.

From optical rotation readings, the percent inversion was calculated by using calibration curves. The calibration method is described in appendix C.

4.2 RESIN PREPARATION FOR EXPERIMENTS

The resin was supplied in sodium form. Wet sieving was done with ASTM standard sieves in tap water to separate the resin beads into different cuts according to their diameters. Each portion of the separated resin was wet sieved many times, and by rejecting oversizes and undersizes, one cut of resin with very uniform diameter was obtained.

Each cut of resin was then aged by converting it repeatedly into hydrogen form and then into sodium form. 2N commercial hydrochloric acid and 2N sodium chloride solution were used for this purpose. The cycle was repeated for about 10 times over a few days.

Each resin cut was then converted to hydrogen form by washing with 2N hydrochloric acid solution. Excess acid was washed out with distilled water. The resin was wet sieved again, this time by using distilled water, and a final cut of resin was obtained by rejecting oversizes and undersizes.

The final cut of resin was taken in a glass column and washed with 1N analytical grade hydrochloric acid solution. Acid washing was done slowly by using at least 15 times of the theoretical acid requirement and continued for more than 24 hours to ensure compete removal of all cations. The resin was then washed thoroughly with deionized distilled water until the effluent water conductivity was

close to that of the feed water. 60 ml. (free settled) of this resin was measured out and used in the experiment.

4.3 EXPERIMENTAL RUN

Solution of specified concentration was prepared by using analytical grade sucrose and deionized distilled water and taken in the feed tank. During start-up, the resin column and all lines were filled with solution and air bubbles were removed. The feed solution and the resin column were heated to the specified temperature. Flow rate through the resin bed was controlled and monitored by using the rotameters.

After steady state temperature and flow rate were reached, sample was collected from the outlet of the resin bed and taken to a thermostatic bath maintained at 30^0C. After the sample had reached 30^0C, its optical rotation was measured quickly. Measurements for different samples were continued until steady optical readings were obtained. The flow rate was then changed and the procedure repeated.

During sampling interval, the flow rate was measured by collecting outlet solution in a measuring cylinder for a definite period of time. During a single set of reading the flow rate was kept steady by monitoring it on the rotameters.

The solution flow rate was changed from low to high values for a fixed temperature. The experiment was repeated for five different temperatures for each resin size and solution concentration. Five different resin sizes and three solution concentrations were used.
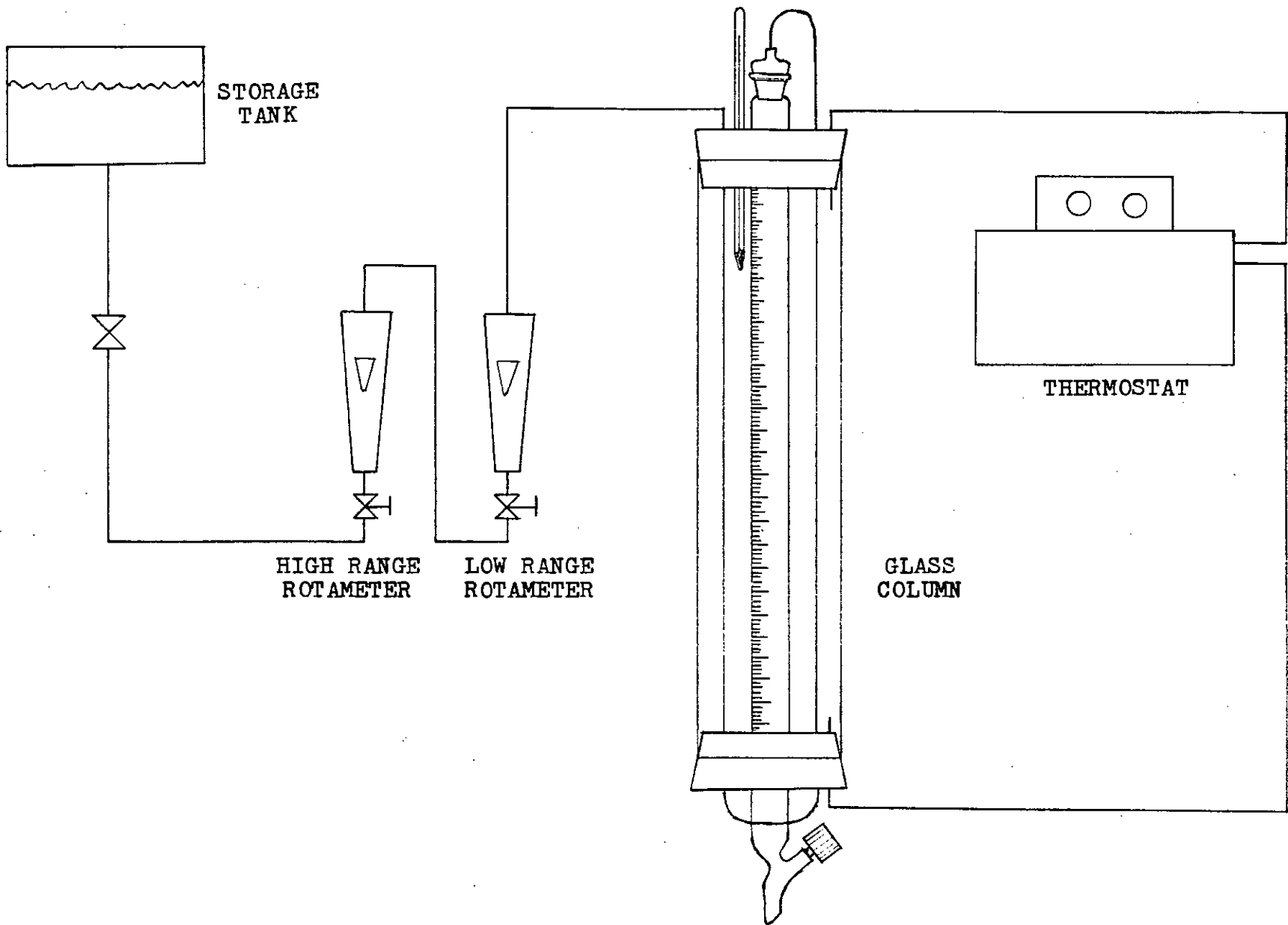
FIGURE 4.1 : SCHEMATIC FLOW DIAGRAM OF THE EXPERIMENTAL SET-UP

STORAGE TANK

HIGH RANGE ROTAMETER

LOW RANGE ROTAMETER

GLASS COLUMN

THERMOSTAT

CHAPTER-5

RESULTS
AND
DISCUSSIONS

CHAPTER-5

RESULTS AND DISCUSSIONS

Catalytic inversion of sucrose solution has been studied in a column packed with strongly acidic cation exchange resin. The resin used was Duolite C-20, a commercially available gel-type resin with 8% divinyl benzene cross-linking. The variable studied were: reaction temperature (30-70^{0}C); feed flow rate (0.9-26 ml/min), feed concentration (20-40%) and resin particle diameter (0.362-1.09 mm). Detailed description of the experimental set-up and method of experiment have been described in Chapter 4. Percent inversion of sucrose solution was measured with a calibrated polarimeter. The calibration procedure has been described in Appendix C.

The measured values of percent inversion of sucrose solutions of different concentrations at different temperatures and flow rates for a specified resin particle size are presented in Table A.1.1 to A.3.5 and plotted in Figure B.1.1 to B.3.5. The curves shown in Figure B.1.1 to B.3.5 show a consistent pattern. Inversion of sucrose is favoured at higher space-time i.e. lower velocity and higher temperature and this is expected. Conversion also increases with decreasing particle size. As the size decreases the specific surface area and hence interfacial mass transfer area increases. In addition the resistance to diffusion decreases as the particles becomes smaller. The effect of particle size is however, more pronounced at higher temperature. As the temperature increases rate of chemical reaction increases rapidly. At the same time resistance

to diffusion is also lowered significantly. Inversion is also favoured as the concentration of solution increases. This is because reaction rate is high at high concentration. The effect of different variables on reaction rate can be best explained when fundamental kinetic and mass transfer data are available and this will be done in the following sections.

Residual sucrose concentrations are plotted against space-time for different feed concentrations and resin sizes with temperature as a parameter in Figure B.4.1 to B.6.5. It may be seen from these Figure that at low values of space-time the data fall on a straight line. As the space-time increases the data deviate from straight line and in most instances the experimental data lie above the straight lines correlating the low space-time data points.

The reason why the lower space-time data in Figure B.4.1 to B.6.5 fall on a straight line can be explained in terms of rate determining factor. Lower values of space-time mean higher velocities and thus film diffusion would be less important as the space-time decreases. Eq. (3.17) gives the concentration profile in a packed bed for a first order reaction (as in the present case) neglecting film diffusion resistance. In this case the overall rate is controlled by a combination of intraparticle reaction and intraparticle diffusion. For this case the residual sucrose concentration vs space-time would lie in a straight line in a semi-log plot. As space-time increases i.e. as the velocity decreases, the effect of film diffusion control cannot be neglected. The onset of the effect of film diffusion depends on particle size, temperature and solution concentration. The effect is more

pronounced at low temperatures and for larger particle sizes. The importance of film diffusion is most evident at a space-time above 40-50 min but this can also be observed at about 20 min in some cases.

The slopes of the straight lines in Figure B.4.1 to B.6.5 give the values of the over-all rate constant, $\bar{k}\lambda\eta$. This follows from the above argument and Eq. (3.17). These over-all rate constants are presented in Table A.4.1 to A.6.5. The over-all rate constant, expresses the combined effect of reaction and diffusion as indicated by the terms $\bar{k}$ and $\lambda\eta$ respectively. The constant λ connects the bulk liquid phase concentration and interfacial resin phase concentration as given in Eq. (3.10).

In order to extract intrinsic rate data, diffusion co-efficient and distribution co-efficient from the over-all data it will be helpful to consider Eq. (3.9) given for a single particle when the Thiele modulus, W>15. It may be seen that when w>15, values of over-all rate constant vs resin particle radius in log-log plots would give straight lines of slope-1.

Since $W = r_0\,(\bar{k}/d_{eff})^{1/2}$ one cannot say a prior the value of r_0 for which W>15 as both $\bar{k}$ and D_{eff} are unknown. However, as W is directly proportional to r_0, it is expected that over-all rate constant for the larger particle sizes would be correlated as discussed above. These plots are shown in Figure B.7.1 to B.7.3 and it is clear that for particle size above 0.04 cm the data lie on a straight line having a slope of -1. Thus the accuracy of overall rate constant data can be checked for the larger size particles.

These over-all rate constant and the corresponding resin radius values which gave straight line in the above plot were subjected to non-linear regression analysis along with equation (3.9) to estimate the parameters λ_e, k and D_{eff}. An available programme was used for this purpose.

It may appear that the regression analysis has been unduly restrictive since in most cases only three data points corresponding to W>15 have been used instead of the entire set for a given temperature. This is because the accuracy of the data in this range can be checked as explained above. In the alternative case if all the data points are used some uncertainty is introduced in the regression analysis. This uncertainty is easily avoided by considering data for higher particle radius only. A regression analysis with all the data points give values of distribution co-efficients which are difficult to explain and hence this was not done.

Estimated values of distribution co-efficient, specific rate constant and effective diffusivity at different temperatures and solution concentrations are presented in Table A.7 to A.9 and plotted in Figure B.8 to B.10.

Variation of intrinsic rate with temperature and the variation of over-all rate with temperature for different resin sizes and different concentrations are plotted in Figure B.11 to B.14. From these plots activation energy and Arrhenius constant were found for the intrinsic rate as well as for the over-all rates. These values are presented in Table A.10 and plotted in Figure B.15 and B.16.

5.1 OVER-ALL RATE

Over-all rate values at different temperatures and solution concentrations are presented in Table A.4.1 to A.6.5. The over-all rate involves diffusion as well as the intrinsic chemical reaction and for obvious reasons increases with temperatures. This is the usual behaviour of chemical reaction with diffusion.

For a given concentration, the over-all rate decreases with increasing particle size. As a typical case, at 50^0C and for 30% sucrose solution the over-all rate decreases from 0.10252 to 0.04419 min^{-1} for resin diameter of 0.362 to 1.09 mm. This indicate that diffusional resistances play a strong role in the over-all process.

Table A.4.1 to A.6.5 show that the over-all rate increases with solution concentration. For example, at 50^0C and for 0.78 mm resin diameter the over-all rates are 0.5061, 0.6043 and 0.647 min^{-1} for 20, 30 and 40% sucrose solutions respectively. Similar observation has been reported earlier by Siegers and Martinola (5).

5.2 SPECIFIC AND INTRINSIC RATE CONSTANTS

As mentioned earlier, specific rate constant values were estimated from the over-all rate values by regression analysis. These values are presented in Table A.7 to A.9 and plotted in Figure B.9. For a given temperature the specific rate constant increases linearly with solution concentration. Extrapolating these values to zero concentration, the intrinsic rate constants at different temperatures were obtained. These values are 0.0075,

0.031, 0.11, 0.293 and 0.563 min^{-1} for 30, 40, 50, 60 and 70^{0}C respectively.

5.3 DISTRIBUTION CO-EFFICIENT AND EFFECTIVE DIFFUSIVITY

Values of distribution co-efficient and effective diffusivity at different temperatures for different solution concentrations are presented in Table A.7 to A.9 and plotted in Figure B.8 and B.10. Most of the distribution co-efficient values are close to 1.0 and deviate slightly with temperature and concentration.

Effective diffusivity increases slowly with increasing concentration and increases rapidly with temperature. At 50^{0}C the diffusivity values are 5.976 x 10^{-8}, 6.768 x 10^{-8} and 7.147 x 10^{-8} cm^2/sec for 20, 30 and 40% solutions respectively. For 30% sucrose solution diffusivity increases from 3.826 x 10^{-8} to 18.951 x 10^{-8} cm^2/sec for the temperature range of 30 to 70^{0}C. The increase of diffusivity from 60 to 70^{0}C is very rapid and the value at 70^{0}C is about twice that of at 60^{0}C. As a rule the increase in mobility with temperature is somewhat greater in ion exchangers than in ordinary aqueous solution. The activation energy of diffusion is about 6-10 kcal/mole, as compared to 3-6 kcal/mole in solution. Likely explanations are that as temperature increases, resin phase interactions become weaker and the matrix becomes flexible. It may be noted that the recommended maximum operating temperature for cation resin of the type used in the experiments is about 100^{0}C.

A further factor may be that at high temperature, the reaction rate is high enough to control the mass transfer rate. In this case reaction occurs in a thin shell at the surface of the particle and

diffusion is not important. In this case evaluation of diffusion coefficient at high temperature by the present method would be suspect.

5.4 ACTIVATION ENERGY AND ARRHENIUS CONSTANT

Temperature dependence of intrinsic rate constant is expressed by Arrhenius equation $k=Ae^{-(B/RT)}$. In the present case the observed over-all rate also obey similar relationship and an "apparent" activation energy can be obtained along with intrinsic rate.

Activation energy and Arrhenius constant for the intrinsic rate was found to be 24.93 kcal/g.mol and 7.66×10^{-15} min^{-1} respectively from Figure B.1.1. The value of activation energy is close to the published value of 25.8 kcal/g.mole for inversion of sucrose by acid in a homogeneous system (22).

Apparent activation energy and Arrhenius constant for the over-all rate for different resin diameters and solution concentrations were found from Figure B.12 to B.14. These values are presented in Table A.10 and plotted in Figure B.15 and B.16. Both apparent activation energy and Arrhenius constant decrease with increasing solution concentration and resin diameter. For higher values of resin diameter the apparent activation energy approaches a value of about 14-15 kcal/mol and the reason for this is explained below.

If the over-all rate is affected by diffusion, the apparent activation energy differs from that of the chemical reaction. With rate limitation by intraparticle diffusion, the apparent activation energy is a crossbreed between those of diffusion and of the

chemical reaction. As a rule, the activation energy of intraparticle diffusion is of the order of 6-10 kcal/g.mol and is usually lower than that of the chemical reaction. In the limiting case of strong diffusion limitation (W>15), the apparent activation energy approaches the arithmetic mean of those of reaction and diffusion (17):

$$E_{app} = 1/2 \ (E + E_{diff}).$$

The validity of the above equation can be checked by estimating E_{diff} for the present case. This may be estimated from the Arrhenius equation for diffusion which is given by

$$D_{eff} = A_{diff} \ exp \ (-E_{diff}/RT)$$

Table B.17 shows a plot of D_{eff} against 1/T for three different concentrations. The activation energy given by the slopes of these curves correspond to about 6 kcal/mole. It should be noted that when correlating, the data at 70^0C have been neglected, as these show a marked deviation from the other data. It has been explained that at this temperature the mass transfer rate may be controlled by reaction at the surface and that intraparticle diffusion is of no consequence.

The value of E for chemical reaction has been estimated to be about 25 kcal/mole and hence E_{app} is about 15 kcal/mole. This may be seen in Figure B.15 where the asymptotic values for higher particle sizes correspond to limiting case of activation energy under strong diffusional limitation.

5.5 EFFECT OF FILM DIFFUSION CONTROL

It has been mentioned earlier that as space-time increases i.e. as the flow rate decreases, the effect of film diffusion resistance to mass transfer become more noticeable. This may be seen by examining the Figure B.4.1 to B.6.5. It has been explained that when film diffusion resistance can be neglected, the data in the above figures would lie in a straight line. When this resistance cannot be neglected, the total mass transfer resistance would increase and thereby inversion of sucrose would decrease.

The quantitative prediction of film diffusion effect from theoretical or empirical considerations is not possible in the present case. Literature on mass and heat transfer in packed and fluidized beds are essentially for Newtonian fluids and mass transfer data are usually expressed as

$$Sh = C_1 / \beta \; Re_p^m \; Sc^n$$

where,

$$Sh = \frac{K_L D_p}{D} \qquad Re_p = \frac{D_p V \rho}{\mu} \qquad \text{and} \qquad Sc = \frac{\mu}{\rho D}$$

Usually the values of $C_1 = 0.81$, $m = 0.5$ and $n = 0.33$. The limitation of the above correlation for a highly viscous system is obvious. In addition the relevant physical properties are not available for sucrose-glucose-fructose system for the evaluation of the above dimensionless groups.

It is, however, possible to calculate the mass transfer coefficient from experimental data using Eq.(3.20). Already k, and λ have been estimated and using these values in Eq. (3.20), the liquid film mass transfer coefficient, K_L, can be calculated. A few typical values of K_L are shown in Table A.11. It may be seen from

these values that the K_L values are of the order of 10^{-5} cm/sec, whereas typical values for Newtonian fluids in packed bed of ion exchange resins are of the order of 10^{-3} cm/sec. A difference of the order of two orders of magnitude indicate that mass transfer data for the present system cannot possibly be correlated by existing correlations. No attempt was, however, made to correlate the present data because of lack of viscosity and diffusion coefficient data in the fluid phase. It should be noted that physical properties of the fluid vary along the length of the bed and this should be taken into consideration in correlating mass transfer data.

CHAPTER-6

CONCLUSIONS
AND
SUGGESTIONS

CHAPTER-6

CONCLUSIONS AND SUGGESTIONS

6.1 CONCLUSIONS

The present study on inversion of sucrose solution with strongly acidic cation exchange resin (Duolite C-20) leads to the following conclusions:

1) Inversion of sucrose decreases with increasing flow rate and resin particle size and increases with increasing temperature.

2) Over-all rate ($\overline{k}\lambda\eta$) increases with increasing temperature and solution concentration and decreases with increasing resin particle size.

3) Distribution co-efficient for the system is around 1.0.

4) Specific rate constant increases with increasing concentration

5) Effective diffusivity increases with increasing temperature. The change in diffusivity value is very rapid in the temperature range 60 to 70^{0}C.

6) Apparent activation energy and Arrhenius constant decreases with increasing resin particle size and solution concentration and approach a constant value for large particle size.

7) Mass transfer co-efficient in the liquid film is of the order of 10^{-5} cm/sec.

6.2 <u>SUGGESTIONS FOR FUTURE WORK</u>

The following suggestions can be put forward for future investigations:

1) Experiments may be carried out by varying the degree of crosslinking of the resin beads.

2) Experiments may be carried out by using macroporous resins.

3) Investigations may be done to find the effect of the presence of other cations in the feed solution or by using partially regenerated resins.

4) Studies may be carried out for the catalyst life in this system, especially at higher temperatures.

REFERENCES

1.   Mariani, E., *Ann. Chim Applicata*, 39, 283-90 (1949).

2.   Mariani, E., *Ibid*, 40, 1-12 (1950).

3.   Bodamer, G., and R.Kunin, *Ind. Eng. Chem.* 43, 1082-85 (1951).

4.   Gilliand, E.R., H.J.Bixler, and J.E.O`Connell, *Ind. Eng. Chem. Fundam.* 10, No.2, 185-191 (1971).

5.   Siegers, G., and F.Martinola, monograph "Extensive Inversion of Sucrose Solutions with Strongly Acidic Cation Exchange Resins", Bayer AG, OC Division, Leverkusen, 1984.

6.   McGarvey, F.X., and R.Kunin, in "Ion Exchange Technology", p.272, F.C.Nachod and J.Schubert (eds.), Academic Press, Inc., New York, 1956.

7.   Jaeger, F.M., *Trans. Faraday Soc.* 25, 320-45 (1929), "On the constitution and Structure of Ultramarine".

8.   Rice, F.E., and S.Osugi, Soil Sci., 5, 333-58 (1918).

9.   Puri, A.N., and A.G.Asghar, *Soil Sci.*, 45, 359-67 (1938), "Titration Curves and Dissociation Constants of Soil Acidoids".

10. Puri, A.N., and A.N.Dua, *Soil Sci.*, 46, 113-28 (1938).

11. Thomas, G.G., *Ind. Eng. Chem.*, 41, 2564 (1949).

12. Tacke, B., and H.Suchting, *Landw. Jahrb.*, 41, 717-54 (1911).

13. Hanley, J.A., *J. Agr. Sci.*, 6, 63-76 (1914).

14. Parker, F.W., and O.C.Bryan, *Soil Sci.*, 15, 99-107 (1923).

15. Sussman, S., *Ind. Eng. Chem.*, 38, 1228-30 (1946).

16. Ananda, M.M., and T.R.Rauha, B.Sc.Engg.Thesis, Chem. Engg. Dept., Bangladesh Univ. of Engg. and Technology (1991).

17. Helfferich, F., "Ion Exchange", McGraw-Hill Book Company, Inc., New York, 1962.

18. Bernhard, S.A., and L.P.Hammett, *J. Am. Chem. Soc.*, 75, 1798 (1953).

19. Levesque, C.L., and A.M.Craig, *Ind. Eng. Chem.*, 40, 96 (1946).

20. Haskell, V.C., and L.P.Hammett, *J. Am. Chem. Soc.*, 17, 1284 (1949).

21. Bird, R.B., W.E.Stewart, and E.N.Lightfoot, "Transport Phenomena", p.542, John Wiley & Sons, Inc., New York, 1960.

22. Moore, W.J., "Physical Chemistry", p.299, 3rd ed., Prentice-Hall, Inc., Englewood Cliffs, N.J., 1962.

APPENDIX-A

TABLES

TABLE NO. A.1: <u>EXPERIMENTAL DATA ON PERCENT INVERSION OF 20%</u>
<u>SUCROSE SOLUTION AT DIFFERENT TEMPERATURES AND</u>
<u>FLOW RATES</u>

<u>TABLE NO. A.1.1</u>

Diameter of resin bead : 1.09 mm
Sucrose concentration in feed solution : 20%
Bed volume : 58.74 ml

Tempe-rature (^0C)	Volumetric flow rate (ml/min)	Optical rotation (degree)	Percent inversion (x)	Space time (min)	Residual sucrose (100-x)
30	1.30	10.75	19.51	45.18	80.49
	3.30	12.70	8.79	17.80	91.21
	5.70	13.45	4.67	10.31	95.33
	10.00	13.80	2.75	5.87	97.25
40	1.25	6.70	41.76	46.99	58.24
	2.80	10.65	20.05	20.98	79.95
	5.40	12.20	11.54	10.88	88.46
	9.20	13.05	6.87	6.38	93.13
	13.40	13.55	4.12	4.38	95.88
50	1.26	2.90	62.64	46.62	37.36
	3.10	8.15	33.79	18.95	66.21
	5.80	10.50	20.88	10.13	79.12
	9.20	11.95	12.91	6.38	87.09
	13.70	12.80	8.24	4.29	91.76
60	1.20	-0.50	81.32	48.95	18.68
	4.40	6.30	43.96	13.35	56.04
	8.90	9.35	27.20	6.60	72.80
	13.00	10.95	18.41	4.52	81.59
	16.70	11.65	14.56	3.52	85.44
70	1.20	-3.05	95.33	48.95	4.67
	2.85	-0.25	79.95	20.61	20.05
	5.10	2.40	65.38	11.52	34.62
	8.50	5.50	48.35	6.91	51.65
	12.70	7.80	35.71	4.63	64.29
	17.00	9.40	26.92	3.46	73.08

TABLE NO. A.1.2

Diameter of resin bead   : 0.925 mm
Sucrose concentration in feed solution : 20%
Bed volume   : 59.29 ml

Tempe-rature (^{0}C)	Volumetric flow rate (ml/min)	Optical rotation (degree)	Percent inversion (x)	Space time (min)	Residual sucrose (100-x)
30	1.12	10.20	22.53	52.94	77.47
	2.90	12.10	12.09	20.44	87.91
	7.40	13.50	4.40	8.01	95.60
	11.20	13.80	2.75	5.29	97.25
40	1.08	5.70	47.25	54.90	52.75
	3.30	10.25	22.25	17.97	77.75
	7.20	12.40	10.44	8.23	89.56
	10.40	13.05	6.87	5.70	93.13
	14.00	13.45	4.67	4.24	95.33
50	1.15	1.75	68.96	51.56	31.04
	2.80	6.65	42.03	21.18	57.97
	6.00	10.15	22.80	9.88	77.20
	9.80	11.75	14.01	6.05	85.99
	13.70	12.40	10.44	4.33	89.56
60	1.35	-1.85	88.74	43.92	11.26
	3.20	2.60	64.29	18.53	35.71
	6.00	6.50	42.86	9.88	57.14
	11.80	10.00	23.63	5.02	76.37
	18.00	11.40	15.93	3.29	84.07
70	3.00	-1.50	86.81	19.76	13.19
	6.50	2.80	63.19	9.12	36.81
	11.00	6.15	44.78	5.39	55.22
	16.00	8.50	31.87	3.71	68.13
	18.30	9.25	27.75	3.24	72.25

TABLE NO. A.1.3

Diameter of resin bead   : 0.78 mm
Sucrose concentration in feed solution : 20%
Bed volume   : 59.29 ml

Tempe-rature (^{0}C)	Volumetric flow rate (ml/min)	Optical rotation (degree)	Percent inversion (x)	Space time (min)	Residual sucrose (100-x)
30	1.66	10.75	19.51	35.72	80.49
	3.60	12.35	10.71	16.47	89.29
	6.80	13.35	5.22	8.72	94.78
	12.00	13.75	3.02	4.94	96.98
40	1.08	5.15	50.27	54.90	49.73
	2.45	8.50	31.87	24.20	68.13
	4.50	11.00	18.13	13.18	81.87
	7.70	12.35	10.71	7.70	89.29
	11.50	13.05	6.87	5.16	93.13
	16.20	13.50	4.40	3.66	95.60
50	1.05	0.20	77.47	56.47	22.53
	3.00	5.55	48.08	19.76	51.92
	6.33	9.75	25.00	9.37	75.00
	10.80	11.50	15.38	5.49	84.62
	16.00	12.35	10.71	3.71	89.29
60	1.20	-3.25	96.43	49.41	3.57
	2.70	0.70	74.73	21.96	25.27
	6.50	6.05	45.33	9.12	54.67
	12.00	9.50	26.37	4.94	73.63
	16.80	10.70	19.78	3.53	80.22
70	2.80	-2.80	93.96	21.18	6.04
	6.30	1.40	70.88	9.41	29.12
	10.10	3.90	57.14	5.87	42.86
	13.00	6.55	42.58	4.56	57.42
	17.00	8.00	34.62	3.49	65.38

TABLE NO. A.1.4

Diameter of resin bead   : 0.55 mm
Sucrose concentration in feed solution : 20%
Bed volume   : 58.56 ml

Tempe-rature (^{0}C)	Volumetric flow rate (ml/min)	Optical rotation (degree)	Percent inversion (x)	Space time (min)	Residual sucrose (100-x)
30	1.20	10.00	23.63	48.80	76.37
	2.50	11.35	16.21	23.42	83.79
	5.00	12.80	8.24	11.71	91.76
	8.20	13.50	4.40	7.14	95.60
40	1.40	4.75	52.47	41.83	47.53
	3.30	8.65	31.04	17.75	68.96
	4.60	10.10	23.08	12.73	76.92
	8.20	12.05	12.36	7.14	87.64
	12.60	12.90	7.69	4.65	92.31
50	1.70	1.10	72.53	34.45	27.47
	5.40	7.90	35.16	10.84	64.84
	7.70	9.55	26.10	7.61	73.90
	11.30	10.85	18.96	5.18	81.04
	16.60	11.85	13.46	3.53	86.54
60	2.05	-2.15	90.38	28.57	9.62
	4.70	1.95	67.86	12.46	32.14
	7.40	4.95	51.37	7.91	48.63
	10.20	7.00	40.11	5.74	59.89
	13.70	8.60	31.32	4.27	68.68
	20.30	10.40	21.43	2.88	78.57
70	2.80	-3.20	96.15	20.91	3.85
	4.70	-1.00	84.07	12.46	15.93
	8.70	2.10	67.03	6.73	32.97
	14.20	4.95	51.37	4.12	48.63
	20.00	6.70	41.76	2.93	58.24

TABLE NO. A.1.5

Diameter of resin bead   : 0.362 mm
Sucrose concentration in feed solution : 20%
Bed volume   : 59.48 ml

Tempe-rature (^{0}C)	Volumetric flow rate (ml/min)	Optical rotation (degree)	Percent inversion (x)	Space time (min)	Residual sucrose (100-x)
30	0.96	9.50	26.37	61.96	73.63
	1.90	10.15	22.80	31.31	77.20
	2.67	11.40	15.93	22.28	84.07
	5.60	12.90	7.69	10.62	92.31
	9.00	13.55	4.12	6.61	95.88
40	0.90	2.50	64.84	66.09	35.16
	3.00	7.70	36.26	19.83	63.74
	5.90	10.55	20.60	10.08	79.40
	9.60	12.10	12.09	6.20	87.91
	13.70	12.70	8.79	4.34	91.21
50	1.15	-2.60	92.86	51.72	7.14
	3.20	2.75	63.46	18.59	36.54
	7.20	7.35	38.19	8.26	61.81
	11.80	9.85	24.45	5.04	75.55
	17.80	11.30	16.48	3.34	83.52
60	4.70	0.15	77.75	12.66	22.25
	9.00	4.05	56.32	6.61	43.68
	12.60	6.30	43.96	4.72	56.04
	19.00	8.60	31.32	3.13	68.68
	25.00	10.00	23.63	2.38	76.37
70	6.80	-0.85	83.24	8.75	16.76
	11.10	2.15	66.76	5.36	33.24
	16.00	4.10	56.04	3.72	43.96
	21.20	5.60	47.80	2.81	52.20
	26.00	6.30	43.96	2.29	56.04

TABLE NO. A.2: <u>EXPERIMENTAL DATA ON PERCENT INVERSION OF 30%</u>
<u>SUCROSE SOLUTION AT DIFFERENT TEMPERATURES AND</u>
<u>FLOW RATES</u>

<u>TABLE NO. A.2.1</u>

Diameter of resin bead   : 1.09 mm
Sucrose concentration in feed solution : 30%
Bed volume   : 57.64 ml

Temperature (^{0}C)	Volumetric flow rate (ml/min)	Optical rotation (degree)	Percent inversion (x)	Space time (min)	Residual sucrose (100-x)
30	1.00	15.15	25.13	57.64	74.87
	2.55	18.80	12.39	22.60	87.61
	5.50	20.60	6.11	10.48	93.89
	10.50	21.55	2.79	5.49	97.21
40	1.15	9.50	44.85	50.12	55.15
	3.40	16.35	20.94	16.95	79.06
	5.80	18.90	12.04	9.94	87.96
	9.20	20.20	7.50	6.27	92.50
	13.60	20.90	5.06	4.24	94.94
50	1.30	2.85	68.06	44.34	31.94
	3.20	11.30	38.57	18.01	61.43
	6.50	16.65	19.90	8.87	80.10
	10.60	18.80	12.39	5.44	87.61
	16.50	19.80	8.90	3.49	91.10
60	1.40	-1.80	84.29	41.17	15.71
	3.70	5.40	59.16	15.58	40.84
	6.40	10.85	40.14	9.01	59.86
	10.00	14.80	26.35	5.76	73.65
	14.20	16.90	19.02	4.06	80.98
	20.00	18.05	15.01	2.88	84.99
70	3.30	-1.05	81.68	17.47	18.32
	6.67	5.75	57.94	8.64	42.06
	11.40	11.10	39.27	5.06	60.73
	15.40	13.35	31.41	3.74	68.59
	21.80	14.80	26.35	2.64	73.65

TABLE NO. A.2.2

Diameter of resin bead   : 0.925 mm
Sucrose concentration in feed solution : 30%
Bed volume   : 58.19 ml

Tempe-rature (^{0}C)	Volumetric flow rate (ml/min)	Optical rotation (degree)	Percent inversion (x)	Space time (min)	Residual sucrose (100-x)
30	0.90	14.00	29.14	64.66	70.86
	3.50	18.85	12.22	16.63	87.78
	5.20	20.05	8.03	11.19	91.97
	9.40	21.20	4.01	6.19	95.99
40	1.15	8.45	48.52	50.60	51.48
	3.20	15.40	24.26	18.18	75.74
	6.40	18.75	12.57	9.09	87.43
	9.20	19.80	8.90	6.33	91.10
	13.00	20.55	6.28	4.48	93.72
50	1.37	2.00	71.03	42.47	28.97
	3.90	10.70	40.66	14.92	59.34
	7.00	15.95	22.34	8.31	77.66
	10.70	18.00	15.18	5.44	84.82
	14.00	18.95	11.87	4.16	88.13
60	1.53	-2.50	86.74	38.03	13.26
	3.80	4.25	63.18	15.31	36.82
	6.80	10.50	41.36	8.56	58.64
	10.40	14.20	28.45	5.60	71.55
	14.60	16.20	21.47	3.99	78.53
70	4.10	-0.95	81.33	14.19	18.67
	7.20	4.80	61.26	8.08	38.74
	11.00	9.20	45.90	5.29	54.10
	14.70	11.70	37.17	3.96	62.83
	19.00	13.00	32.64	3.06	67.36

TABLE NO. A.2.3

Diameter of resin bead   : 0.78 mm
Sucrose concentration in feed solution : 30%
Bed volume   : 58.74 ml

Tempe-rature (°C)	Volumetric flow rate (ml/min)	Optical rotation (degree)	Percent inversion (x)	Space time (min)	Residual sucrose (100-x)
30	1.30	14.30	28.10	45.18	71.90
	3.70	18.85	12.22	15.88	87.78
	8.10	20.85	5.24	7.25	94.76
	11.00	21.25	3.84	5.34	96.16
40	1.28	8.05	49.91	45.89	50.09
	3.40	14.65	26.88	17.28	73.12
	6.50	18.00	15.18	9.04	84.82
	11.00	19.90	8.55	5.34	91.45
50	1.26	0.60	75.92	46.62	24.08
	3.80	9.50	44.85	15.46	55.15
	6.40	14.30	28.10	9.18	71.90
	11.00	17.25	17.80	5.34	82.20
60	1.30	-4.05	92.15	45.18	7.85
	3.40	2.10	70.68	17.28	29.32
	6.70	9.00	46.60	8.77	53.40
	11.50	13.55	30.72	5.11	69.28
	14.25	15.05	25.48	4.12	74.52
70	3.30	-3.05	88.66	17.80	11.34
	6.33	2.65	68.76	9.28	31.24
	10.60	7.00	53.58	5.54	46.42
	16.00	10.15	42.58	3.67	57.42
	20.40	11.40	38.22	2.88	61.78

TABLE NO. A.2.4

Diameter of resin bead   : 0.55 mm
Sucrose concentration in feed solution : 30%
Bed volume   : 57.83 ml

Tempe-rature (^{0}C)	Volumetric flow rate (ml/min)	Optical rotation (degree)	Percent inversion (x)	Space time (min)	Residual sucrose (100-x)
30	1.62	14.05	28.97	35.70	71.03
	4.50	18.80	12.39	12.85	87.61
	8.20	20.60	6.11	7.05	93.89
	12.10	21.20	4.01	4.78	95.99
40	1.50	6.45	55.50	38.55	44.50
	3.80	13.55	30.72	15.22	69.28
	7.50	17.75	16.06	7.71	83.94
	11.80	19.55	9.77	4.90	90.23
	16.40	20.35	6.98	3.53	93.02
50	1.50	-1.15	82.02	38.55	17.98
	4.10	7.70	51.13	14.10	48.87
	7.70	13.85	29.67	7.51	70.33
	11.40	16.45	20.59	5.07	79.41
	16.30	18.05	15.01	3.55	84.99
60	2.04	-4.05	92.15	28.35	7.85
	4.50	1.95	71.20	12.85	28.80
	8.20	8.00	50.09	7.05	49.91
	12.25	11.90	36.47	4.72	63.53
	16.75	14.35	27.92	3.45	72.08
	22.00	16.00	22.16	2.63	77.84
70	4.90	-3.00	88.48	11.80	11.52
	8.20	1.55	72.60	7.05	27.40
	12.40	5.85	57.59	4.66	42.41
	16.30	8.25	49.21	3.55	50.79
	21.10	10.20	42.41	2.74	57.59

TABLE NO. A.2.5

Diameter of resin bead			:	0.362 mm
Sucrose concentration in feed solution			:	30%
Bed volume			:	58.56 ml

Tempe-rature (^{0}C)	Volumetric flow rate (ml/min)	Optical rotation (degree)	Percent inversion (x)	Space time (min)	Residual sucrose (100-x)
30	1.60	13.35	31.41	36.60	68.59
	3.90	18.05	15.01	15.02	84.99
	7.60	20.10	7.85	7.71	92.15
	12.00	21.00	4.71	4.88	95.29
40	1.72	4.95	60.73	34.05	39.27
	4.30	13.50	30.89	13.62	69.11
	7.90	17.25	17.80	7.41	82.20
	12.30	19.10	11.34	4.76	88.66
	17.00	20.05	8.03	3.44	91.97
50	1.68	-2.70	87.43	34.86	12.57
	5.30	8.05	49.91	11.05	50.09
	8.80	12.50	34.38	6.65	65.62
	13.40	15.70	23.21	4.37	76.79
	19.80	17.75	16.06	2.96	83.94
60	3.00	-4.45	93.54	19.52	6.46
	5.70	1.05	74.35	10.27	25.65
	10.00	6.25	56.20	5.86	43.80
	14.80	10.40	41.71	3.96	58.29
	20.50	13.30	31.59	2.86	68.41
	25.80	15.20	24.96	2.27	75.04
70	3.85	-5.55	97.38	15.21	2.62
	7.30	-2.05	85.17	8.02	14.83
	11.20	1.10	74.17	5.23	25.83
	16.80	5.00	60.56	3.49	39.44
	22.00	7.95	50.26	2.66	49.74

TABLE NO. A.3: <u>EXPERIMENTAL DATA ON PERCENT INVERSION OF 40%</u>
<u>SUCROSE SOLUTION AT DIFFERENT TEMPERATURES AND</u>
<u>FLOW RATES</u>

<u>TABLE NO. A.3.1</u>

Diameter of resin bead : 1.09 mm
Sucrose concentration in feed solution : 40 Brix
Bed volume : 56.91 ml

Temperature (^{0}C)	Volumetric flow rate (ml/min)	Optical rotation (degree)	Percent inversion (x)	Space time (min)	Residual sucrose (100-x)
30	0.90	19.10	29.80	63.23	70.20
	2.80	24.95	15.21	20.33	84.79
	5.20	28.30	6.86	10.94	93.14
	7.80	29.25	4.49	7.30	95.51
40	0.92	8.40	56.48	61.86	43.52
	2.35	18.45	31.42	24.22	68.58
	5.00	24.80	15.59	11.38	84.41
	7.75	27.25	9.48	7.34	90.52
	15.60	29.20	4.61	3.65	95.39
50	0.92	-0.45	78.55	61.86	21.45
	2.80	14.50	41.27	20.33	58.73
	5.10	20.15	27.18	11.16	72.82
	8.10	23.80	18.08	7.03	81.92
	14.20	26.90	10.35	4.01	89.65
60	2.70	0.50	76.18	21.08	23.82
	5.00	11.35	49.13	11.38	50.87
	7.70	17.10	34.79	7.39	65.21
	10.40	20.70	25.81	5.47	74.19
	15.00	23.15	19.70	3.79	80.30
	20.20	24.10	17.33	2.82	82.67
70	3.03	-4.35	88.28	18.78	11.72
	5.00	2.55	71.07	11.38	28.93
	8.50	10.30	51.75	6.70	48.25
	11.20	13.80	43.02	5.08	56.98
	14.25	15.85	37.91	3.99	62.09
	19.90	18.15	32.17	2.86	67.83

TABLE NO. A.3.2

Diameter of resin bead   : 0.925 ml
Sucrose concentration in feed solution : 40%
Bed volume   : 57.46 ml

Tempe-rature (^{0}C)	Volumetric flow rate (ml/min)	Optical rotation (degree)	Percent inversion (x)	Space time (min)	Residual sucrose (100-x)
	0.92	18.30	31.80	62.46	68.20
30	2.25	22.40	21.57	25.54	78.43
	4.70	27.05	9.97	12.23	90.03
	8.20	29.10	4.86	7.01	95.14
	0.94	7.45	58.85	61.13	41.15
	2.10	14.35	41.65	27.36	58.35
40	4.60	22.90	20.32	12.49	79.68
	7.50	26.50	11.35	7.66	88.65
	11.30	27.70	8.35	5.08	91.65
	0.92	-2.05	82.54	62.46	17.46
	2.60	9.00	54.99	22.10	45.01
50	4.20	15.80	38.03	13.68	61.97
	7.20	21.75	23.19	7.98	76.81
	12.00	25.05	14.96	4.79	85.04
	2.60	-1.10	80.17	22.10	19.83
	4.70	8.45	56.36	12.23	43.64
60	7.40	14.50	41.27	7.76	58.73
	12.20	20.20	27.06	4.71	72.94
	19.00	23.05	19.95	3.02	80.05
	3.60	-3.55	86.28	15.96	13.72
	6.00	2.80	70.45	9.58	29.55
70	9.20	8.85	55.36	6.25	44.64
	14.20	13.80	43.02	4.05	56.98
	20.40	16.75	35.66	2.82	64.34

TABLE NO. A.3.3

```
 Diameter of resin bead                      : 0.78 mm
 Sucrose concentration in feed solution : 40%
 Bed volume                                  : 58.19 ml
```

Tempe-rature (^{0}C)	Volumetric flow rate (ml/min)	Optical rotation (degree)	Percent inversion (x)	Space time (min)	Residual sucrose (100-x)
30	0.98	17.50	33.79	59.38	66.21
	2.20	21.70	23.32	26.45	76.68
	4.00	25.65	13.47	14.55	86.53
	6.70	28.15	7.23	8.69	92.77
	8.80	28.90	5.36	6.61	94.64
40	0.94	5.80	62.97	61.90	37.03
	2.25	13.55	43.64	25.86	56.36
	4.20	20.40	26.56	13.85	73.44
	6.80	25.10	14.84	8.56	85.16
	9.30	26.55	11.22	6.26	88.78
50	1.05	-2.95	84.79	55.42	15.21
	2.60	5.85	62.84	22.38	37.16
	5.30	16.90	35.29	10.98	64.71
	7.30	20.25	26.93	7.97	73.07
	9.50	22.40	21.57	6.13	78.43
60	2.60	-2.60	83.92	22.38	16.08
	5.10	7.30	59.23	11.41	40.77
	8.70	13.80	43.02	6.69	56.98
	14.25	19.40	29.05	4.08	70.95
	19.80	21.75	23.19	2.94	76.81
70	5.60	-0.20	77.93	10.39	22.07
	7.80	4.20	66.96	7.46	33.04
	12.70	10.80	50.50	4.58	49.50
	20.30	15.55	38.65	2.87	61.35

TABLE NO. A.3.4

Diameter of resin bead   : 0.55 mm
Sucrose concentration in feed solution : 40%
Bed volume   : 57.46 ml

Tempe-rature (°C)	Volumetric flow rate (ml/min)	Optical rotation (degree)	Percent inversion (x)	Space time (min)	Residual sucrose (100-x)
30	1.27	16.85	35.41	45.24	64.59
	2.80	22.10	22.32	20.52	77.68
	4.86	25.55	13.72	11.82	86.28
	7.90	27.40	9.10	7.27	90.90
	10.50	28.40	6.61	5.47	93.39
40	1.15	4.60	65.96	49.97	34.04
	3.00	14.70	40.77	19.15	59.23
	5.90	22.00	22.57	9.74	77.43
	9.00	25.00	15.09	6.38	84.91
	12.40	26.35	11.72	4.63	88.28
50	1.50	-3.95	87.28	38.31	12.72
	2.90	4.45	66.33	19.81	33.67
	5.20	13.10	44.76	11.05	55.24
	8.40	18.75	30.67	6.84	69.33
	11.60	21.70	23.32	4.95	76.68
60	3.50	-2.60	83.92	16.42	16.08
	5.60	4.00	67.46	10.26	32.54
	9.40	11.35	49.13	6.11	50.87
	12.20	15.05	39.90	4.71	60.10
	15.40	17.45	33.92	3.73	66.08
	19.80	19.70	28.30	2.90	71.70
70	5.80	-3.10	85.16	9.91	14.84
	8.80	1.95	72.57	6.53	27.43
	12.30	6.35	61.60	4.67	38.40
	15.40	9.80	52.99	3.73	47.01
	20.00	13.20	44.51	2.87	55.49
	23.40	15.00	40.02	2.46	59.98

TABLE NO. A.3.5

Diameter of resin bead   : 0.362 mm
Sucrose concentration in feed solution : 40%
Bed volume   : 57.64 ml

Tempe- rature (^{0}C)	Volumetric flow rate (ml/min)	Optical rotation (degree)	Percent inversion (x)	Space time (min)	Residual sucrose (100-x)
30	1.34	15.25	39.40	43.01	60.60
	2.60	20.55	26.18	22.17	73.82
	4.20	23.80	18.08	13.72	81.92
	8.40	26.85	10.47	6.86	89.53
40	1.55	3.15	69.58	37.19	30.42
	2.95	11.95	47.63	19.54	52.37
	6.10	20.55	26.18	9.45	73.82
	9.00	23.80	18.08	6.40	81.92
	13.00	25.90	12.84	4.43	87.16
50	1.62	-5.40	90.90	35.58	9.10
	2.90	2.05	72.32	19.88	27.68
	5.80	10.25	51.87	9.94	48.13
	9.60	16.55	36.16	6.00	63.84
	14.00	20.45	26.43	4.12	73.57
60	2.25	-8.45	98.50	25.62	1.50
	4.00	-3.70	86.66	14.41	13.34
	7.20	3.25	69.33	8.01	30.67
	10.20	7.65	58.35	5.65	41.65
	14.50	12.50	46.26	3.98	53.74
	18.40	15.45	38.90	3.13	61.10
70	5.40	-7.45	96.01	10.67	3.99
	8.40	-3.40	85.91	6.86	14.09
	11.30	0.10	77.18	5.10	22.82
	15.50	4.35	66.58	3.72	33.42
	21.00	8.90	55.24	2.74	44.76
	25.00	11.75	48.13	2.31	51.87

TABLE NO. A.4: <u>OVER-ALL RATE CONSTANT OF 20% SUCROSE SOLUTION AT DIFFERENT TEMPERATURES</u>

<u>TABLE NO. A.4.1</u>

Diameter of resin bead   : 1.09 mm
Sucrose solution concentration : 20%

Temperature (^{0}C)	Slope $K\lambda\eta(1-\beta)$ (min^{-1})	Overall rate constant $K\lambda\eta$ (min^{-1})
30	0.005215	0.00869
40	0.011234	0.01872
50	0.021890	0.03648
60	0.043861	0.07310
70	0.091191	0.15199

<u>TABLE NO. A.4.2</u>

Diameter of resin bead   : 0.925 mm
Sucrose solution concentration : 20%

Temperature (^{0}C)	Slope $K\lambda\eta(1-\beta)$ (min^{-1})	Overall rate constant $K\lambda\eta$ (min^{-1})
30	0.005945	0.00991
40	0.013676	0.02279
50	0.025547	0.04258
60	0.053130	0.08855
70	0.106600	0.17767

TABLE NO. A.4.3

Diameter of resin bead   : 0.78 mm
Sucrose solution concentration : 20%

Temperature (^{0}C)	Slope $K\lambda\eta\,(1-\beta)$ (min^{-1})	Overall rate constant $K\lambda\eta$ (min^{-1})
30	0.006427	0.01071
40	0.015744	0.02624
50	0.030367	0.05061
60	0.061607	0.10268
70	0.123130	0.20522

TABLE NO. A.4.4

Diameter of resin bead   : 0.55 mm
Sucrose solution concentration : 20%

Temperature (^{0}C)	Slope $K\lambda\eta\,(1-\beta)$ (min^{-1})	Overall rate constant $K\lambda\eta$ (min^{-1})
30	0.007144	0.01191
40	0.020406	0.03401
50	0.039107	0.06518
60	0.086239	0.14373
70	0.167460	0.27910

TABLE NO. A.4.5

Diameter of resin bead   : 0.362 mm
Sucrose solution concentration : 20%

Temperature (^{0}C)	Slope $K\lambda\eta(1-\beta)$ (min^{-1})	Overall rate constant $K\lambda\eta$ (min^{-1})
30	0.007512	0.01252
40	0.023091	0.03848
50	0.054790	0.09132
60	0.119615	0.19936
70	0.224640	0.37440

TABLE NO. A.5: <u>OVER-ALL RATE CONSTANT OF 30% SUCROSE SOLUTION</u>
<u>AT DIFFERENT TEMPERATURES</u>

<u>TABLE NO. A.5.1</u>

Diameter of resin bead   : 1.09 mm
Sucrose solution concentration : 30%

Temperature (^{0}C)	Slope $K\lambda\eta\,(1-\beta)$ (min^{-1})	Overall rate constant $K\lambda\eta$ (min^{-1})
30	0.005819	0.00970
40	0.013090	0.02182
50	0.026515	0.04419
60	0.055308	0.09218
70	0.101435	0.16906

<u>TABLE NO. A.5.2</u>

Diameter of resin bead   : 0.925 mm
Sucrose solution concentration : 30%

Temperature (^{0}C)	Slope $K\lambda\eta\,(1-\beta)$ (min^{-1})	Overall rate constant $K\lambda\eta$ (min^{-1})
30	0.007063	0.01177
40	0.015744	0.02624
50	0.030951	0.05158
60	0.063714	0.10619
70	0.119305	0.19884

TABLE NO. A.5.3

Diameter of resin bead : 0.78 mm
Sucrose solution concentration : 30%

Temperature (^{0}C)	Slope $K\lambda\eta (1-\beta)$ (min^{-1})	Overall rate constant $K\lambda\eta$ (min^{-1})
30	0.007775	0.01296
40	0.018523	0.03087
50	0.036261	0.06043
60	0.071284	0.11881
70	0.144820	0.24136

TABLE NO. A.5.4

Diameter of resin bead : 0.55 mm
Sucrose solution concentration : 30%

Temperature (^{0}C)	Slope $K\lambda\eta (1-\beta)$ (min^{-1})	Overall rate constant $K\lambda\eta$ (min^{-1})
30	0.009425	0.01571
40	0.023224	0.03871
50	0.046650	0.07775
60	0.092103	0.15351
70	0.191880	0.31980

TABLE NO. A.5.5

Diameter of resin bead   : 0.362 mm
Sucrose solution concentration : 30%

Temperature (^{0}C)	Slope $K\lambda\eta(1-\beta)$ (min^{-1})	Overall rate constant $K\lambda\eta$ (min^{-1})
30	0.010193	0.01699
40	0.027654	0.04609
50	0.061510	0.10252
60	0.137468	0.22911
70	0.261660	0.43610

TABLE NO. A.6: <u>OVER-ALL RATE CONSTANT OF 40% SUCROSE SOLUTION AT DIFFERENT TEMPERATURES</u>

<u>TABLE NO. A.6.1</u>

Diameter of resin bead   : 1.09 mm
Sucrose solution concentration : 40%

Temperature (°C)	Slope $K\lambda\eta(1-\beta)$ (min^{-1})	Overall rate constant $K\lambda\eta$ (min^{-1})
30	0.007403	0.01234
40	0.015452	0.02575
50	0.029263	0.04877
60	0.063714	0.10619
70	0.113989	0.18998

<u>TABLE NO. A.6.2</u>

Diameter of resin bead   : 0.925 mm
Sucrose solution concentration : 40%

Temperature (°C)	Slope $K\lambda\eta(1-\beta)$ (min^{-1})	Overall rate constant $K\lambda\eta$ (min^{-1})
30	0.008884	0.01481
40	0.018523	0.03087
50	0.033862	0.05644
60	0.072637	0.12106
70	0.135450	0.22574

TABLE NO. A.6.3

Diameter of resin bead   : 0.78 mm
Sucrose solution concentration : 40%

Temperature (°C)	Slope $K\lambda\eta(1-\beta)$ (min^{-1})	Overall rate constant $K\lambda\eta$ (min^{-1})
30	0.009824	0.01637
40	0.021384	0.03564
50	0.038821	0.06470
60	0.084499	0.14083
70	0.153510	0.25584

TABLE NO. A.6.4

Diameter of resin bead   : 0.55 mm
Sucrose solution concentration : 40%

Temperature (°C)	Slope $K\lambda\eta(1-\beta)$ (min^{-1})	Overall rate constant $K\lambda\eta$ (min^{-1})
30	0.012118	0.02020
40	0.027186	0.04531
50	0.054790	0.09132
60	0.110968	0.18495
70	0.204670	0.34112

TABLE NO. A.6.5

Diameter of resin bead : 0.362 mm
Sucrose solution concentration : 40%

Temperature (^0C)	Slope $K\lambda\eta(1-\beta)$ (min^{-1})	Overall rate constant $K\lambda\eta$ (min^{-1})
30	0.014032	0.02339
40	0.033036	0.05506
50	0.069775	0.11629
60	0.155056	0.25843
70	0.297108	0.49518

TABLE NO. A.7: <u>ESTIMATED VALUES OF DISTRIBUTION CO-EFFICIENT,</u>
<u>SPECIFIC RATE CONSTANT AND EFFECTIVE DIFFUSIVITY</u>
<u>OF 20% SUCROSE SOLUTION AT DIFFERENT TEMPERATURES</u>

Temperature (^{0}C)	Distribution co-efficient	Specific rate constant x10^3 min^{-1}	Effective diffusivity x10^8 cm^2/sec
30	1.01	10.298	3.433
40	1.0	39.817	4.977
50	0.95	134.463	5.976
60	0.98	386.348	8.048
70	1.02	677.100	17.362

TABLE NO. A.8: <u>ESTIMATED VALUES OF DISTRIBUTION CO-EFFICIENT,</u>
<u>SPECIFIC RATE CONSTANT AND EFFECTIVE DIFFUSIVITY</u>
<u>OF 30% SUCROSE SOLUTION AT DIFFERENT TEMPERATURES</u>

Temperature (^{0}C)	Distribution co-efficient	Specific rate constant x10^3 min^{-1}	Effective diffusivity x10^8 cm^2/sec
30	1.07	11.478	3.826
40	1.05	44.068	5.508
50	1.01	152.280	6.768
60	1.04	434.683	9.056
70	1.07	739.091	18.951

TABLE NO. A.9: <u>ESTIMATED VALUES OF DISTRIBUTION CO-EFFICIENT,</u>
<u>SPECIFIC RATE CONSTANT AND EFFECTIVE DIFFUSIVITY</u>
<u>OF 40% SUCROSE SOLUTION AT DIFFERENT TEMPERATURES</u>

Temperature (^{0}C)	Distribution co-efficient	Specific rate constant $\times 10^3$ min^{-1}	Effective diffusivity $\times 10^8$ cm^2/sec
30	1.17	13.327	4.442
40	1.11	48.719	6.090
50	1.04	160.817	7.147
60	1.1	479.369	9.988
70	1.1	785.391	20.138

TABLE NO. A.10: <u>ACTIVATION ENERGY AND ARRHENIUS CONSTANT OF THE OVER-ALL RATE FOR DIFFERENT RESIN DIAMETERS AND SOLUTION CONCENTRATIONS</u>

Solution concentration (%)	Resin diameter (mm)	Activation energy (kCal/g.mol)	Arrhenius constant $\times 10^8$ (min^{-1})
	1.09	14.821	4.165
	0.925	14.975	6.266
20	0.78	15.227	10.580
	0.55	16.355	75.073
	0.362	17.205	384.999
	1.09	14.628	3.557
	0.925	14.635	4.225
30	0.78	15.096	10.008
	0.55	15.565	26.467
	0.362	16.765	216.410
	1.09	14.092	1.810
	0.925	14.157	2.358
40	0.78	14.300	3.358
	0.55	14.727	8.459
	0.362	15.678	48.815
Intrinsic rate		24.9295	7.6573×10^{15}

TABLE NO. A.11: ESTIMATED VALUES OF MASS TRANSFER CO-EFFICIENT
OF 30% SUCROSE SOLUTION FOR 0.78 mm DIAMETER RESIN

Temperature (^{0}C)	Mass transfer co-efficient (cm/sec)
30	≈ 0
40	1.412×10^{-5}
50	1.873×10^{-5}
60	2.957×19^{-5}
70	6.420×10^{-5}

APPENDIX–B

GRAPHS
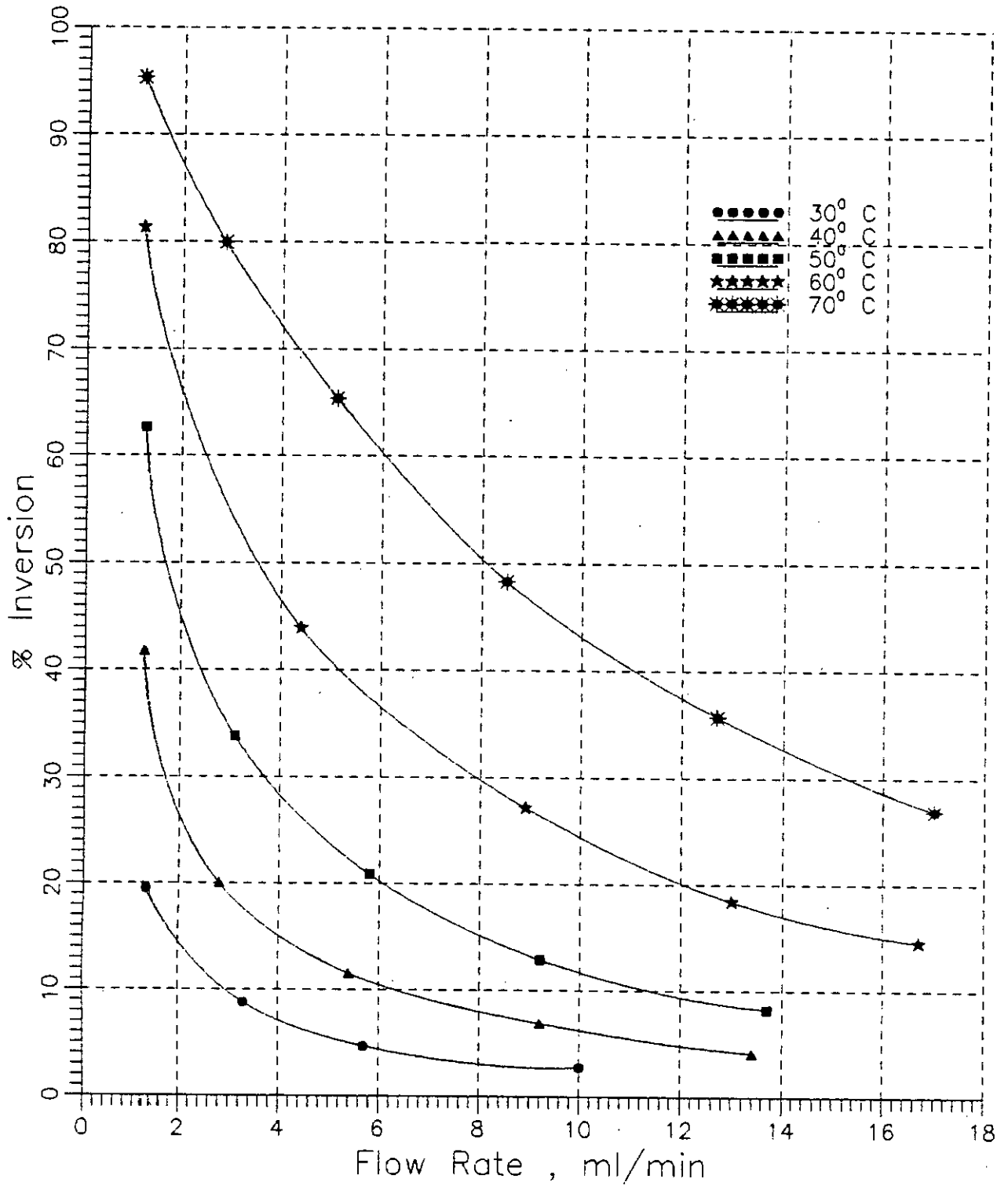
Figure B.1.1: Relation between percent inversion and flow rate of 20% sucrose solution for 1.09 mm diameter resin bead at different temperatures.
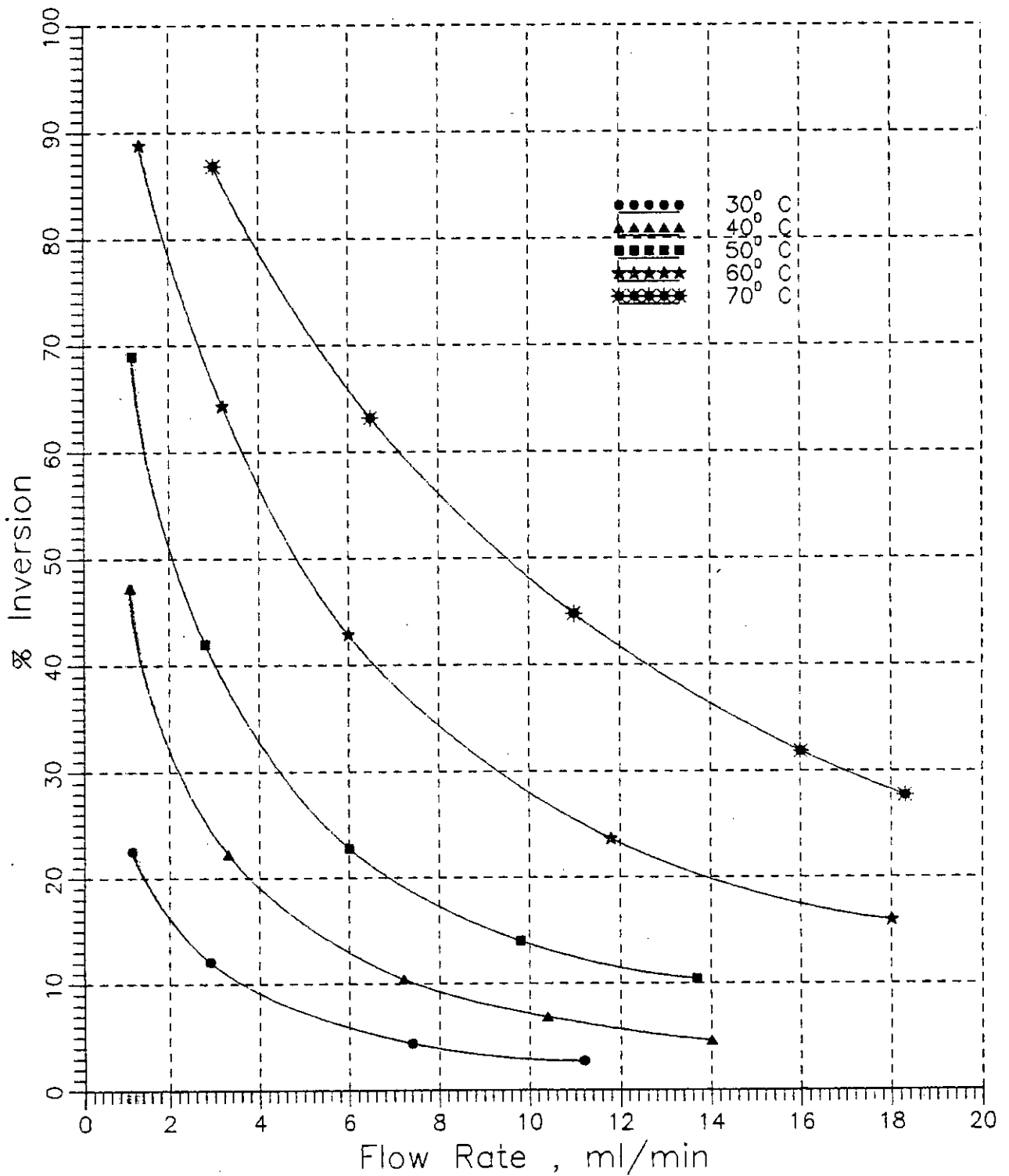
Figure B.1.2: Relation between percent inversion and flow rate of 20% sucrose solution for 0.925 mm diameter resin bead at different temperatures.
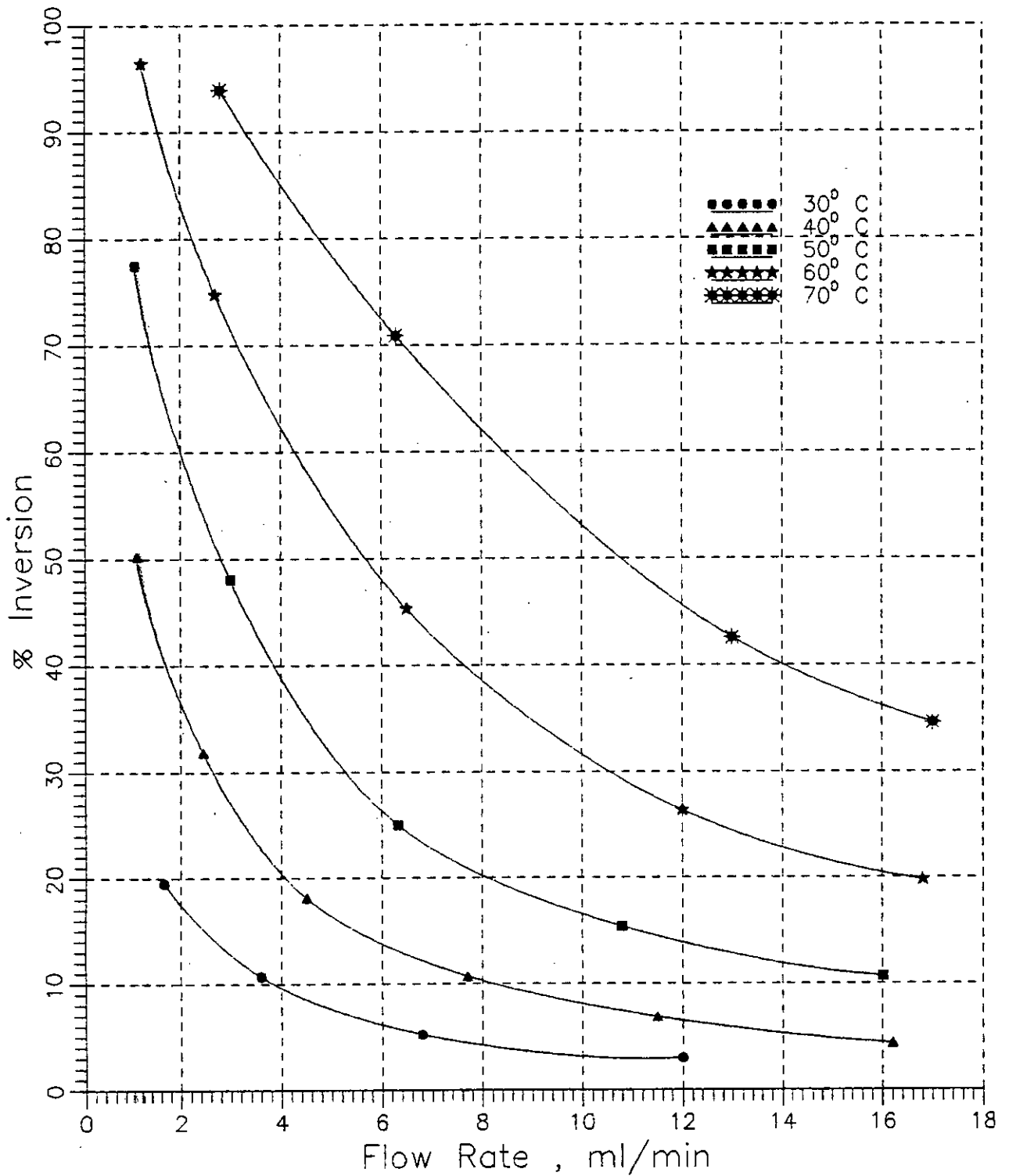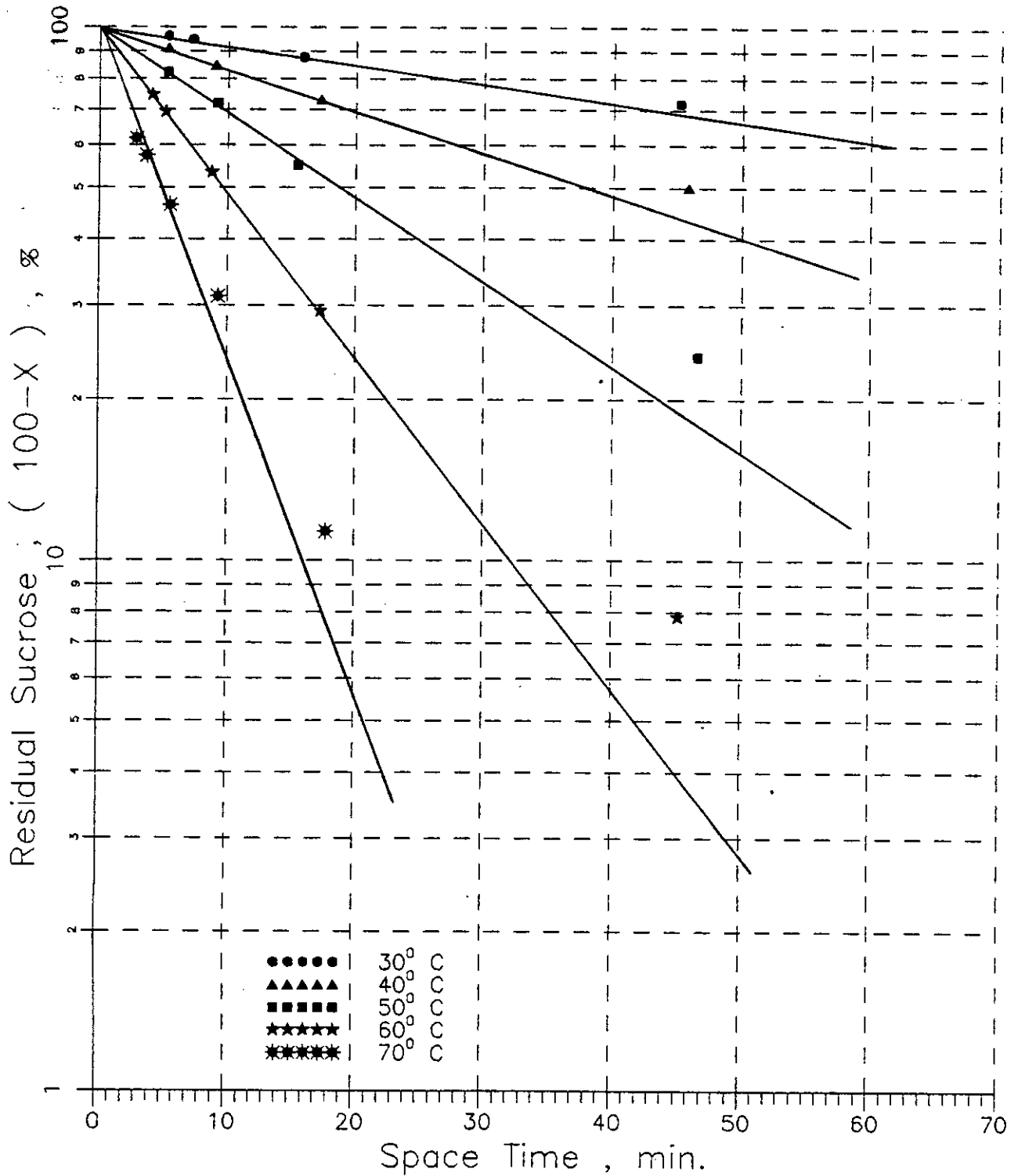
Figure B.1.3: Relation between percent inversion and flow rate
of 20% sucrose solution for 0.78 mm diameter
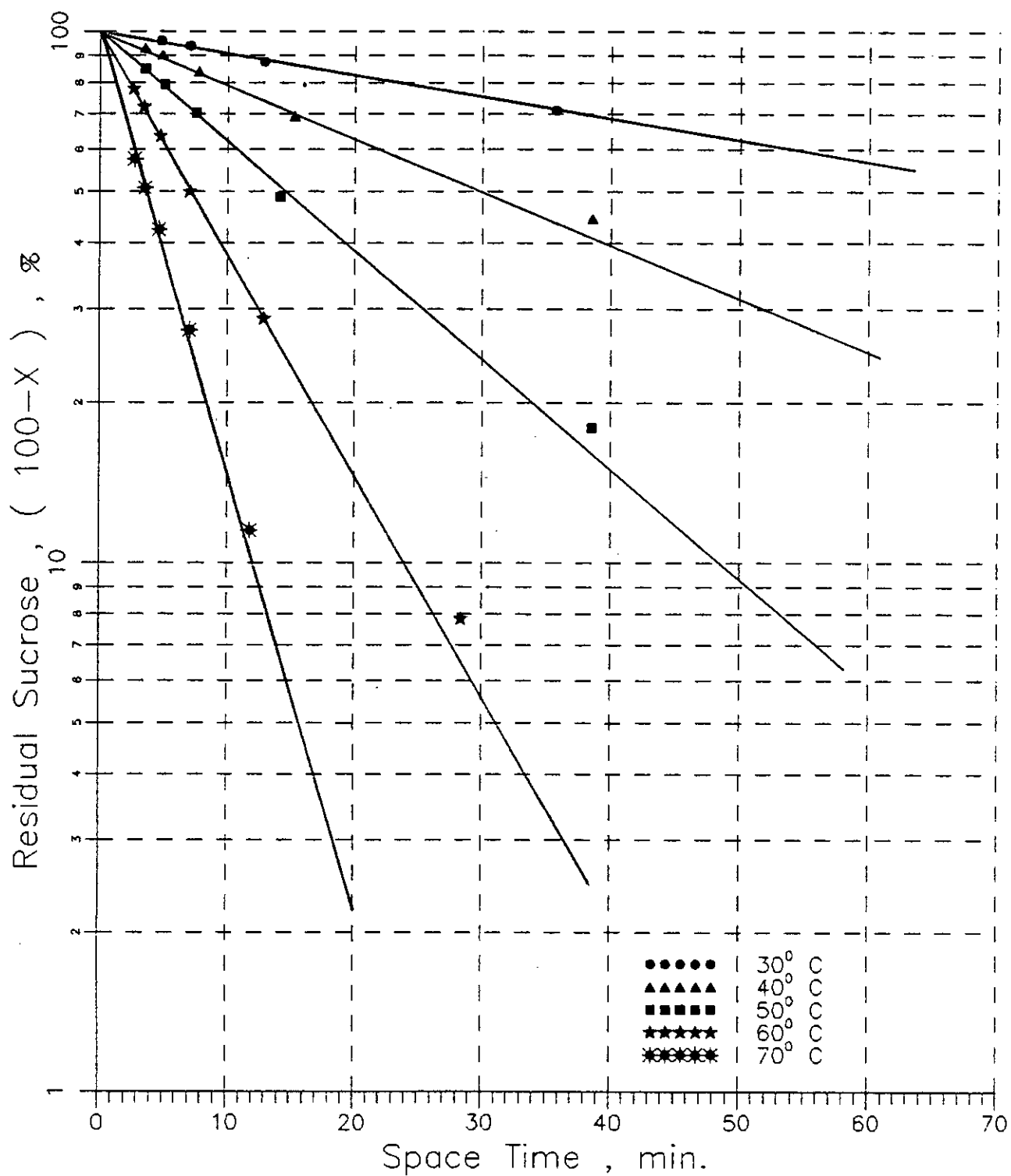resin bead at different temperatures.
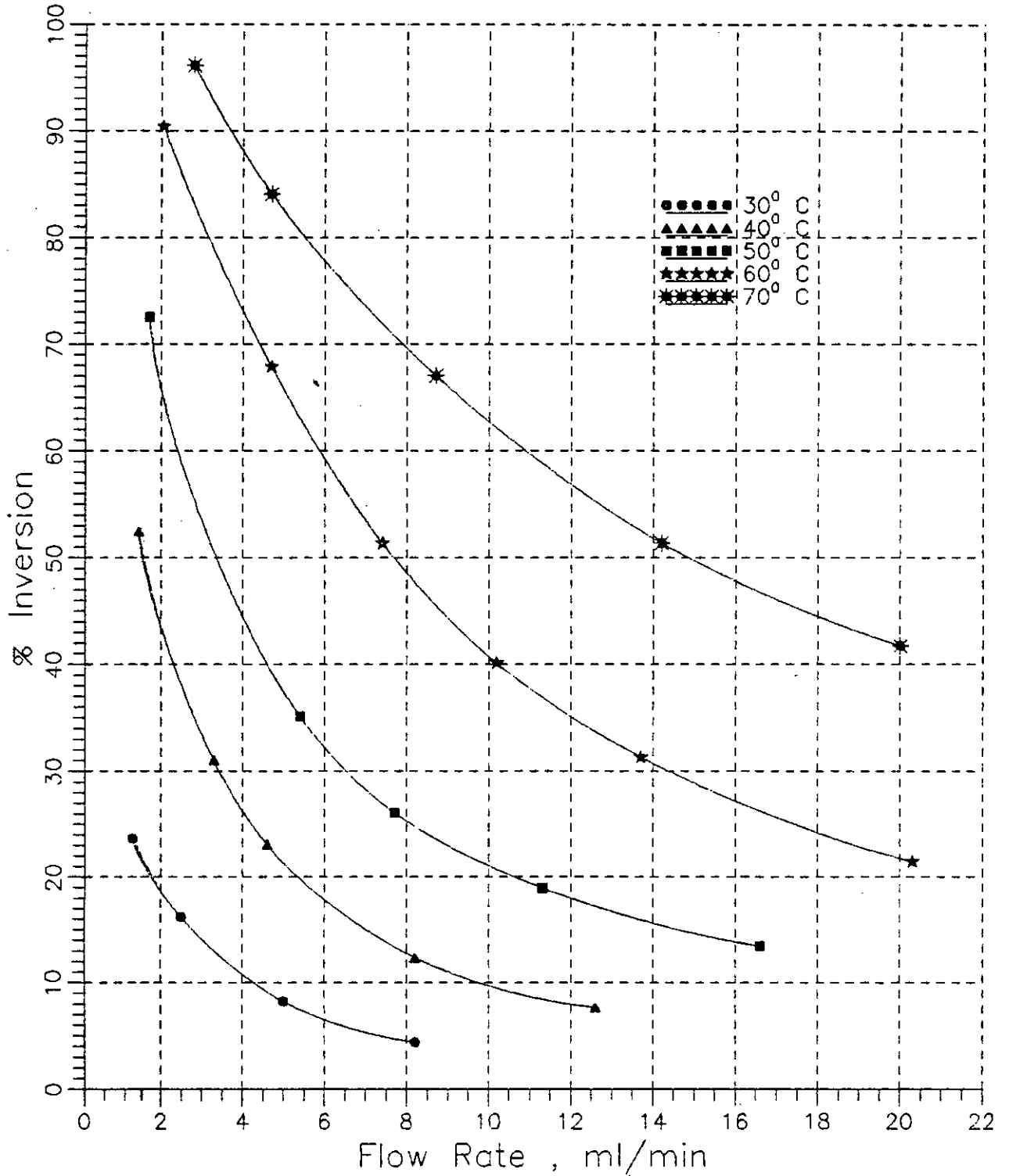
Figure B.1.4: Relation between percent inversion and flow rate of 20% sucrose solution for 0.55 mm diameter resin bead at different temperatures.
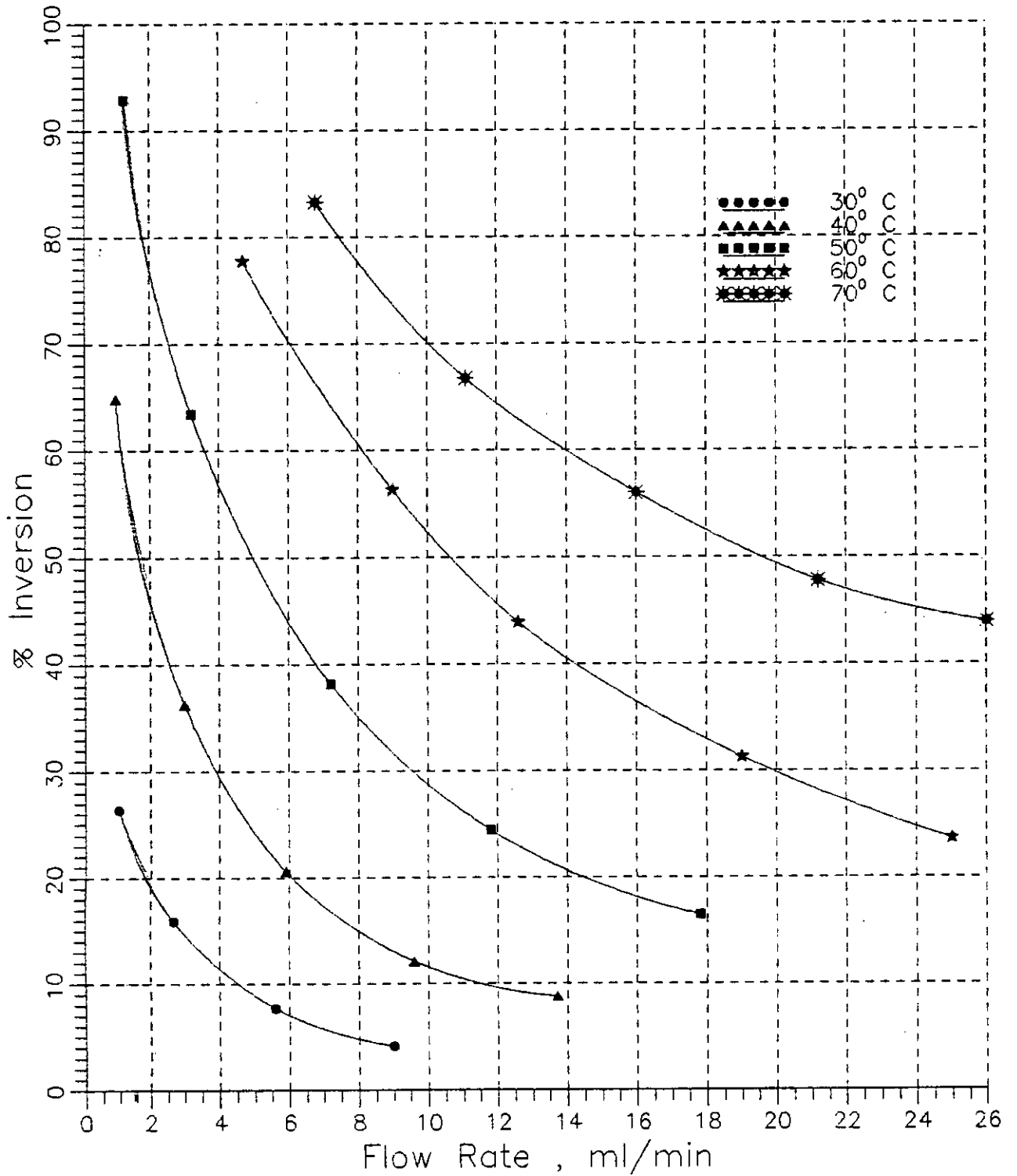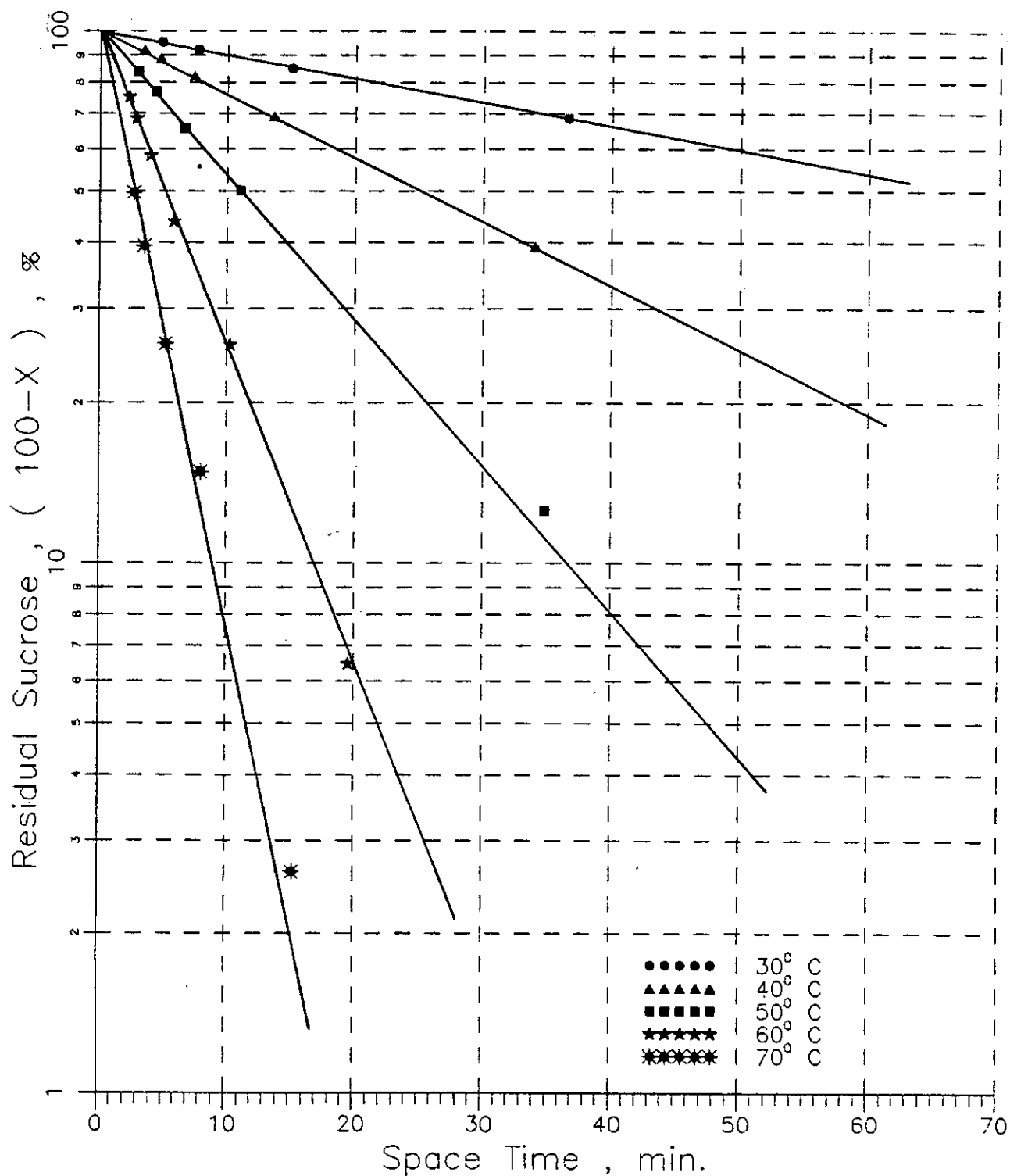
Figure B.1.5: Relation between percent inversion and flow rate of 20% sucrose solution for 0.362 mm diameter resin bead at different temperatures.
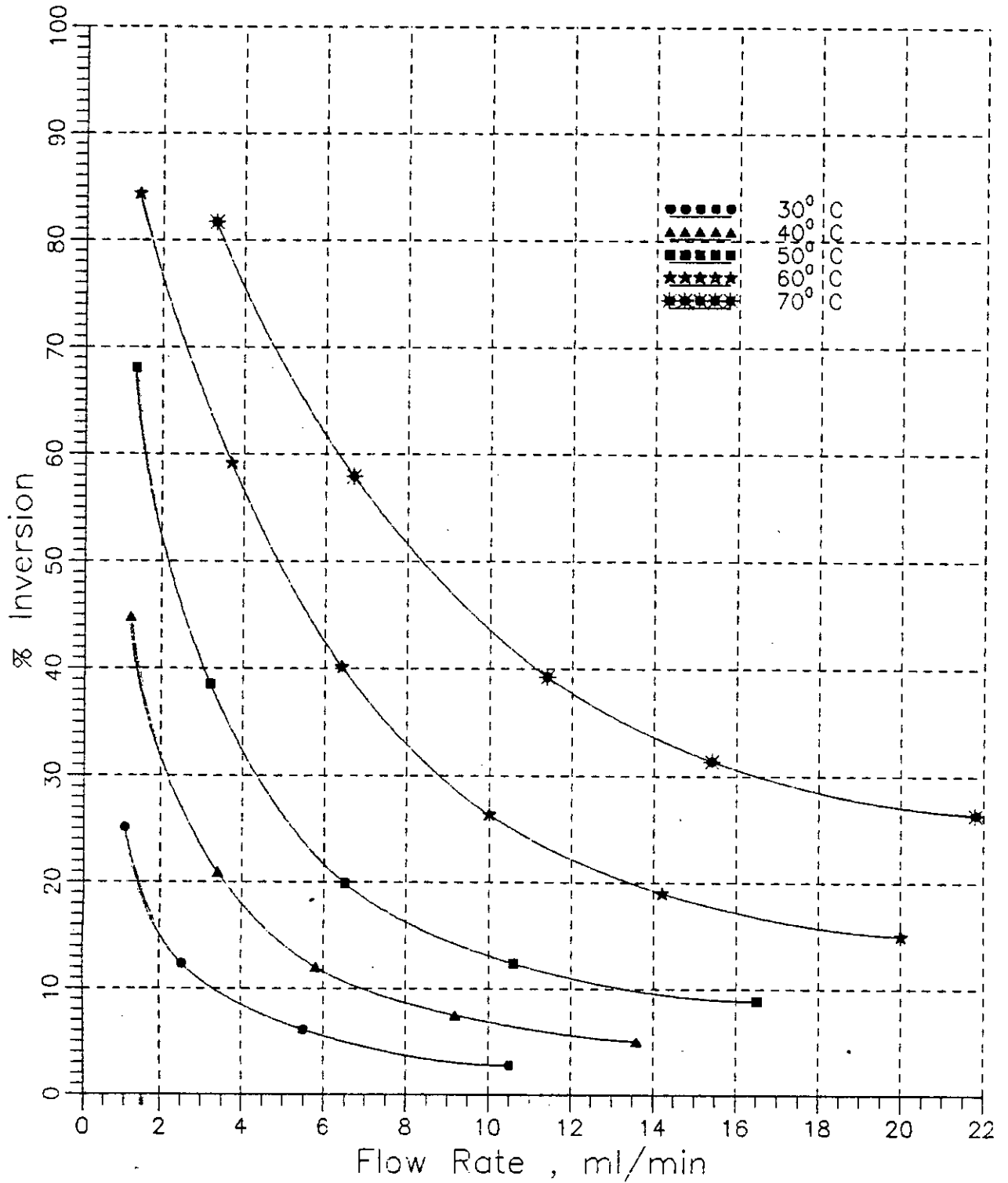
Figure B.2.1: Relation between percent inversion and flow rate of 30% sucrose solution for 1.09 mm diameter resin bead at different temperatures.
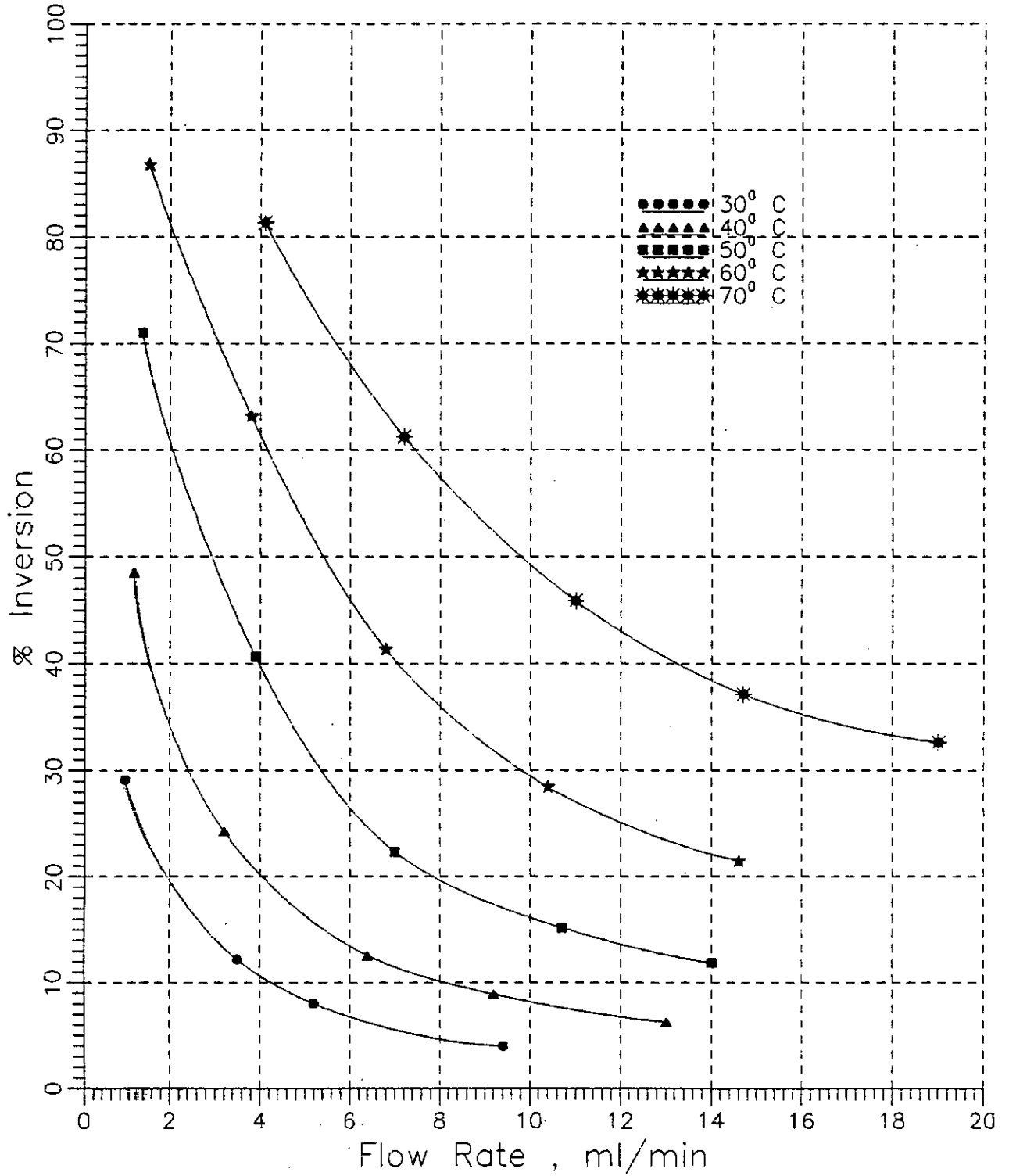
Figure B.2.2: Relation between percent inversion and flow rate of 30% sucrose solution for 0.925 mm diameter resin bead at different temperatures.
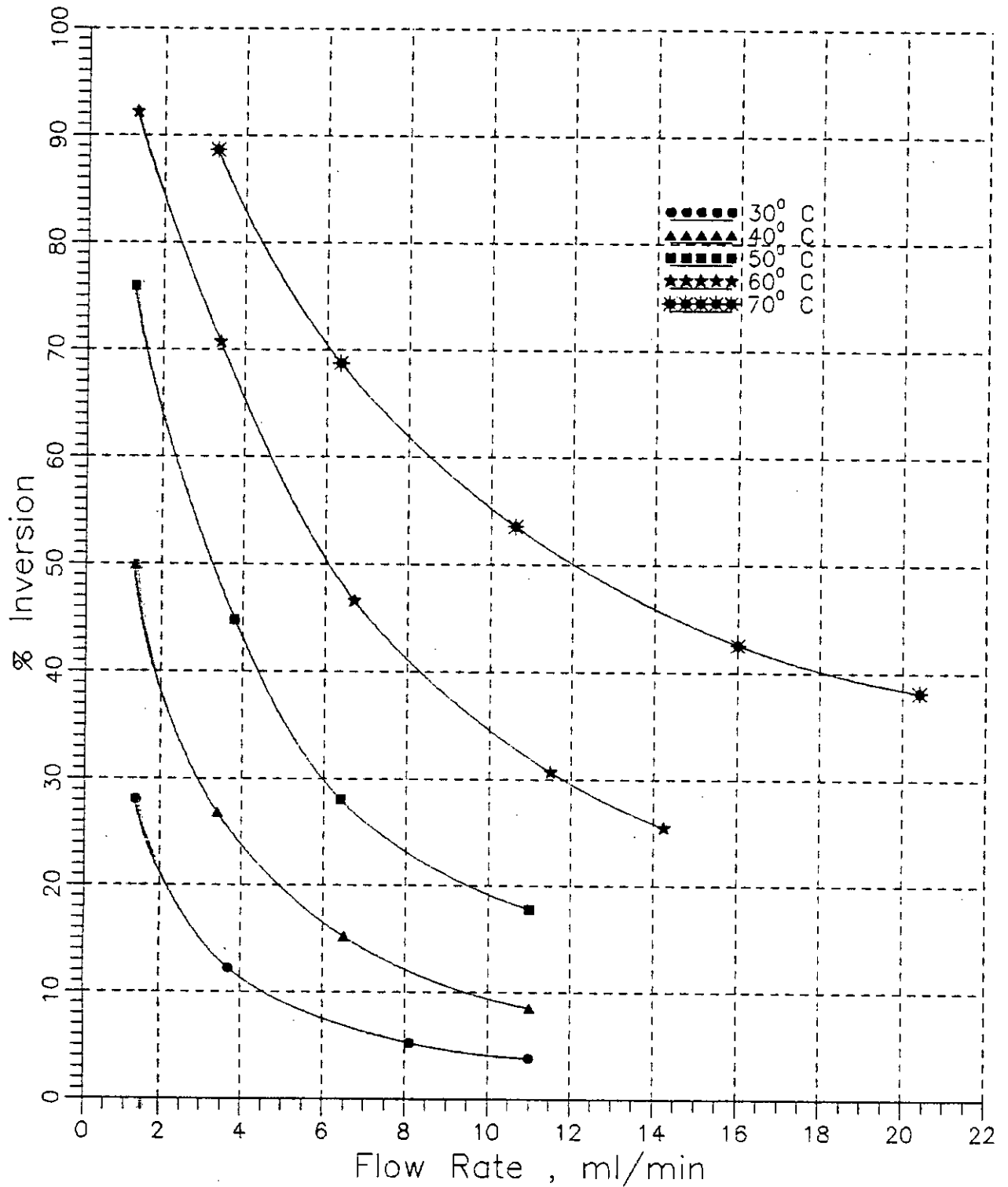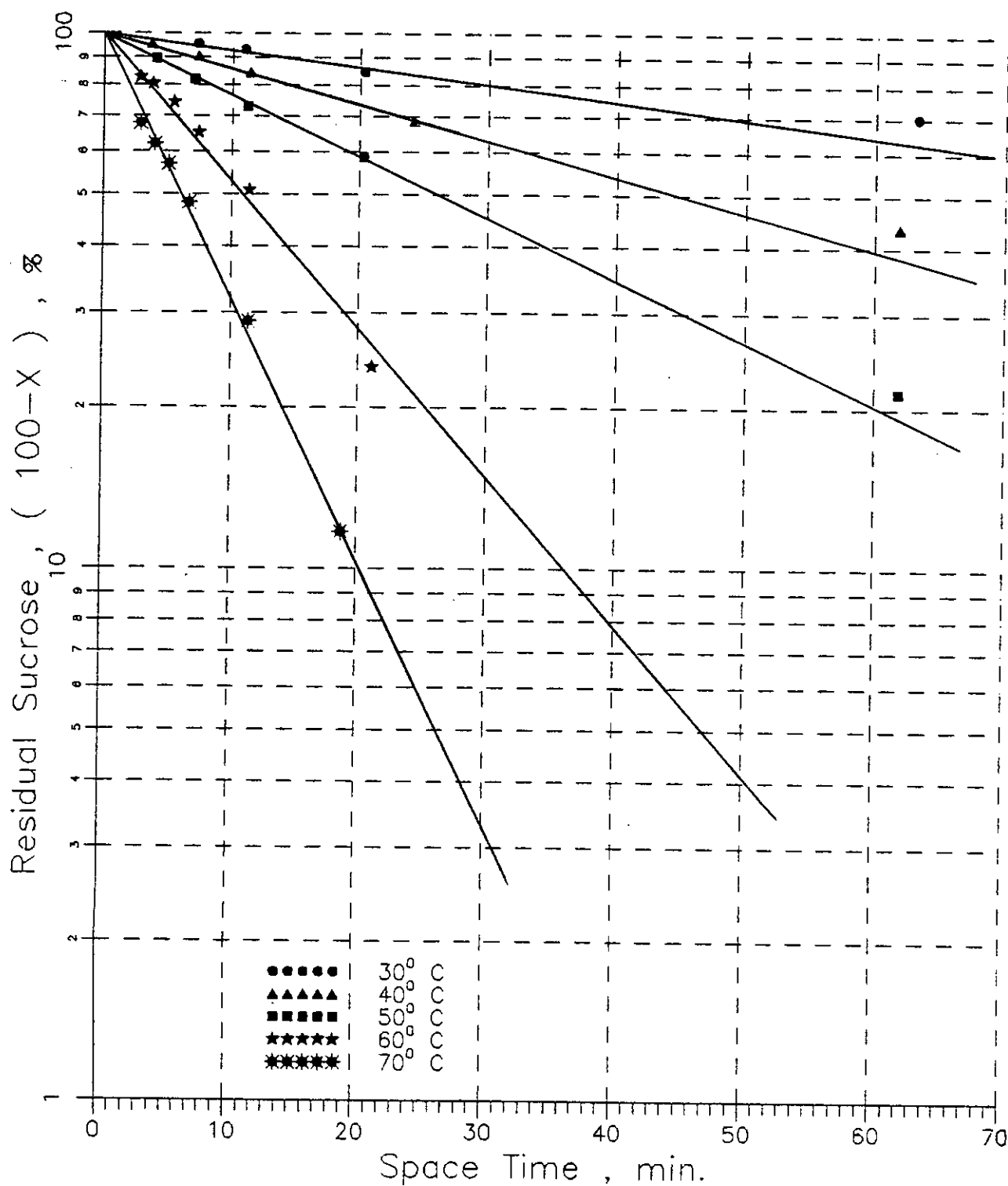
Figure B.2.3: Relation between percent inversion and flow rate of 30% sucrose solution for 0.78 mm diameter resin bead at different temperatures.
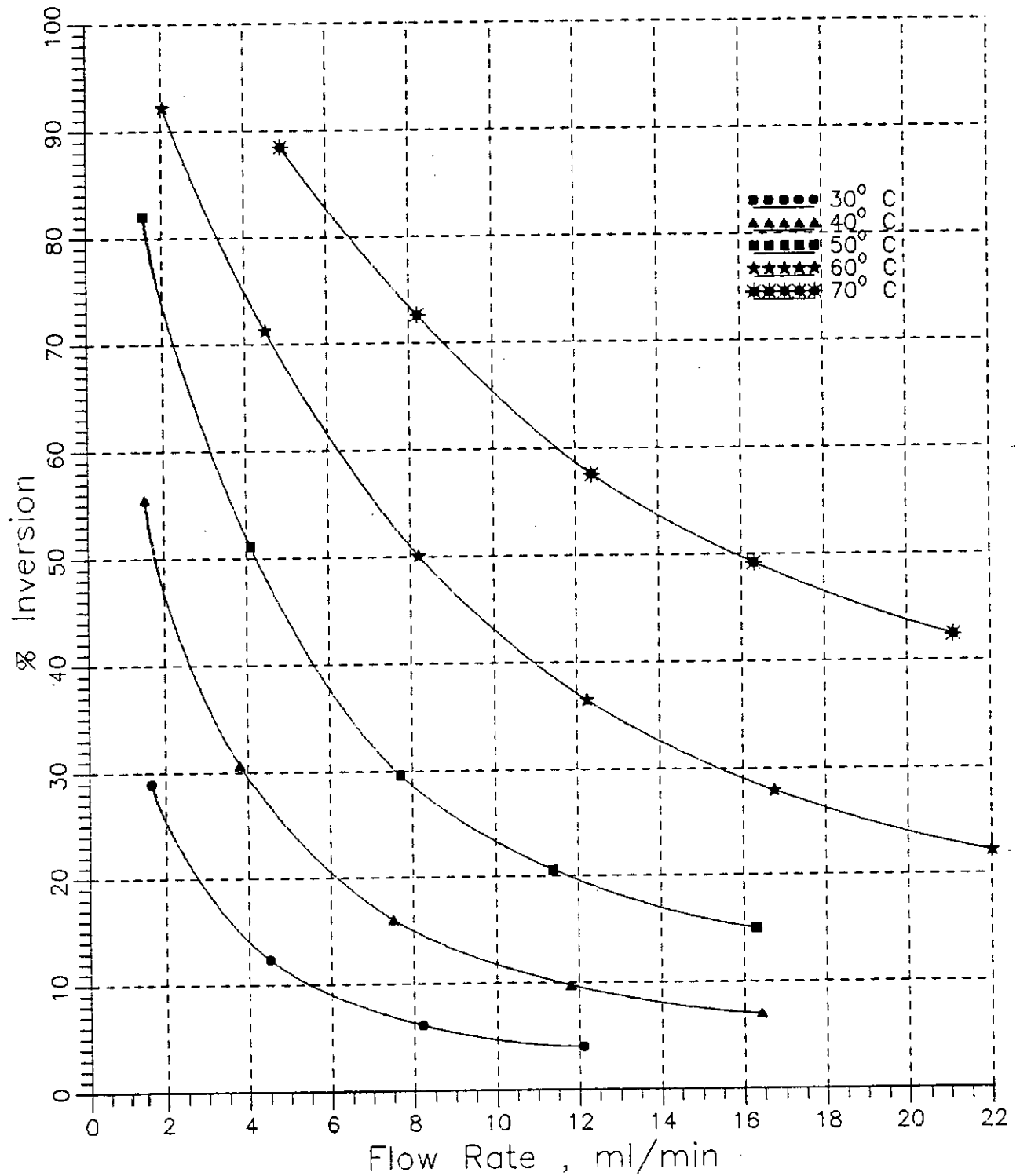
Figure B.2.4: Relation between percent inversion and flow rate of 30% sucrose solution for 0.55 mm diameter resin bead at different temperatures.
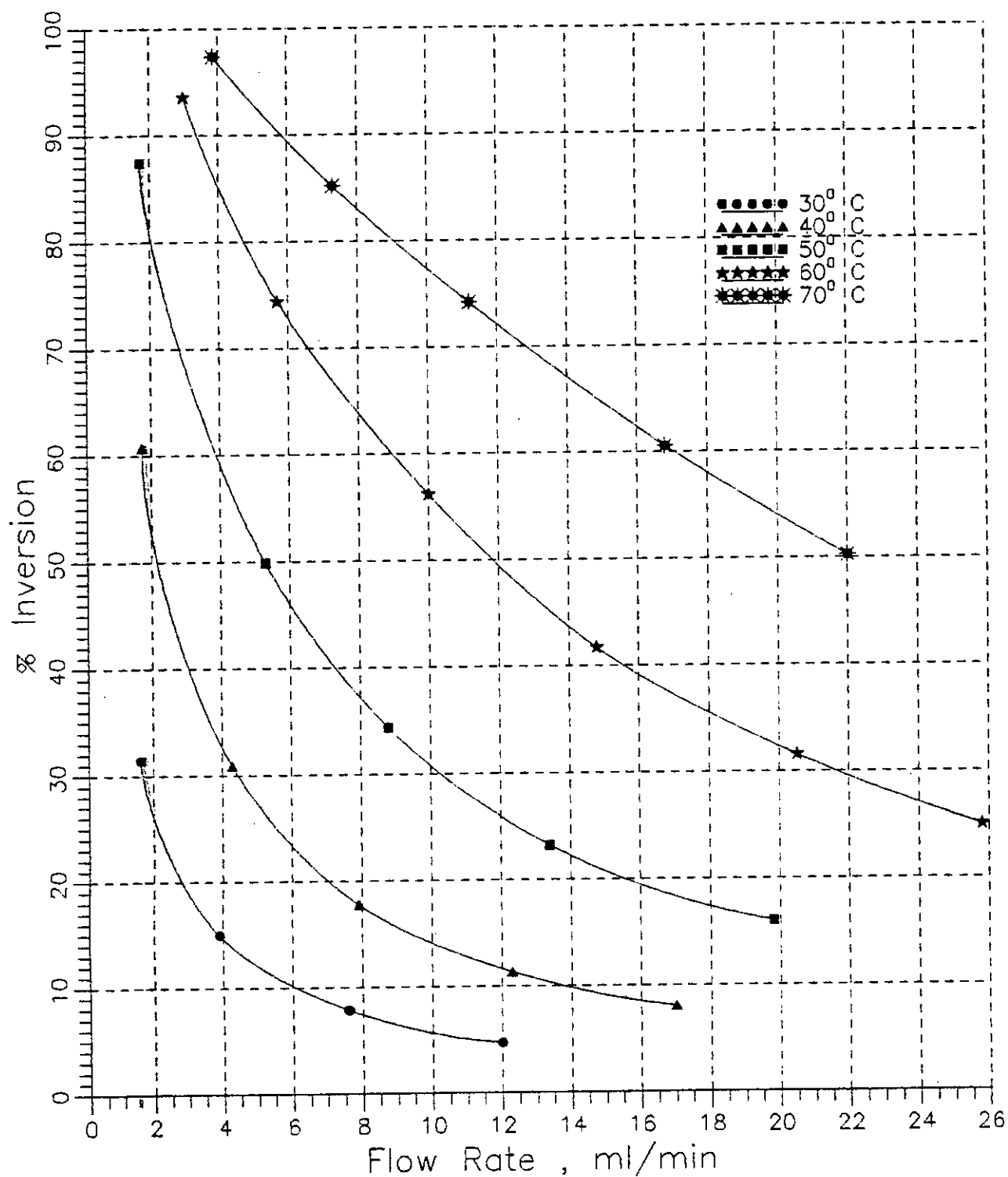
Figure B.2.5: Relation between percent inversion and flow rate of 30% sucrose solution for 0.362 mm diameter resin bead at different temperatures.
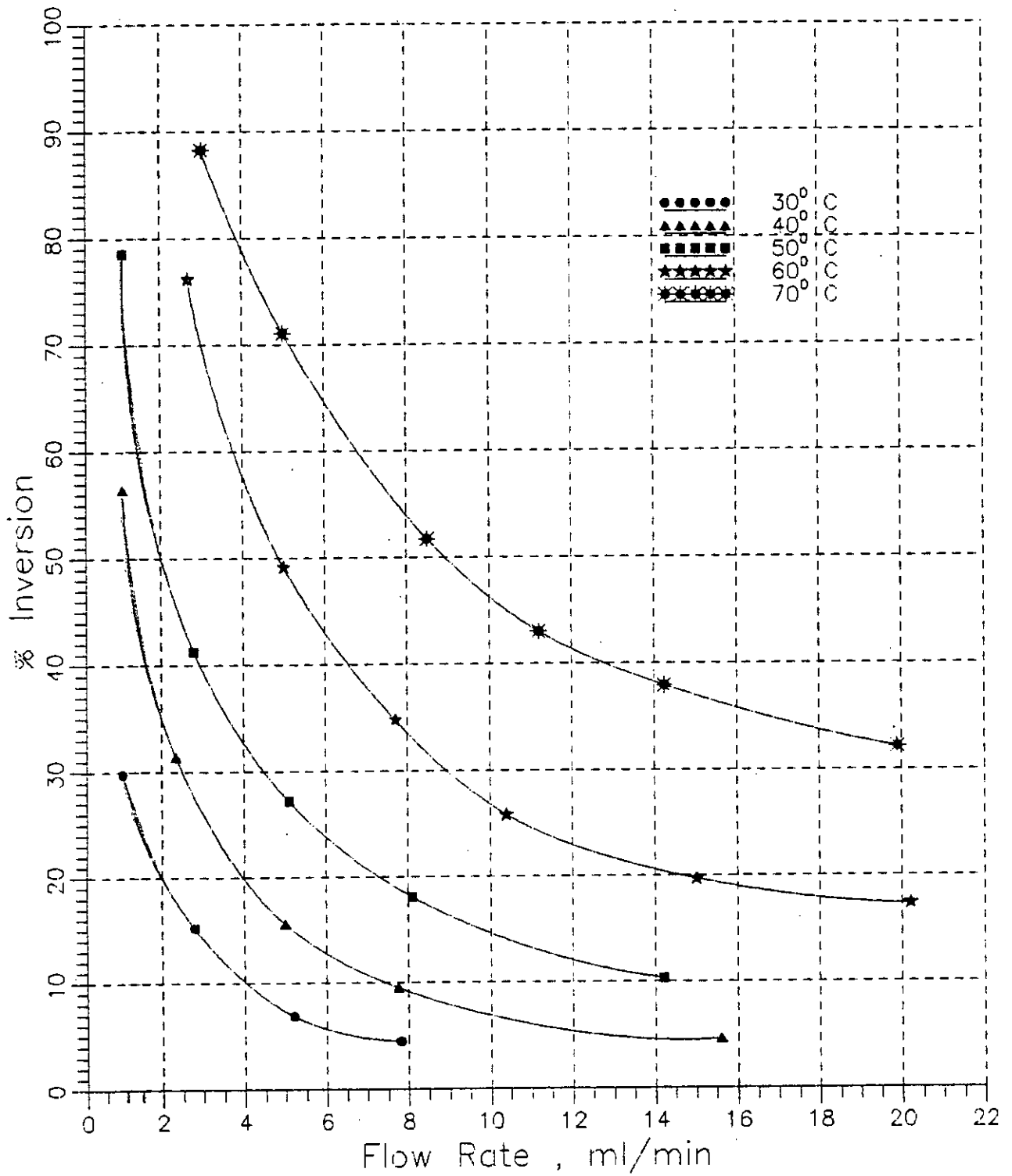
Figure B.3.1: Relation between percent inversion and flow rate of 40% sucrose solution for 1.09 mm diameter resin bead at different temperatures.
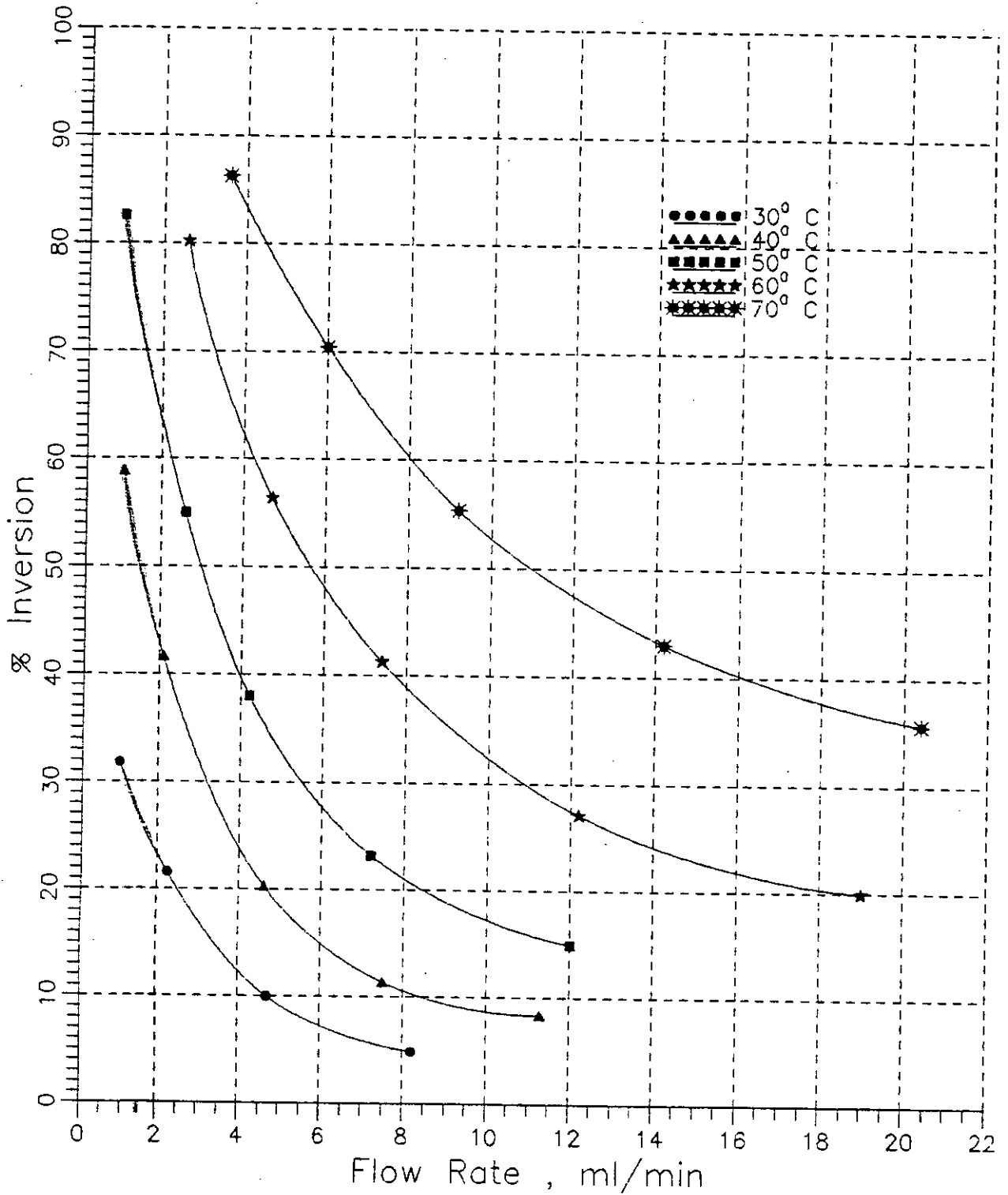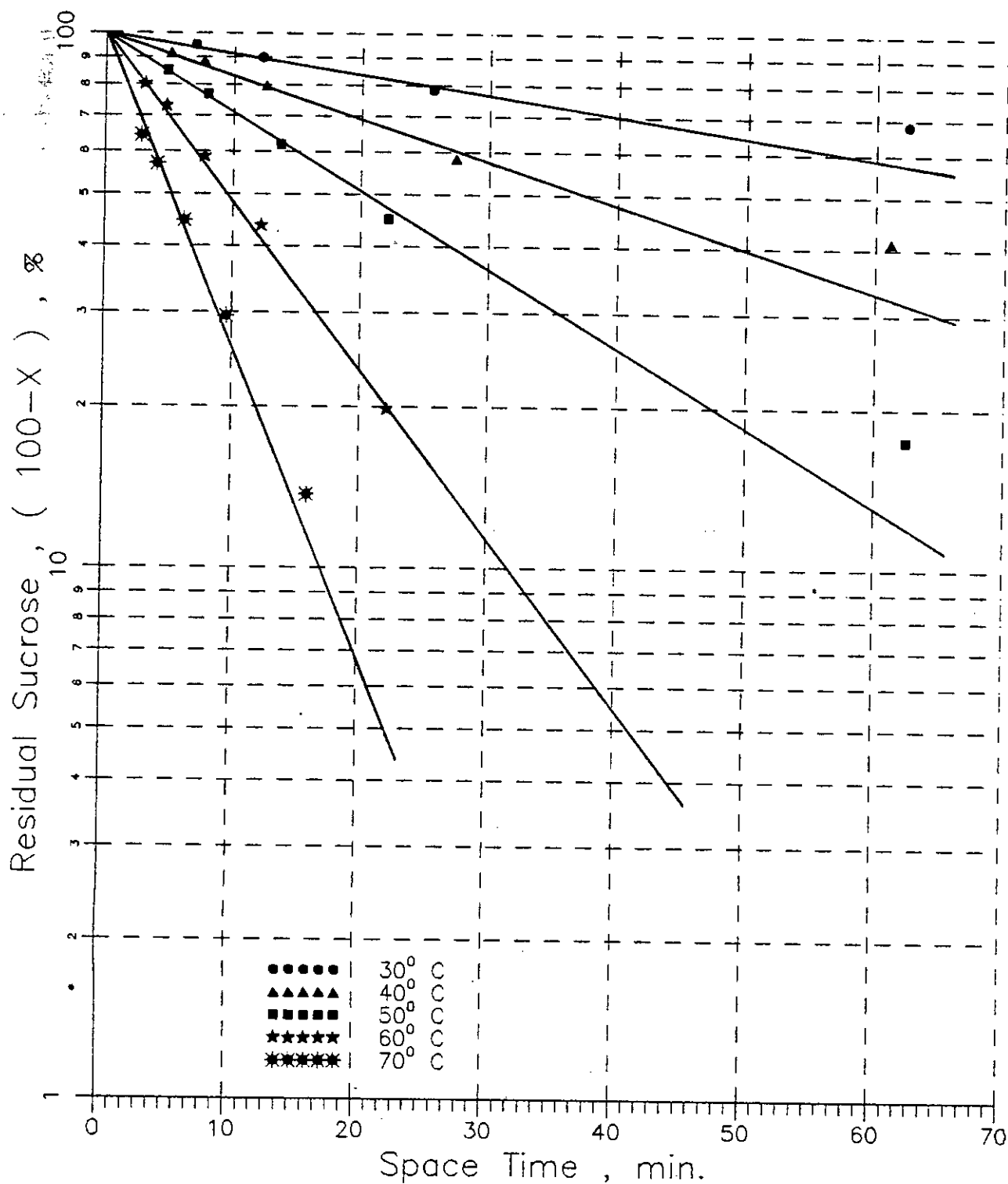
Figure B.3.2: Relation between percent inversion and flow rate of 40% sucrose solution for 0.925 mm diameter resin bead at different temperatures.
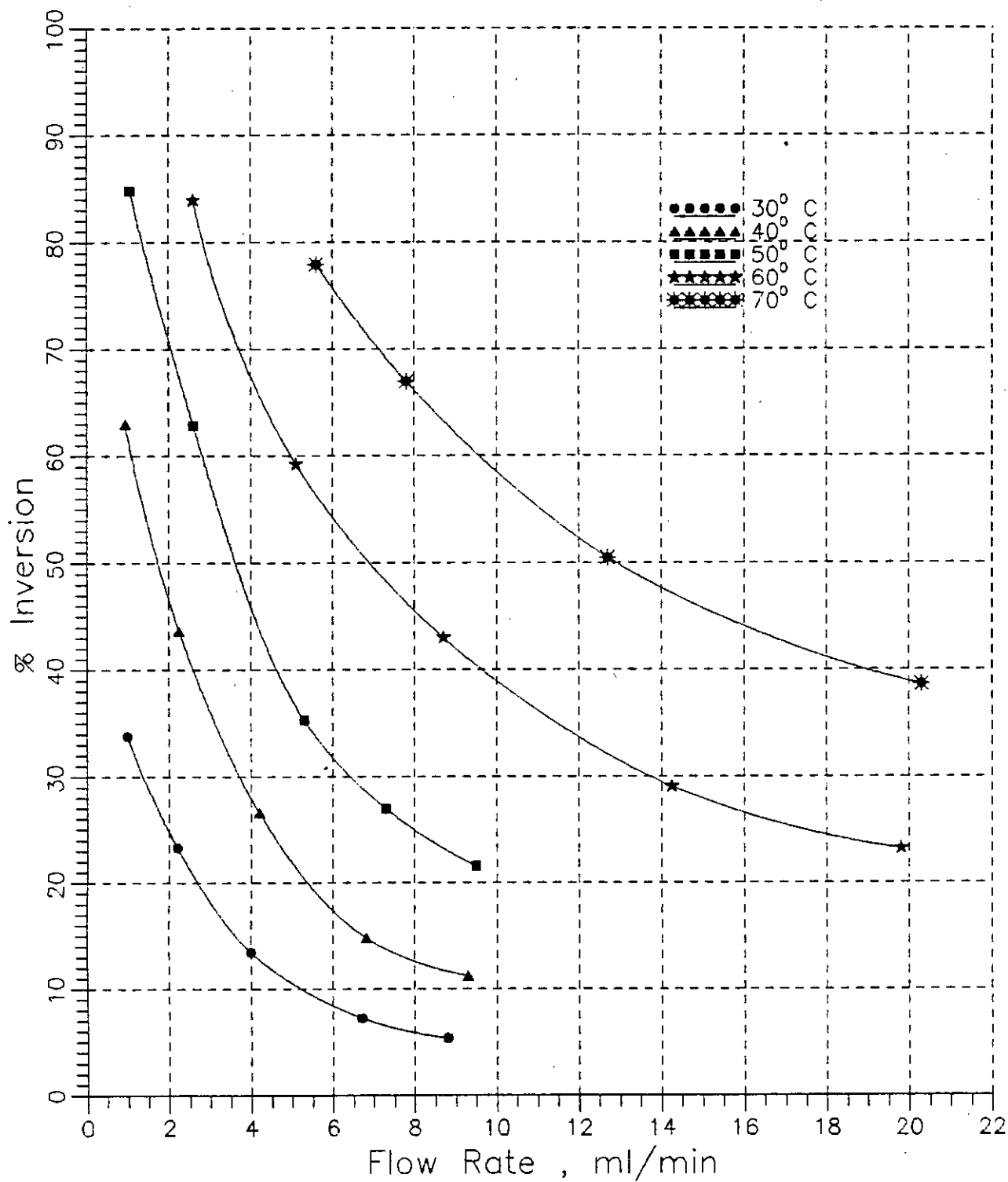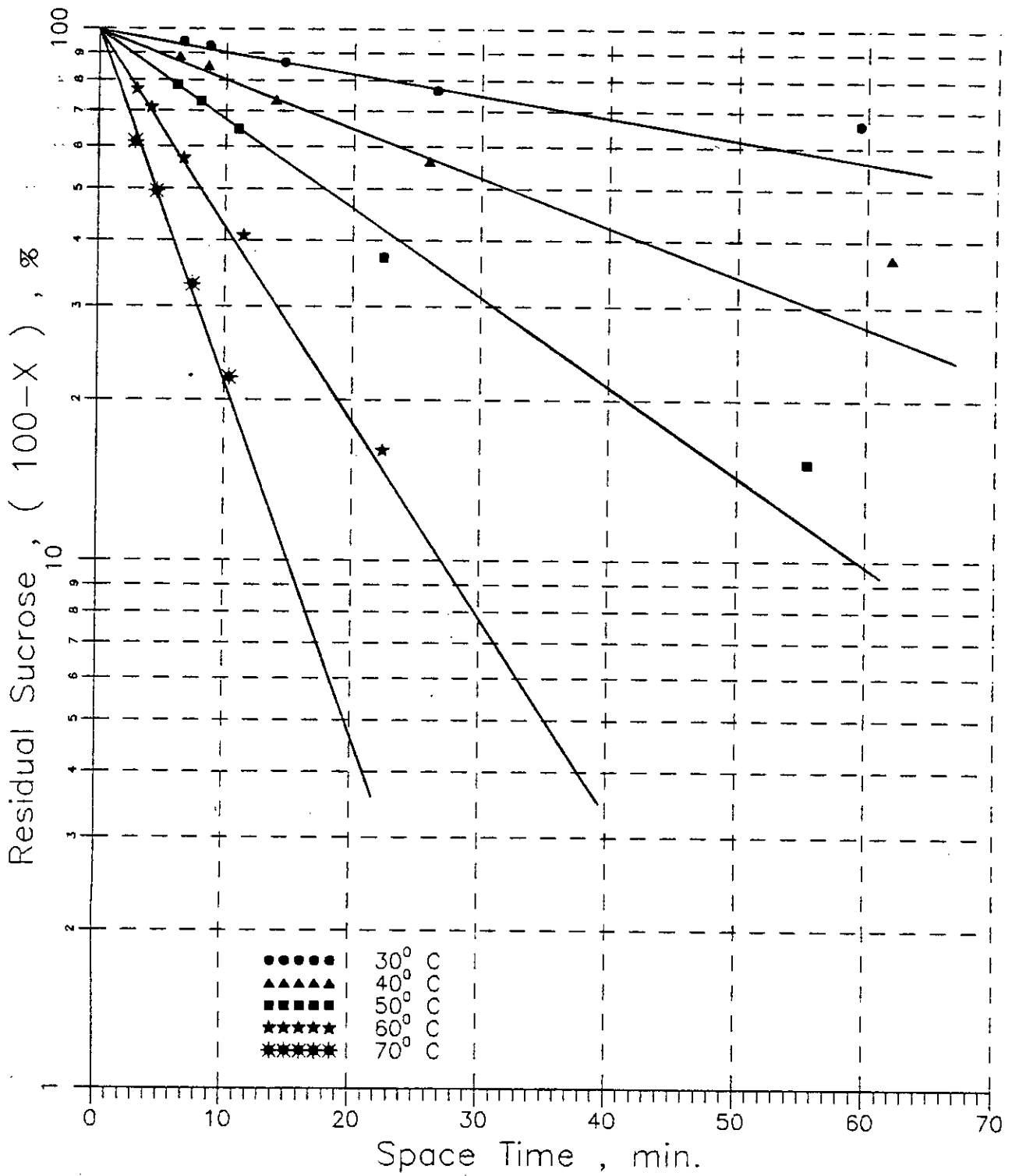
Figure B.3.3: Relation between percent inversion and flow rate of 40% sucrose solution for 0.78 mm diameter resin bead at different temperatures.
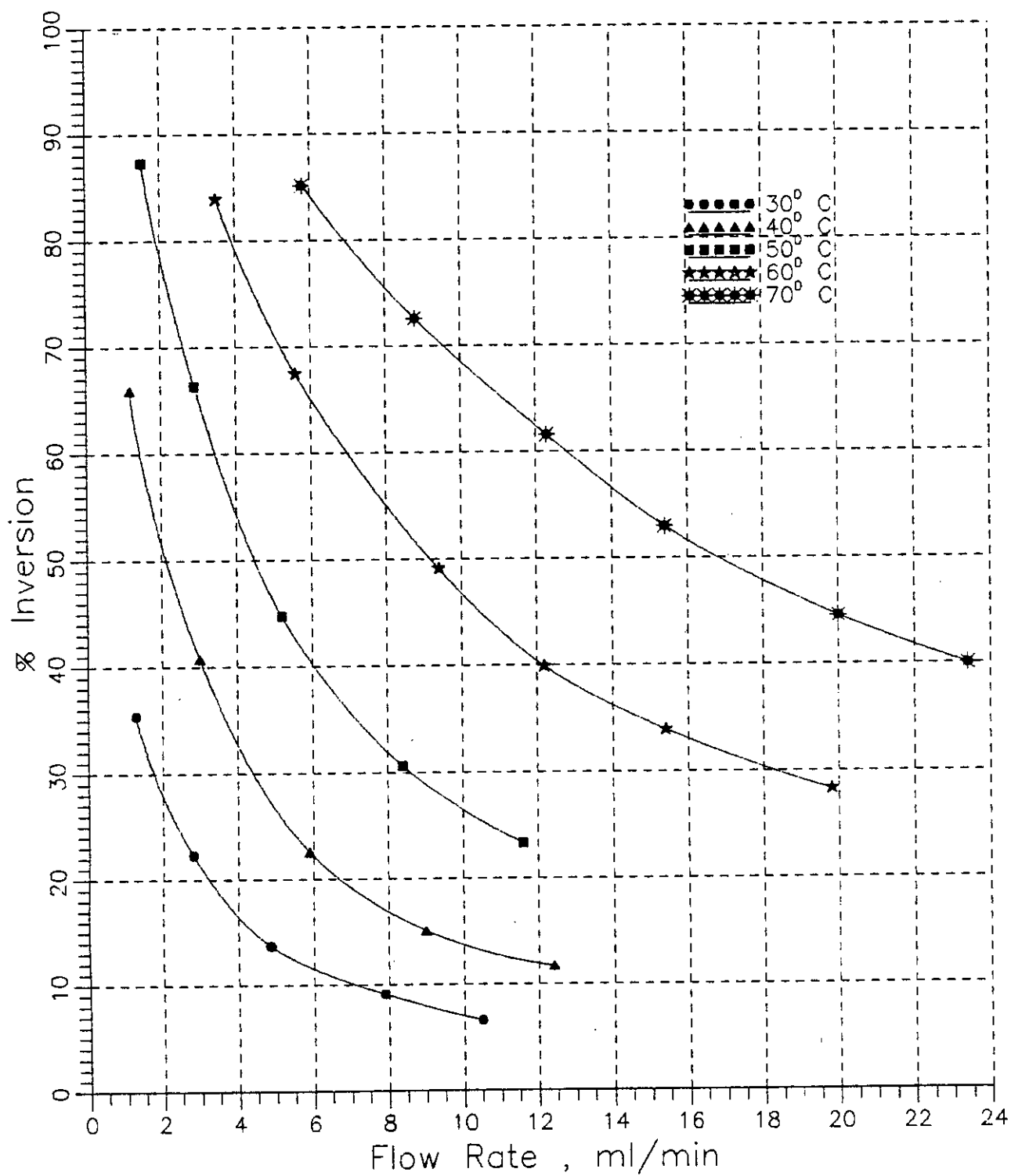
Figure B.3.4: Relation between percent inversion and flow rate of 40% sucrose solution for 0.55 mm diameter resin bead at different temperatures.
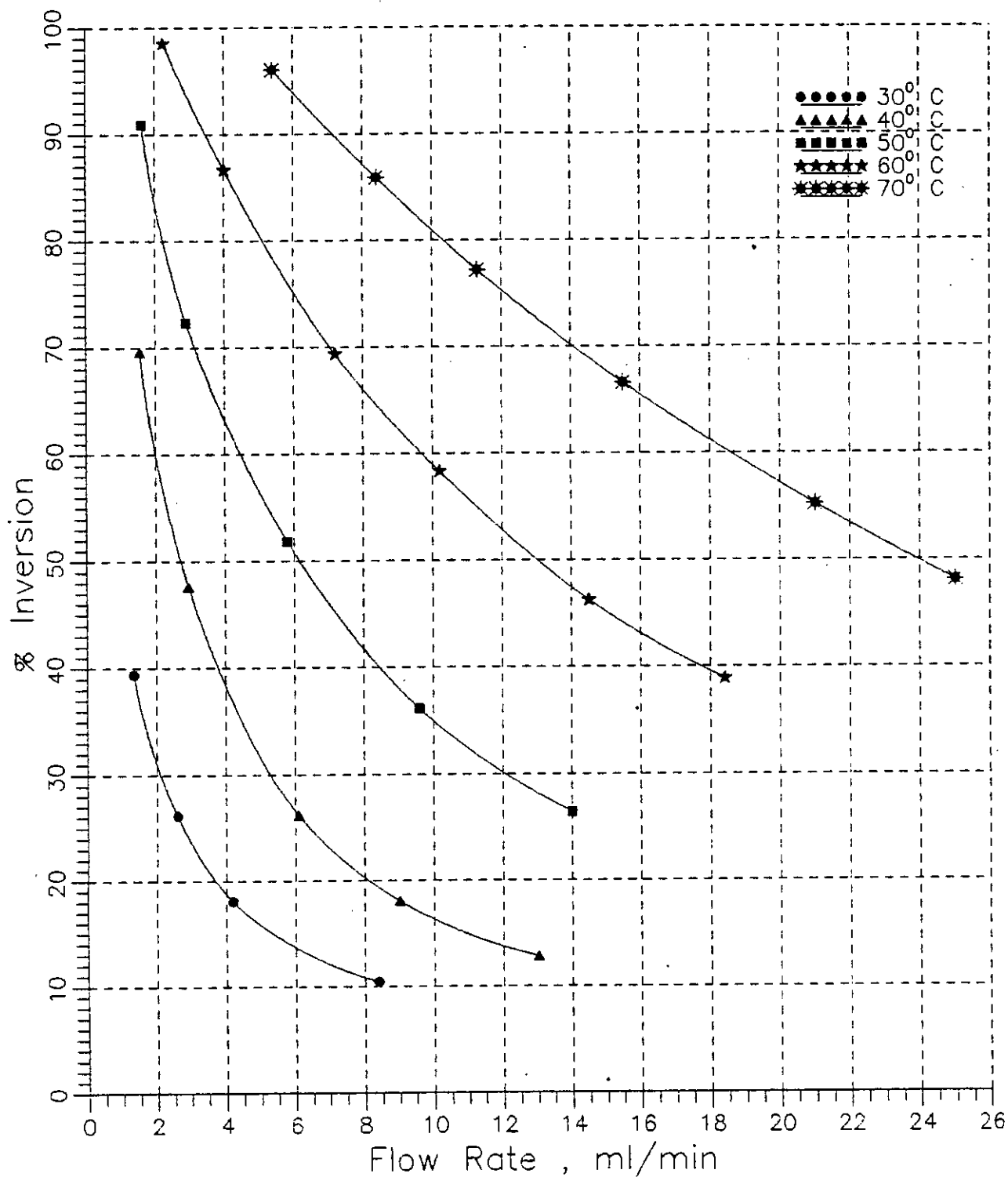
Figure B.3.5: Relation between percent inversion and flow rate of 40% sucrose solution for 0.362 mm diameter resin bead at different temperatures.
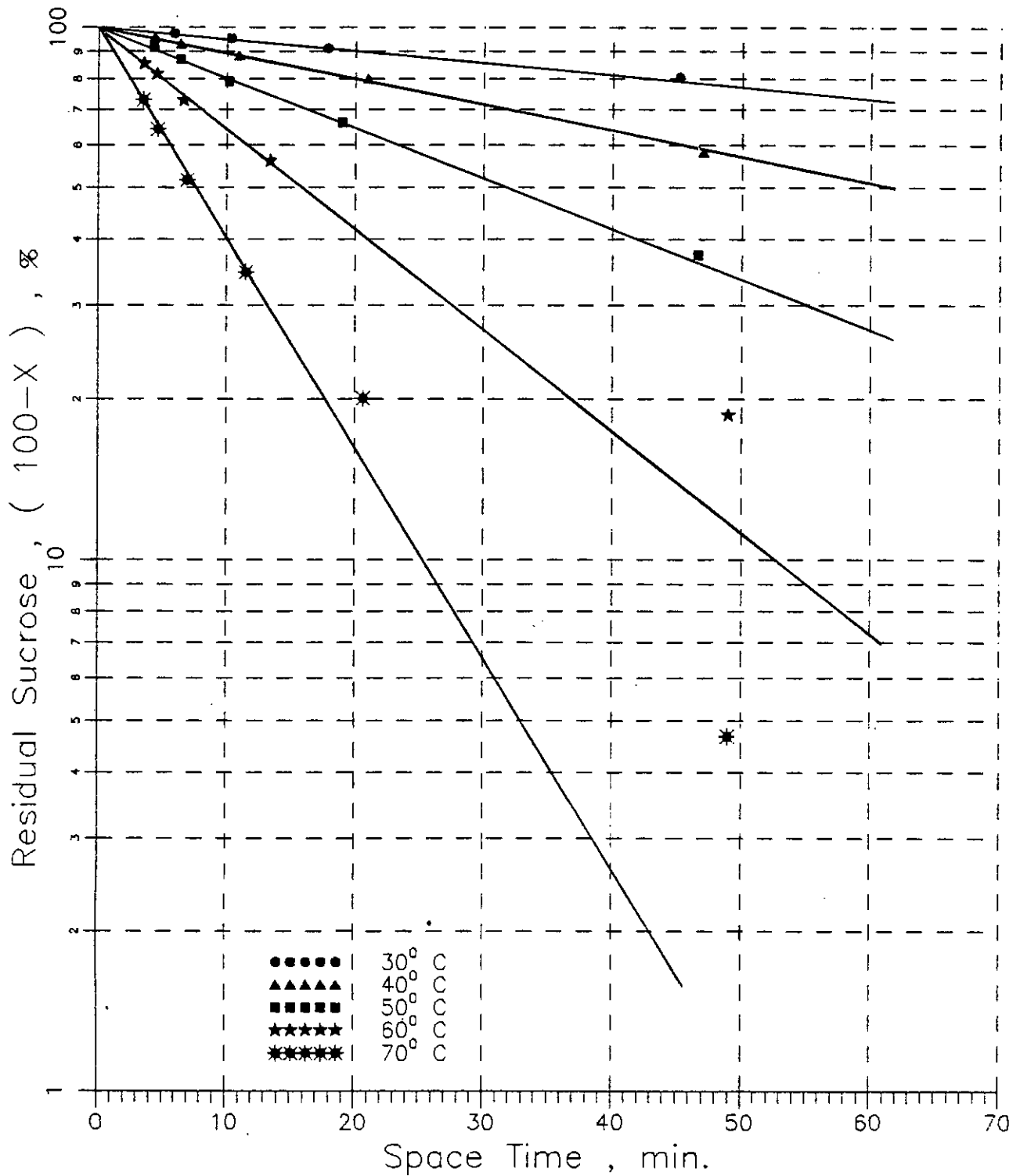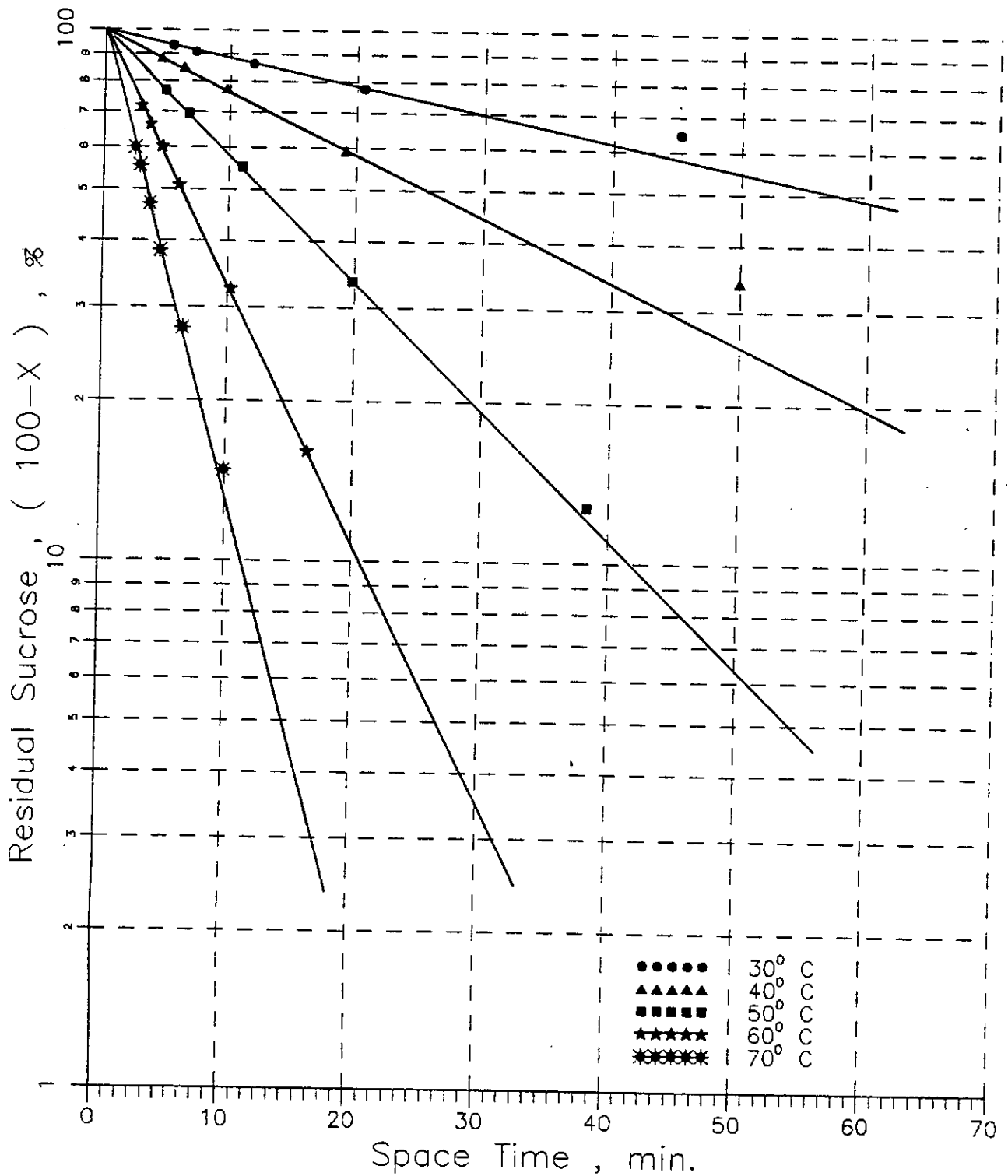
Figure B.4.1: Relation between residual sucrose and space time of 20% sucrose solution for 1.09 mm diameter resin bead at different temperatures.
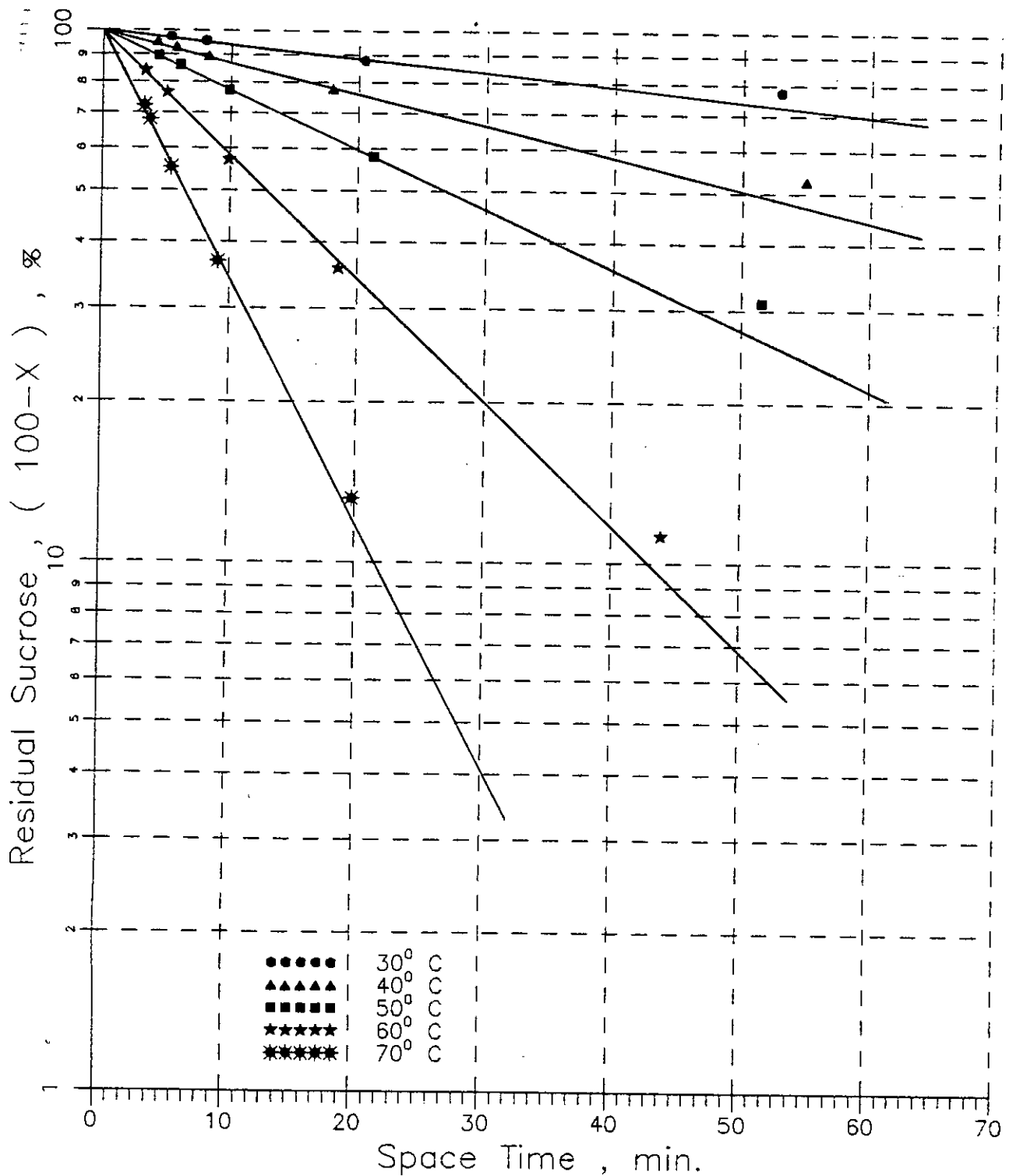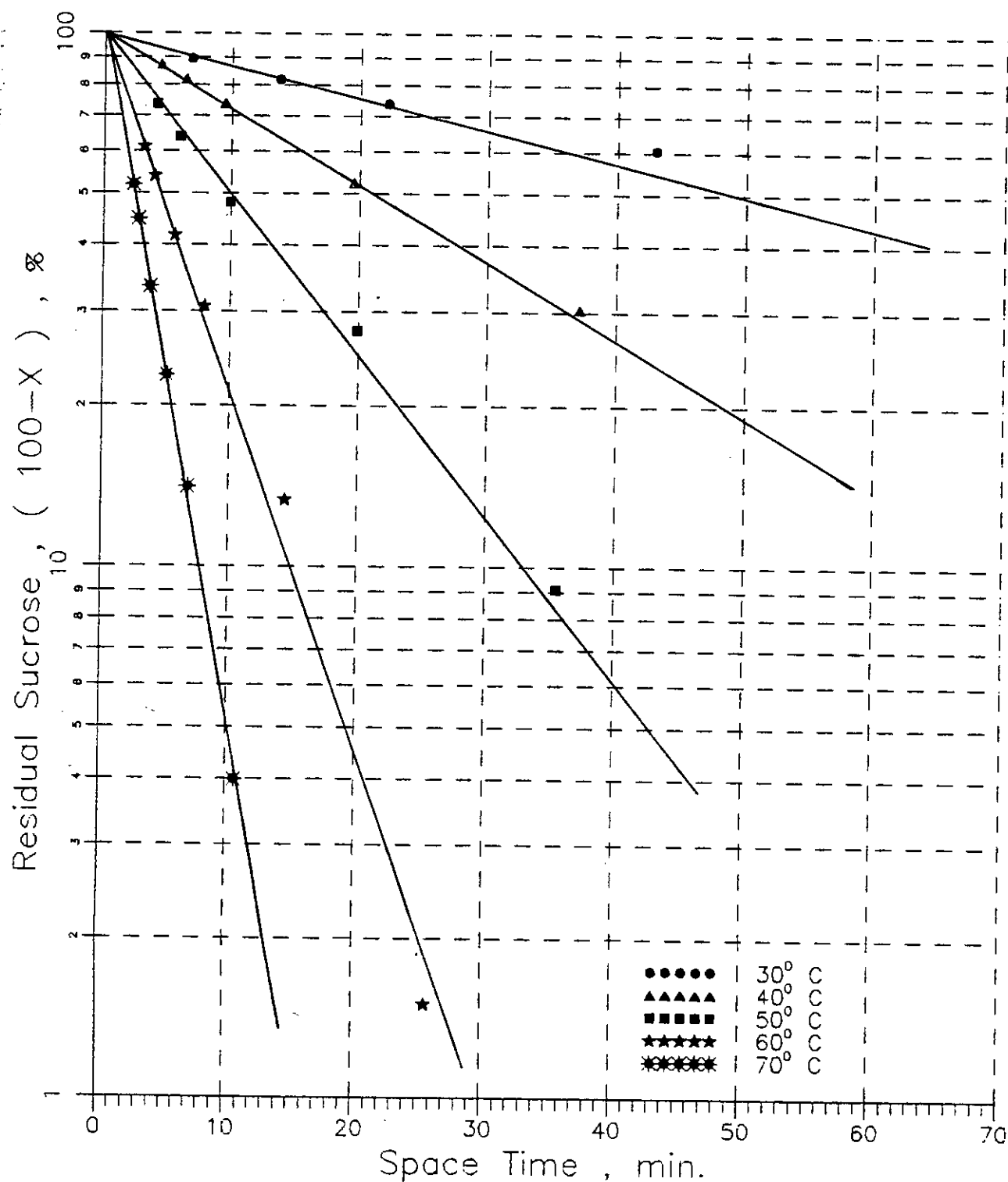
Figure B.4.2: Relation between residual sucrose and space time of 20% sucrose solution for 0.925 mm diameter resin bead at different temperatures.
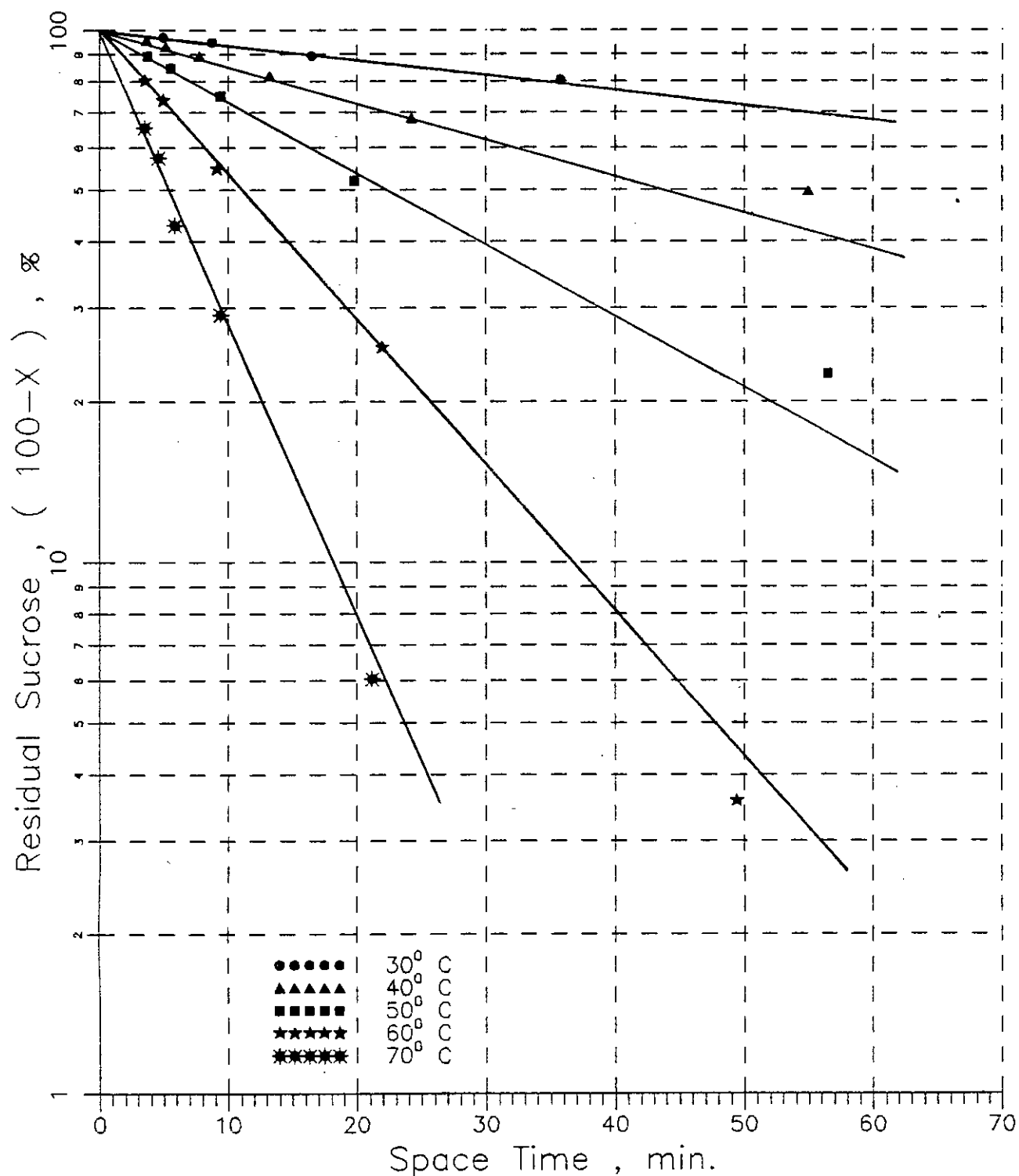
Figure B.4.3: Relation between residual sucrose and space time of 20% sucrose solution for 0.78 mm diameter resin bead at different temperatures.
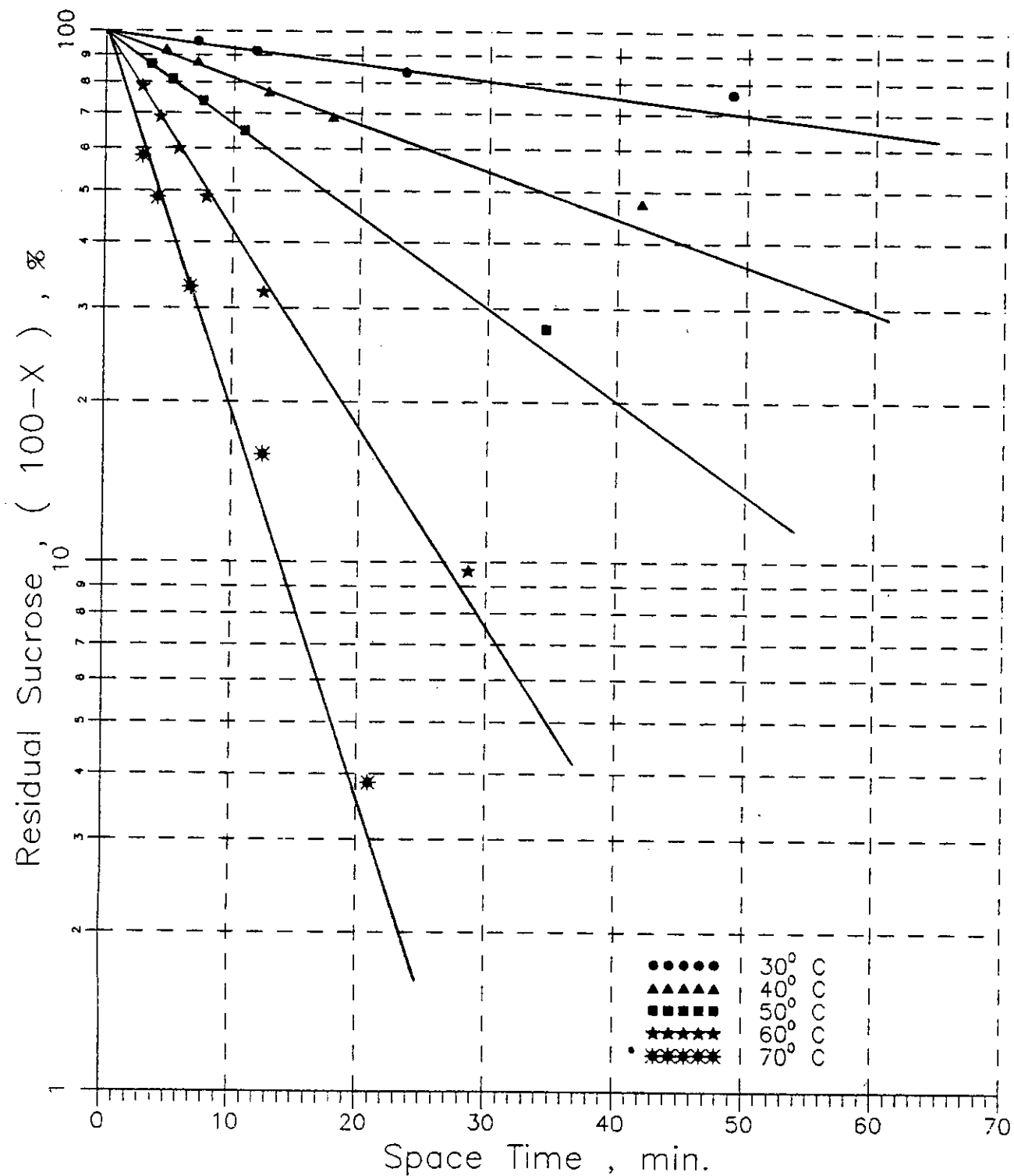
Figure B.4.4: Relation between residual sucrose and space time of 20% sucrose solution for 0.55 mm diameter resin bead at different temperatures.
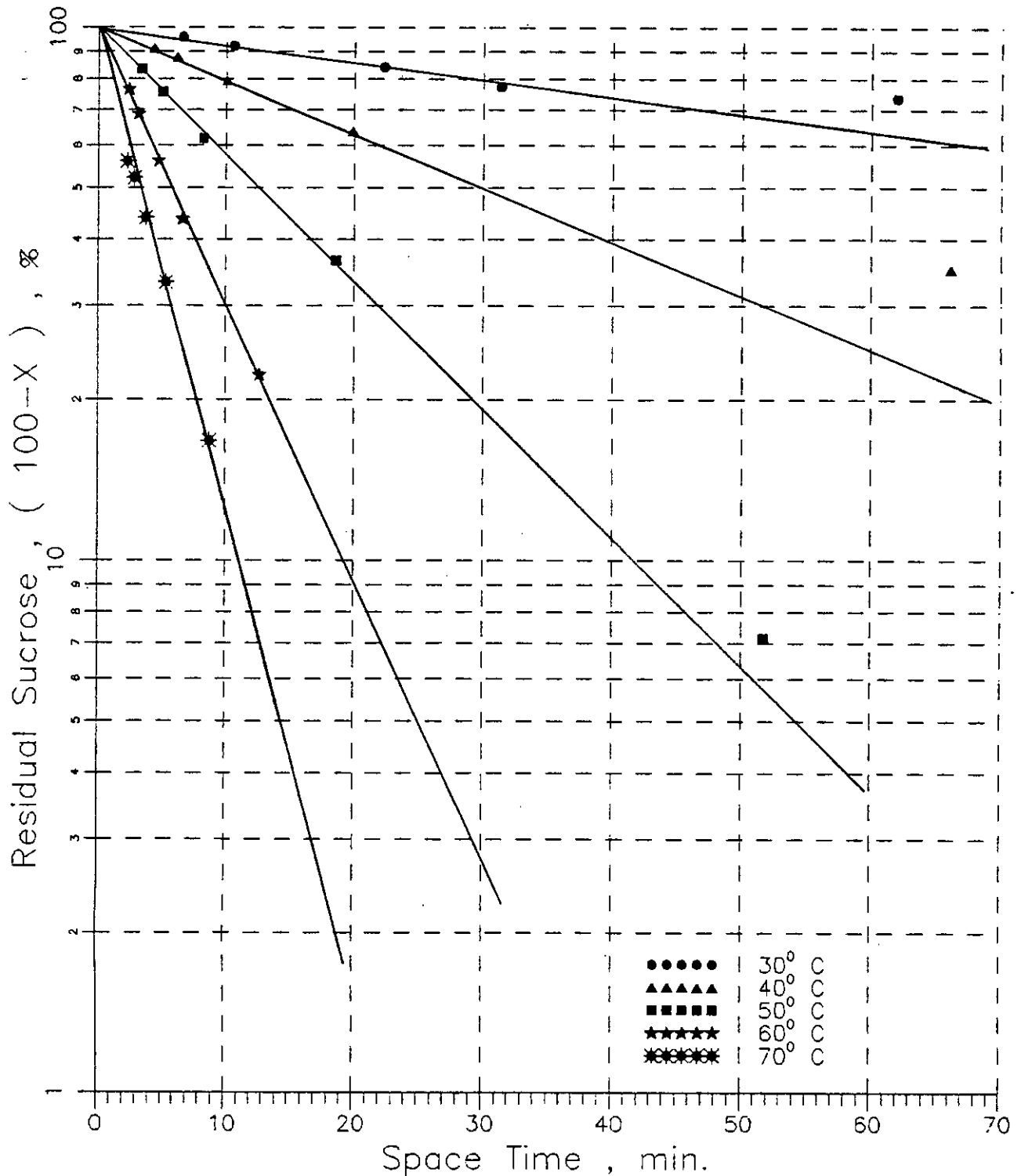
Figure B.4.5: Relation between residual sucrose and space time of 20% sucrose solution for 0.362 mm diameter resin bead at different temperatures.
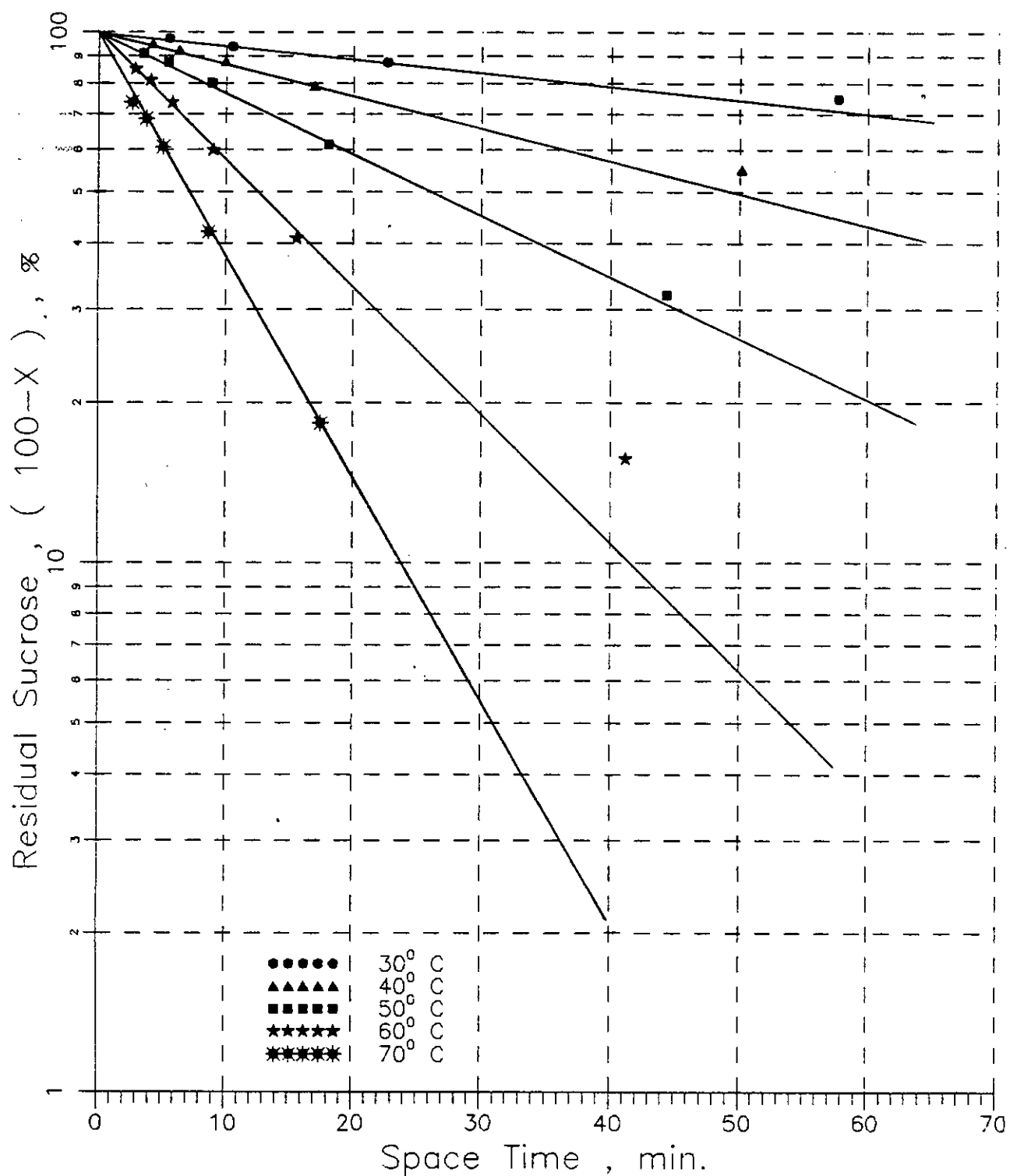
Figure B.5.1: Relation between residual sucrose and space time of 30% sucrose solution for 1.09 mm diameter resin bead at different temperatures.
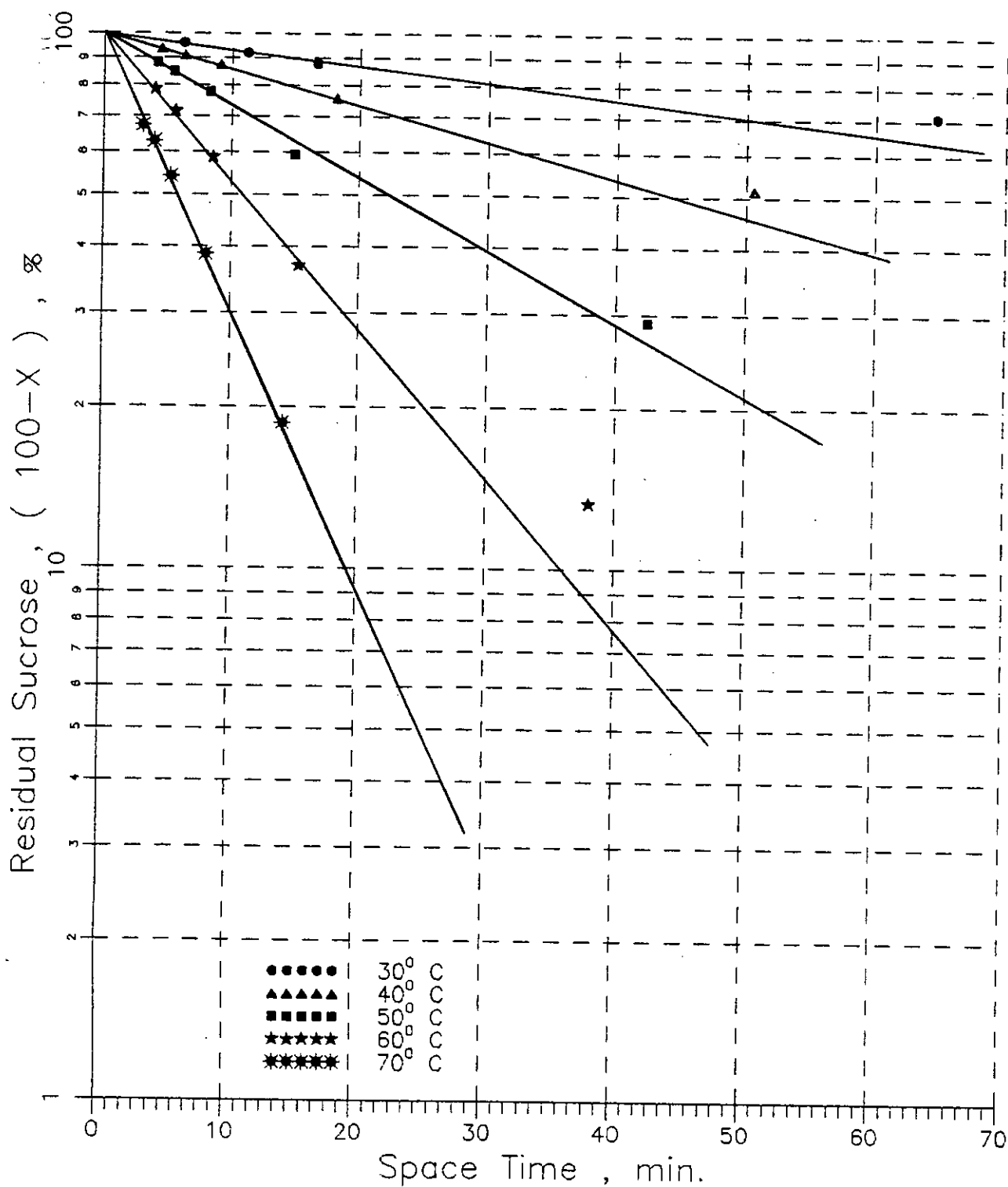
-Figure B.5.2: Relation between residual sucrose and space time
of 30% sucrose solution for 0.925 mm diameter
resin bead at different temperatures.

Figure B.5.3: Relation between residual sucrose and space time of 30% sucrose solution for 0.78 mm diameter resin bead at different temperatures.

Figure B.5.4: Relation between residual sucrose and space time of 30% sucrose solution for 0.55 mm diameter resin bead at different temperatures.

Figure B.5.5: Relation between residual sucrose and space time of 30% sucrose solution for 0.362 mm diameter resin bead at different temperatures.

Figure B.6.1: Relation between residual sucrose and space time of 40% sucrose solution for 1.09 mm diameter resin bead at different temperatures.

Figure B.6.2: Relation between residual sucrose and space time of 40% sucrose solution for 0.925 mm diameter resin bead at different temperatures.

Figure B.6.3: Relation between residual sucrose and space time of 40% sucrose solution for 0.78 mm diameter resin bead at different temperatures.

Figure B.6.4: Relation between residual sucrose and space time of 40% sucrose solution for 0.55 mm diameter resin bead at different temperatures.

Figure B.6.5: Relation between residual sucrose and space time of 40% sucrose solution for 0.362 mm diameter resin bead at different temperatures.
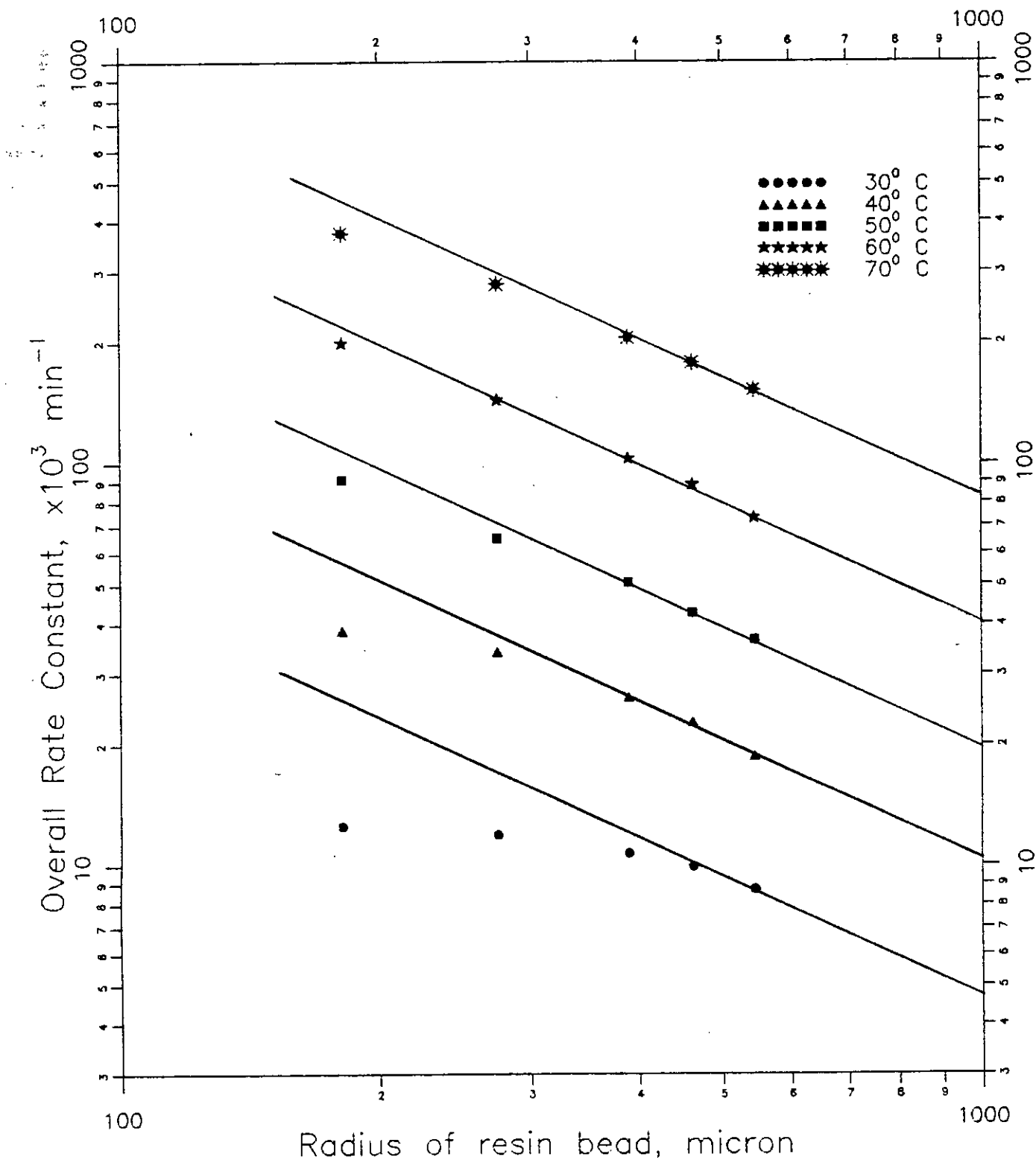
Figure B.7.1: Relation between overall rate constant and particle size of 20% sucrose solution at different temperatures.
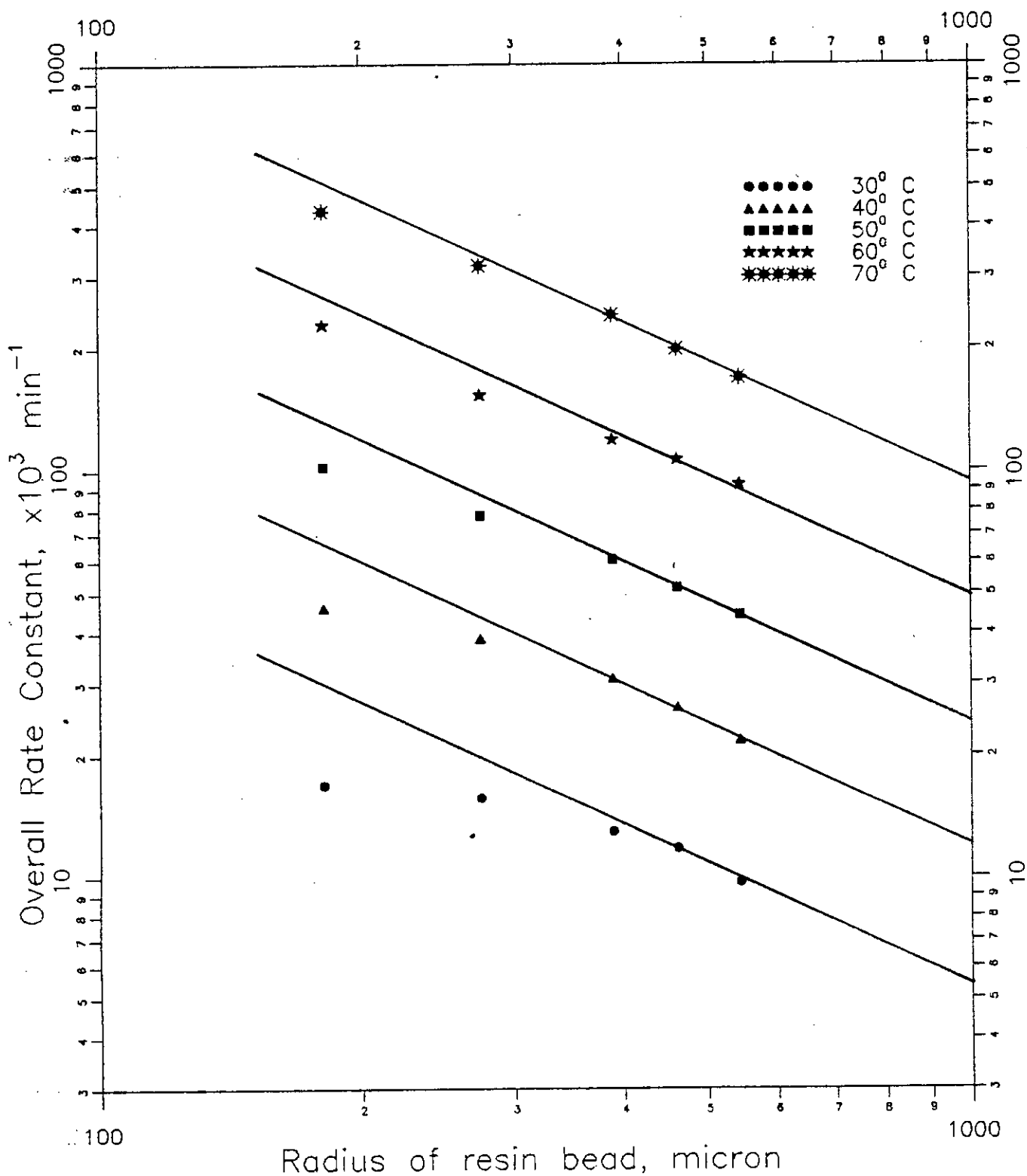
Figure B.7.2: Relation between overall rate constant and particle size of 30% sucrose solution at different temperatures.
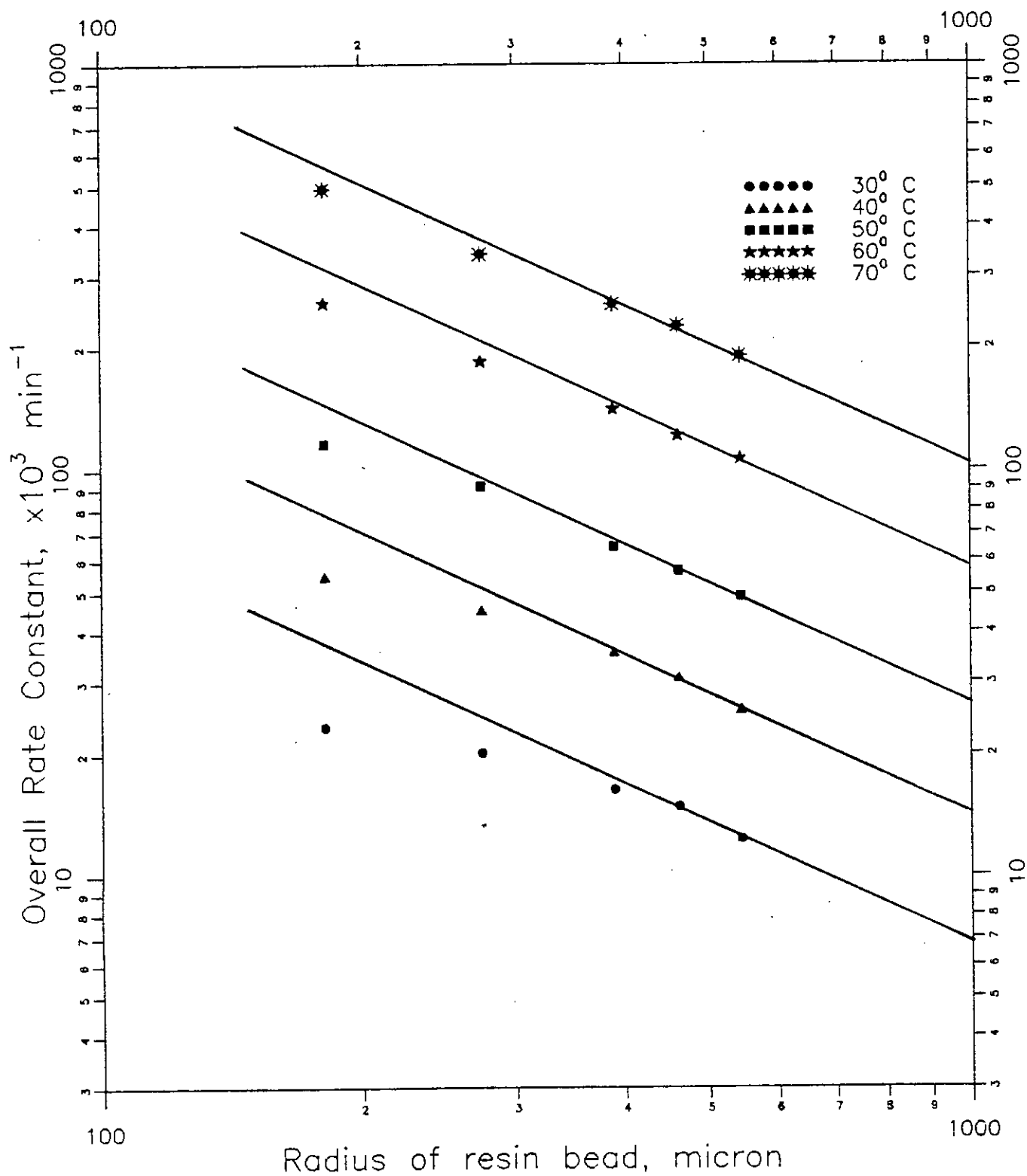
Figure B.7.3: Relation between overall rate constant and particle size of 40% sucrose solution at different temperatures.
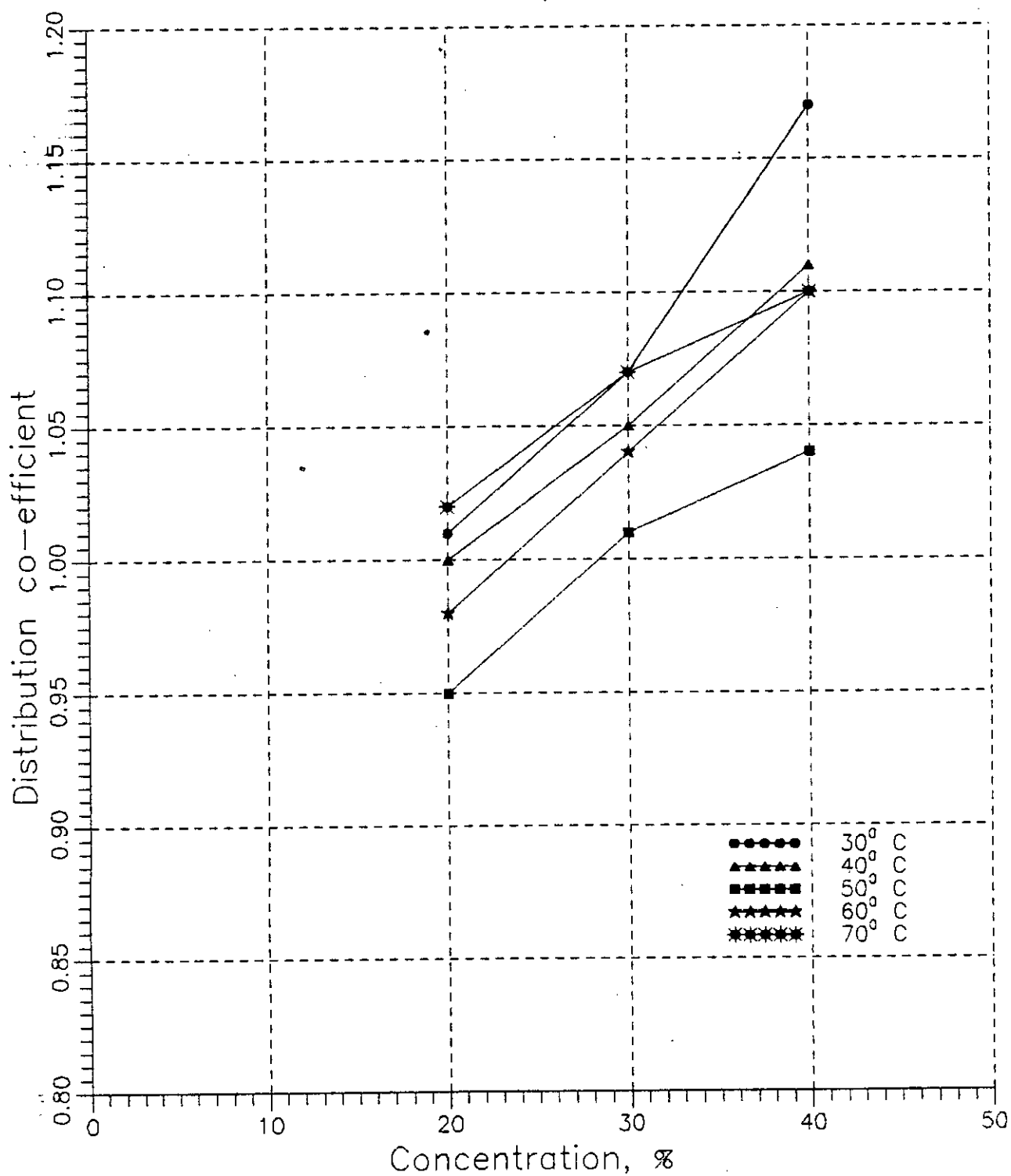
Figure B.8: Variation of distribution co-efficient with concentration at different temperatures.
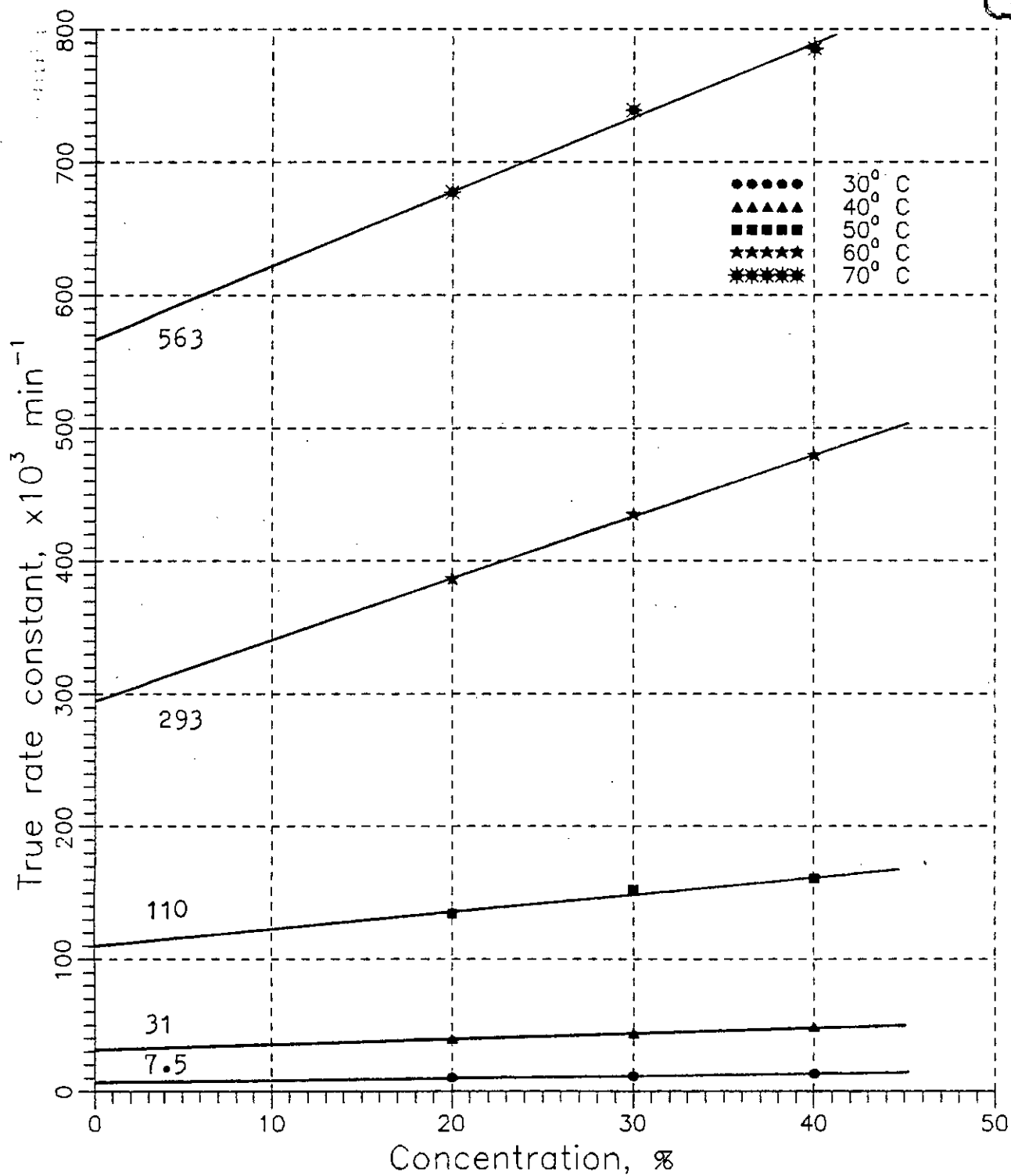
Figure B.9: Variation of rate constant with concentration at different temperatures.
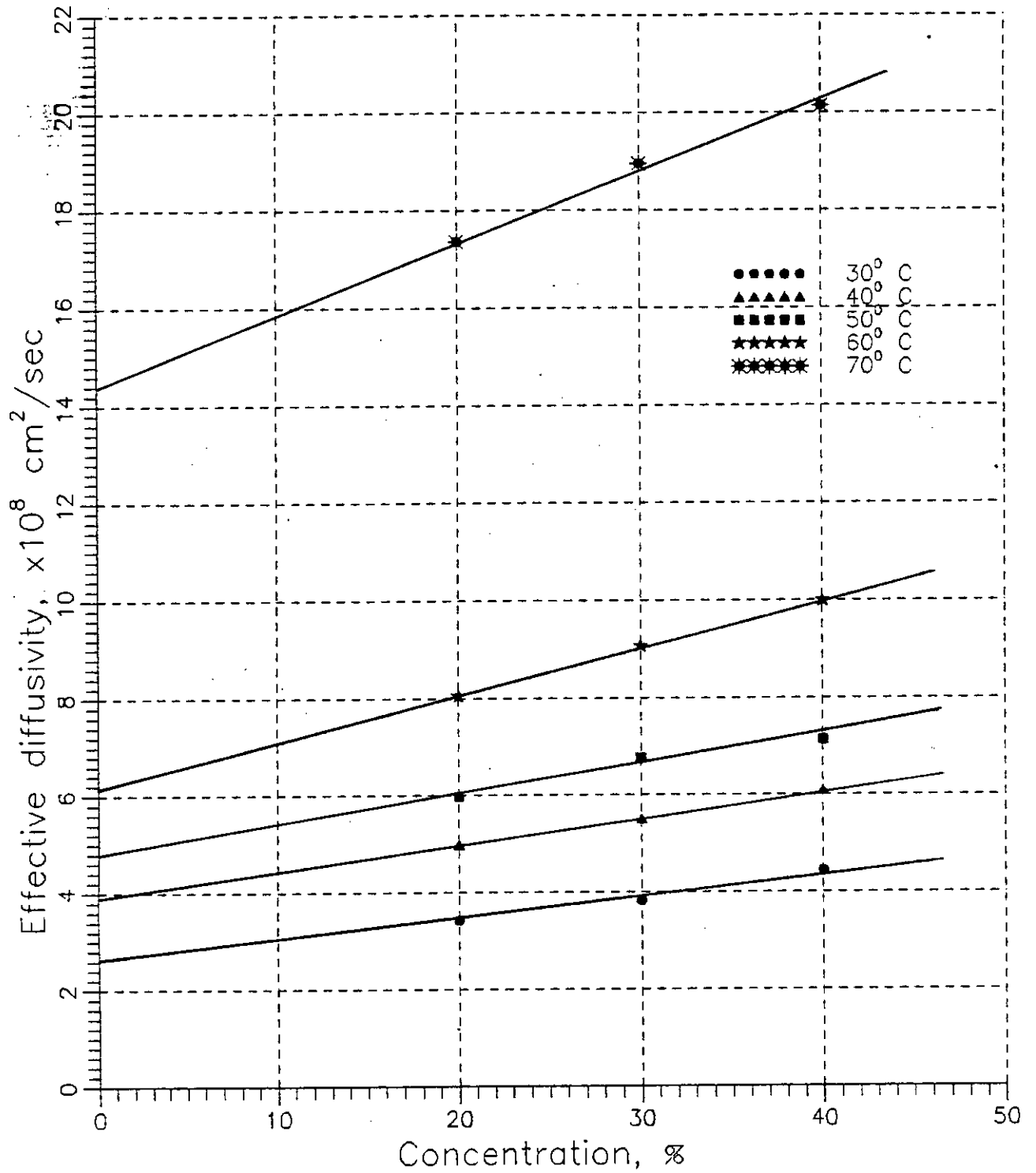
Figure B.10: Variation of effective diffusivity with concentration at different temperatures.
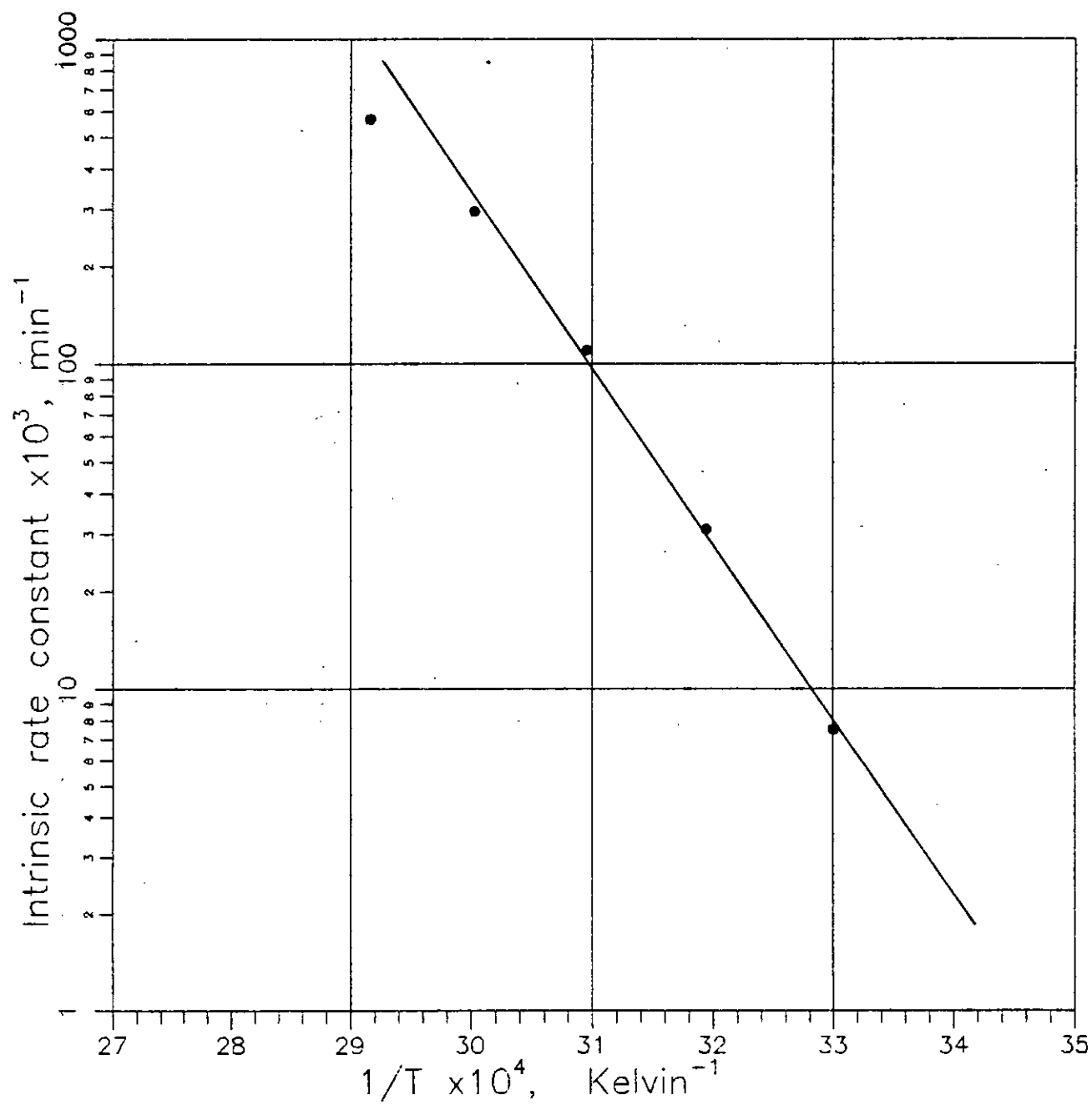
Figure B.11: Relation between intrinsic rate constant and temperature.
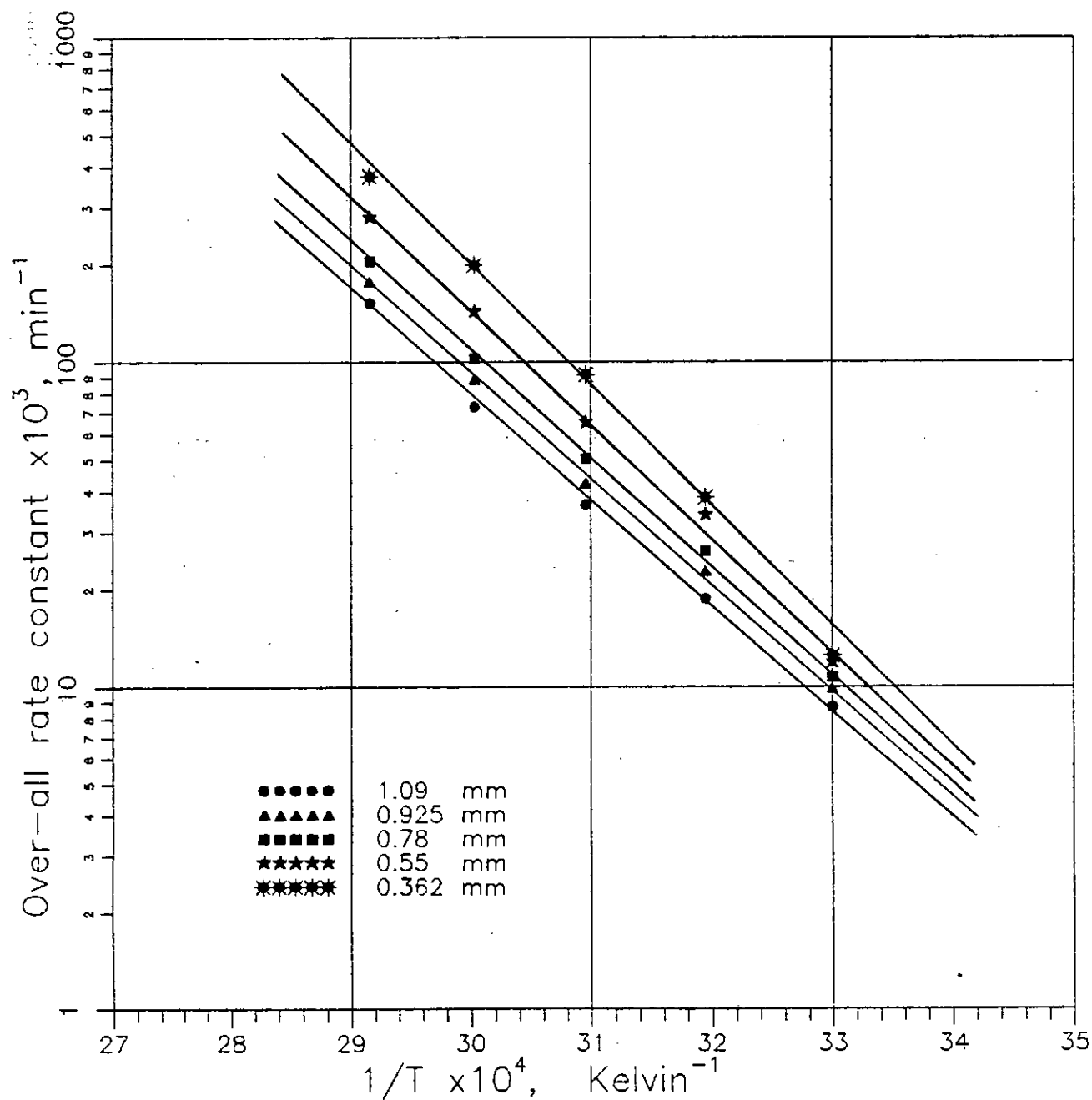
Figure B.12: Relation between over—all rate constant and temperature of 20% sucrose solution for different resin diameters.
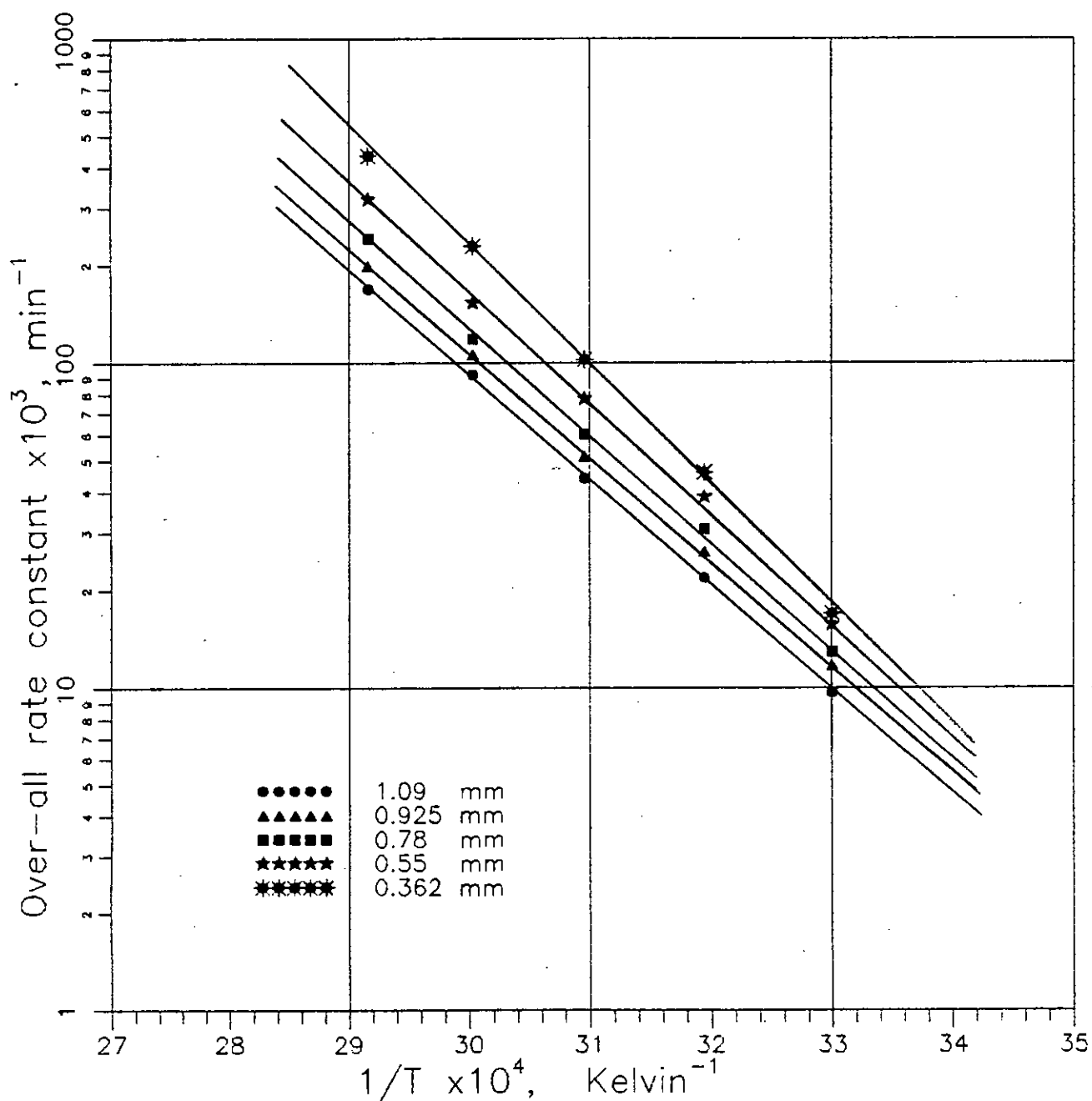
Figure B.13: Relation between over—all rate constant and temperature of 30% sucrose solution for different resin diameters.
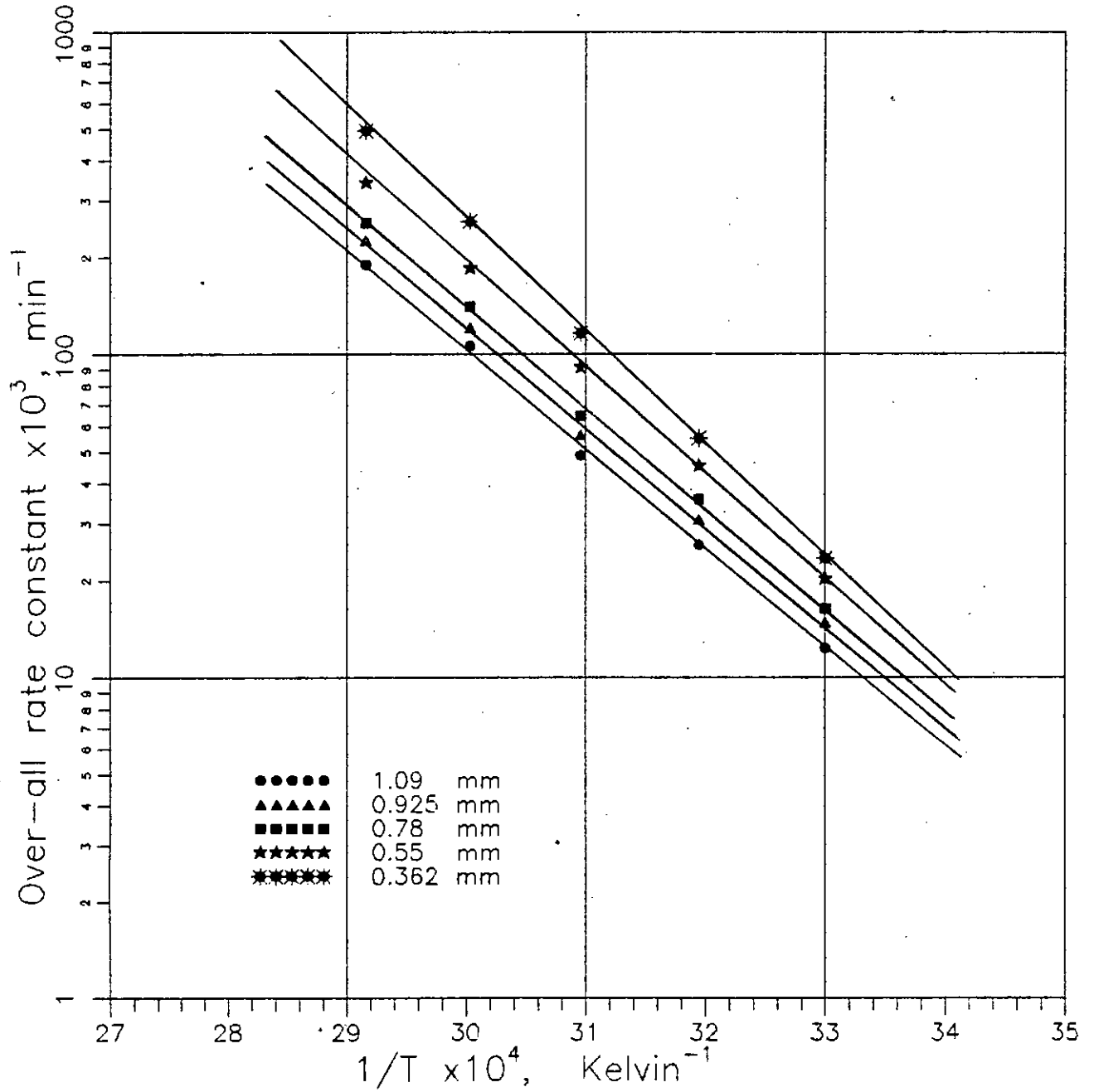
Figure B.14: Relation between over—all rate constant and temperature of 40% sucrose solution for different resin diameters.
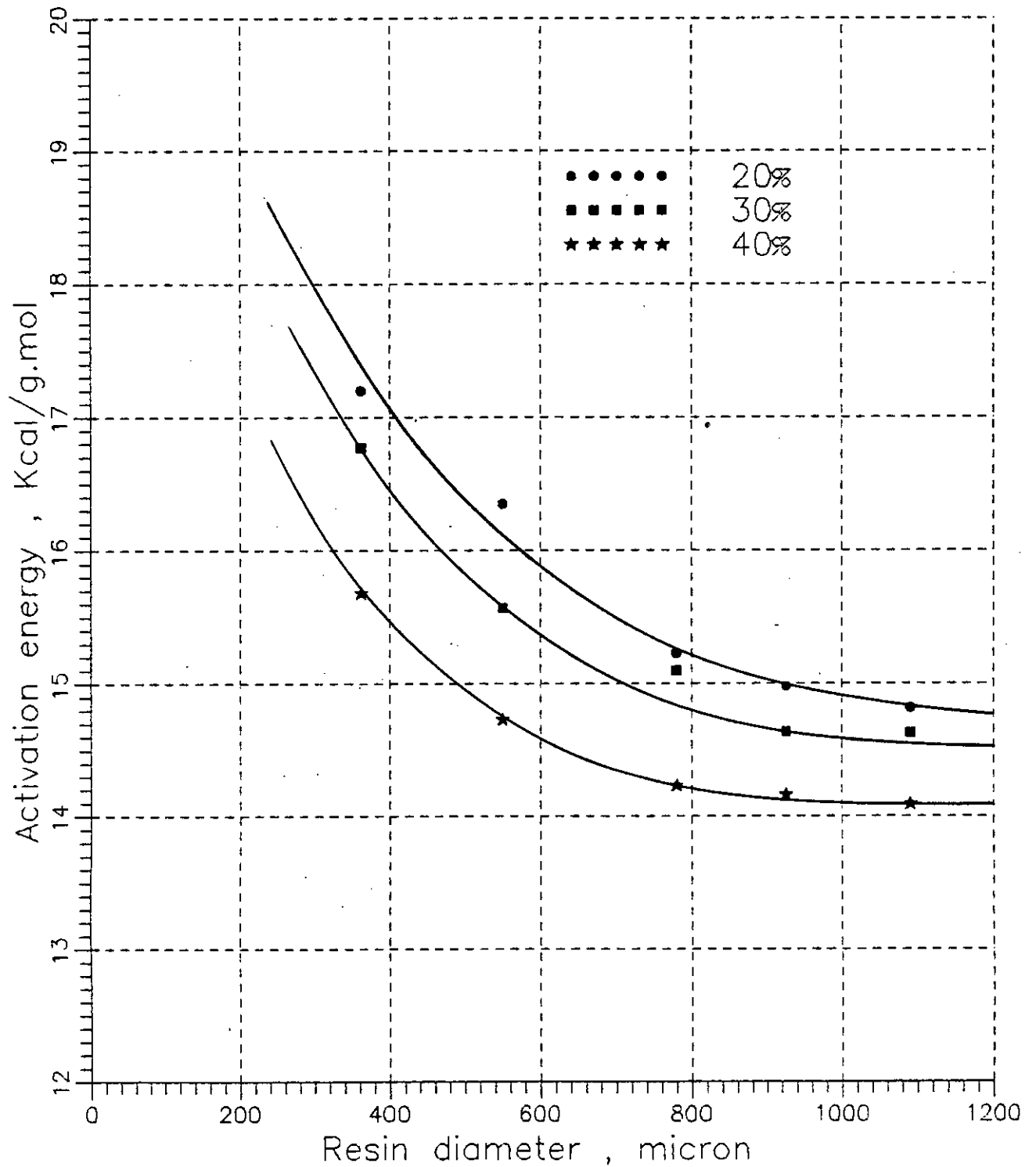
Figure B.15: Relation between activation energy of the over-all
rate and resin particle diameter for different
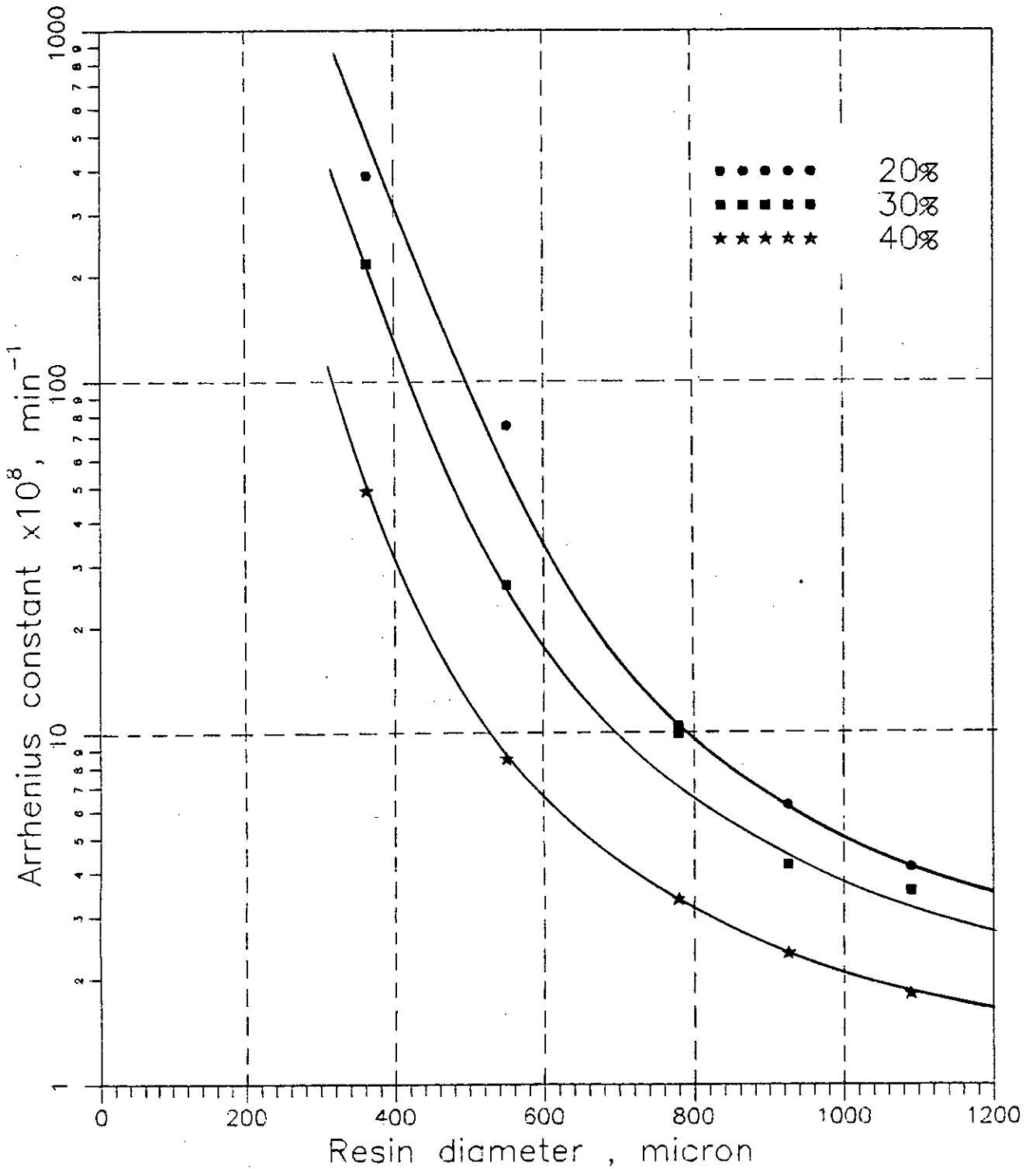concentrations of sucrose solution.

Figure B.16:. Relation between Arrhenious constant of the over—all rate and resin diameter for different concentrations of sucrose solution.
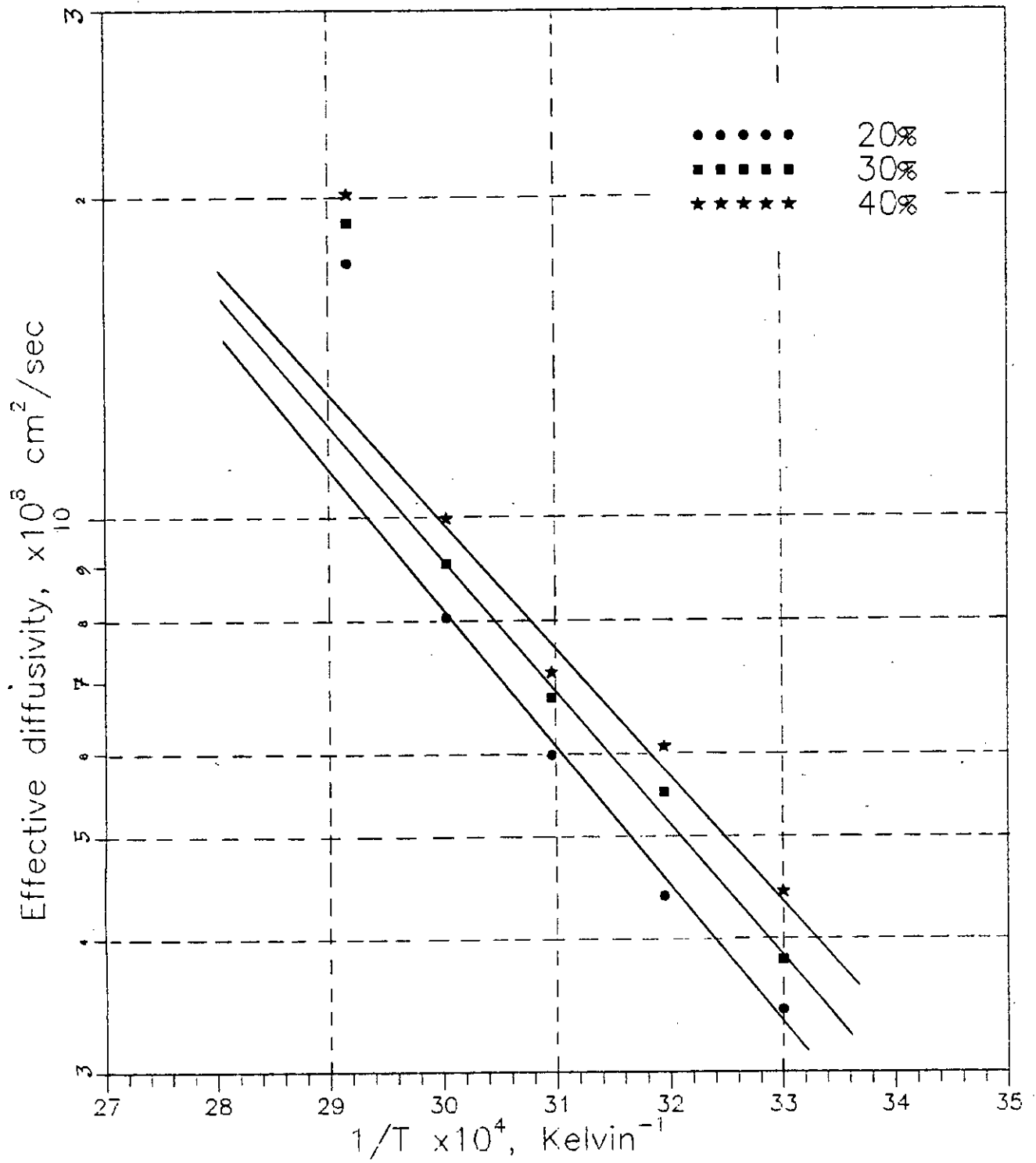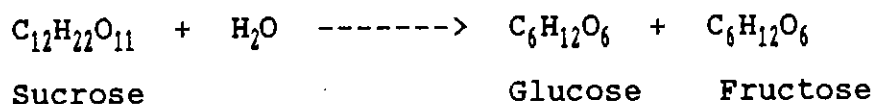
Figure B.17: Relation between effective diffusivity and temperature.

APPENDIX-C

CALIBRATION OF POLARIMETER

Percent inversion values of the sucrose solution was obtained by measuring its optical rotation with a polarimeter. The polarimeter used for this purpose was calibrated at 30^0C. Calibration readings were taken for 20, 30, 40 and 50% sucrose solutions by weight and for 0, 25, 50, 75 and 100% inversions of each concentration.

When sucrose solution is inverted according to the following equation:

$$C_{12}H_{22}O_{11} \quad + \quad H_2O \quad \text{-------->} \quad C_6H_{12}O_6 \quad + \quad C_6H_{12}O_6$$

Sucrose   Glucose   Fructose

Solid percent of the reacting mixture increases gradually with percent inversion. This is due to the fact that water is consumed in the process and the combined weight of glucose and fructose is greater than the equivalent amount of sucrose. This has been given due considerations during calibration.

For example, to prepare 100 gm. calibration samples of 40% sucrose solution at 0, 50 and 100% inversion levels the following amounts of sucrose, glucose, fructose and water were used.

% Inversion	Sucrose	Glucose	Fructose	Water	Total
0	40	0	0	60	100
50	20	10.5263	10.5263	58.9474	100
100	0	21.0526	21.0526	57.8948	100

Calibration data are presented in Table C.1 and plotted in Figure C.1.

TABLE NO. C.1: <u>Optical rotation at 30^{0}C of sucrose solutions of different concentrations at different levels of inversion</u>

Solution Concentra-tion %	Optical rotation, degree				
			% Inversion		
	0	25	50	75	100
20	14.30	9.65	5.25	0.75	-3.90
30	22.35	15.20	8.05	0.95	-6.30
40	31.05	21.00	11.05	1.05	-9.05
50	40.40	27.20	14.15	1.10	-12.15

cell length 1 dm.

Since the calibration was done at 30^{0}C, all polarization readings during actual experiment were also taken at the same temperature. Each sample was cooled to 30^{0}C by keeping it in a thermostatic bath for some time before taking its optical reading. A separate thermostatic bath was used for this purpose.
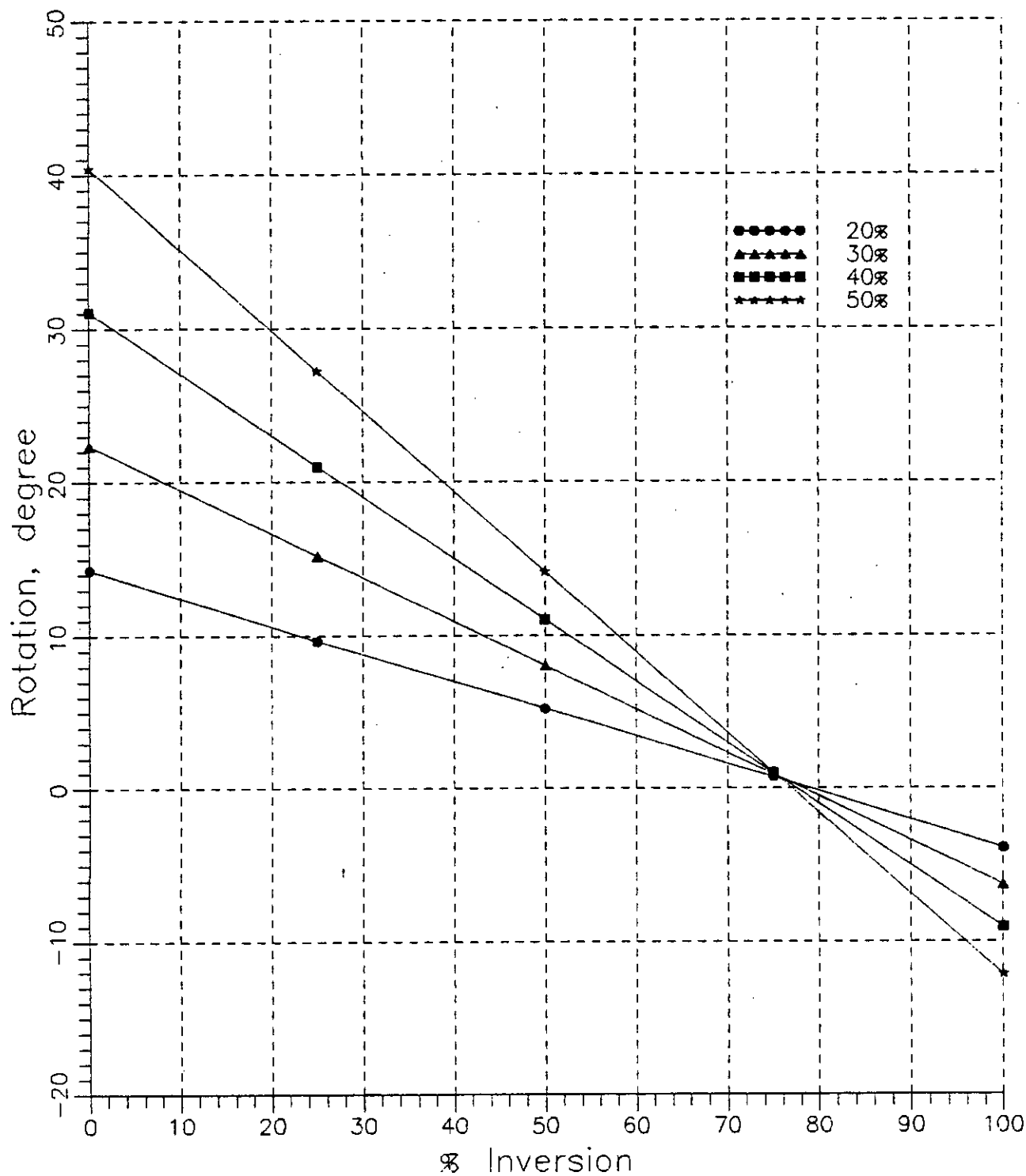
Figure C.1: Relation between optical rotation at 30^0
and percent inversion of sucrose solutions
at different concentrations.